

Supporting Information

Synthesis, Structure and Antileishmanial Evaluation of Endoperoxide–Pyrazole Hybrids

Patrícia S. M. Amado ^{1,2,†}, Inês C. C. Costa ^{1,2}, José A. Paixão ³, Ricardo F. Mendes ⁴, Sofia Cortes ⁵ and Maria L. S. Cristiano ^{1,2,*}

¹ Center of Marine Sciences, CCMAR, Gambelas Campus, University of Algarve, UAlg, 8005-039 Faro Portugal

² Department of Chemistry and Pharmacy, Faculty of Sciences and Technology, FCT, Gambelas Campus, University of Algarve, UAlg, 8005-139 Faro, Portugal

³ CFisUC, Department of Physics, University of Coimbra, 3004-516 Coimbra, Portugal

⁴ CICECO-Aveiro Institute of Materials, University of Aveiro, 3810-193 Aveiro, Portugal

⁵ Global Health and Tropical Medicine-GHTM, Instituto de Higiene e Medicina Tropical-IHMT, Universidade Nova de Lisboa-NOVA, 1349-008 Lisboa, Portugal

* Correspondence: mcristi@ualg.pt; Tel.: +351-289-800-953

† These authors contributed equally to this work.

Table of contents

S1.	¹ H, ¹³ C{ ¹ H} NMR, COSY, HSQC, HMBC spectra of the synthesised compounds	S2
S2.	HRMS spectra of the synthesised compounds	S51
S3.	X-ray crystallography	S60

S1. ^1H , $^{13}\text{C}\{^1\text{H}\}$ NMR, COSY, HSQC, HMBC spectra of the synthesised compounds

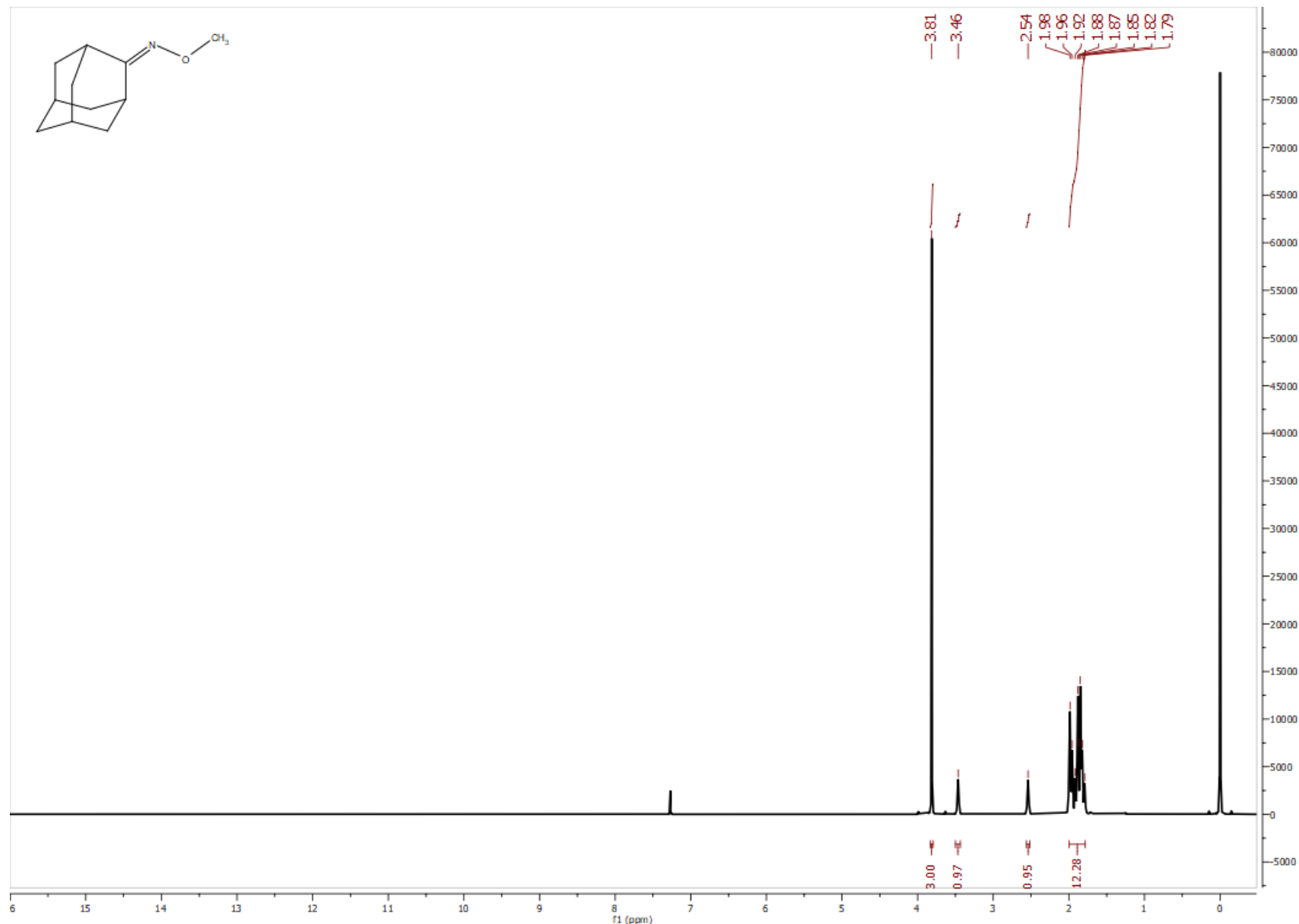


Figure S1. ^1H NMR spectrum (400 MHz) of **1o** in CDCl_3 .

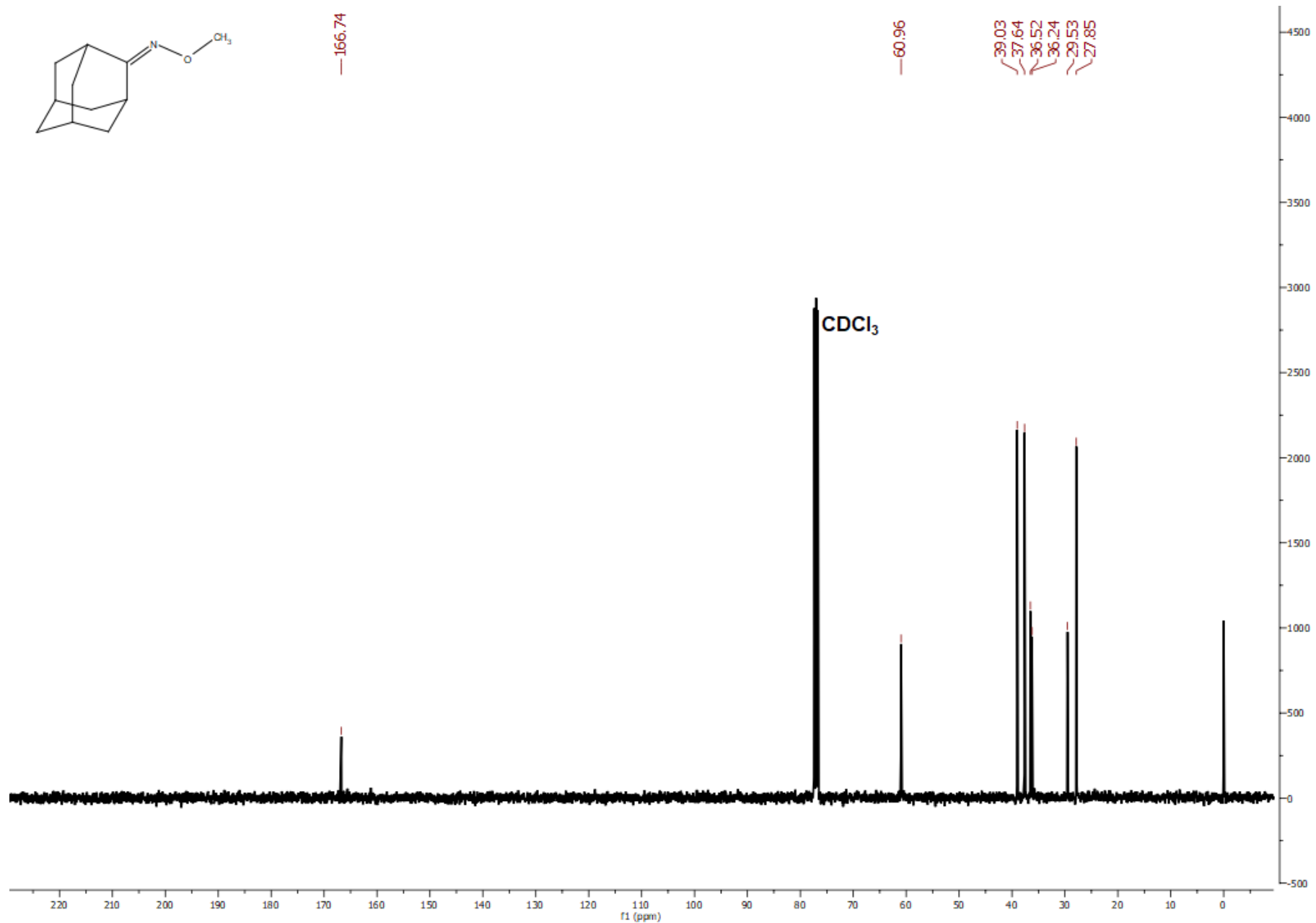


Figure S2. $^{13}\text{C}\{^1\text{H}\}$ NMR spectrum (100 MHz) of **1o** in CDCl_3 .

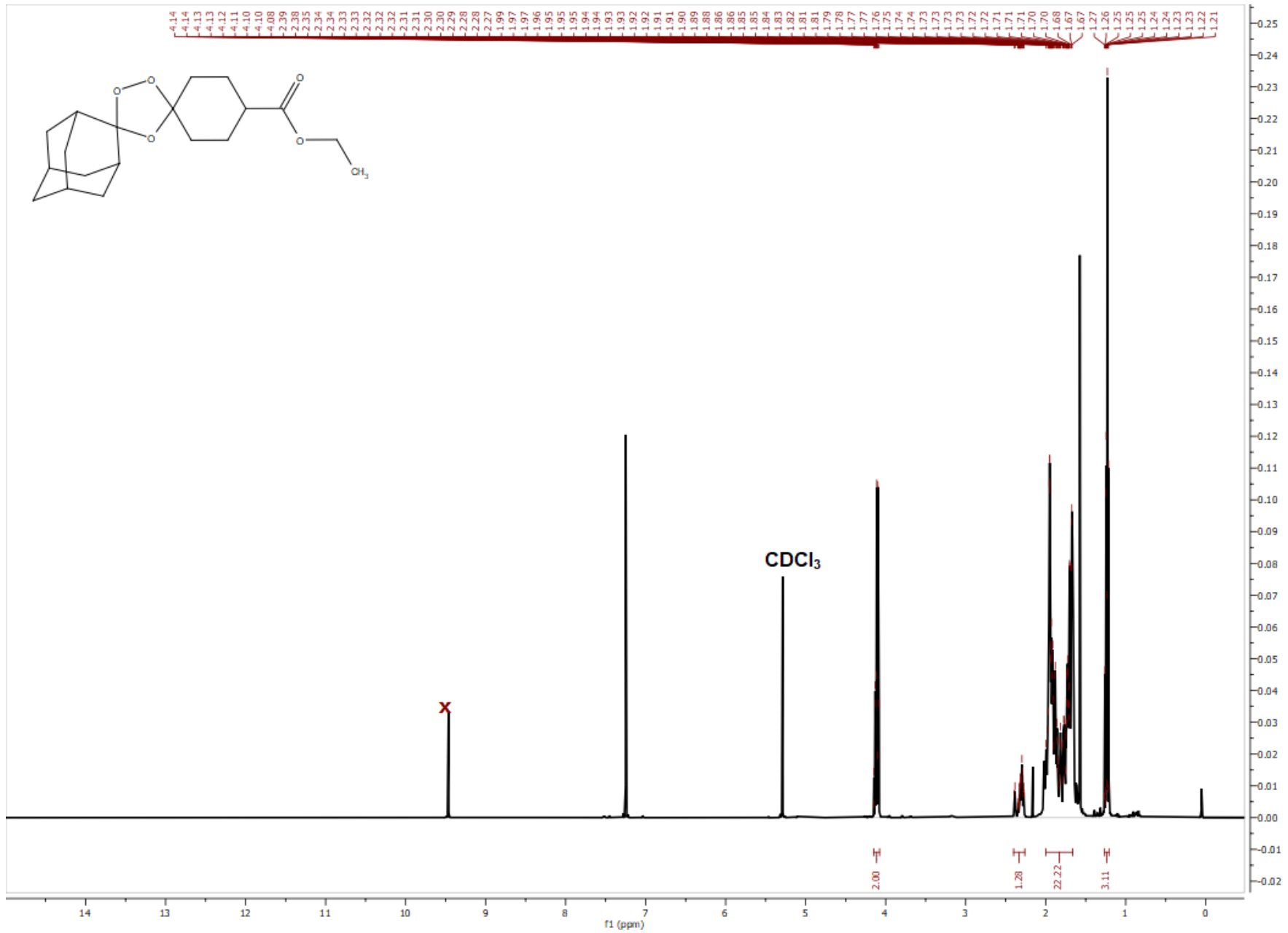


Figure S3. ^1H NMR spectrum (500 MHz) of **2o** in CDCl_3 .

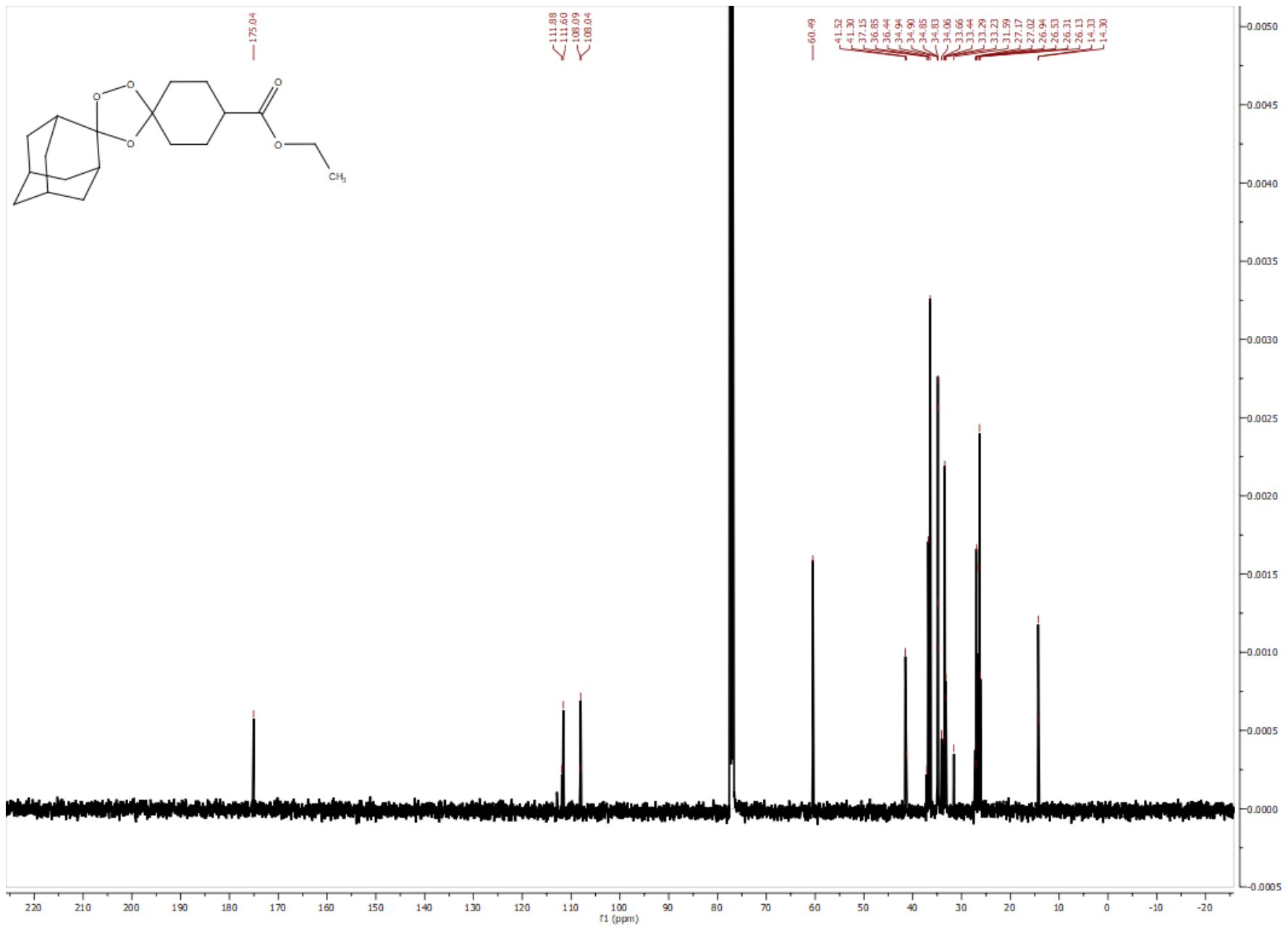


Figure S4. $^{13}\text{C}\{\text{H}\}$ NMR spectrum (126 MHz) of **2o** in CDCl_3 .

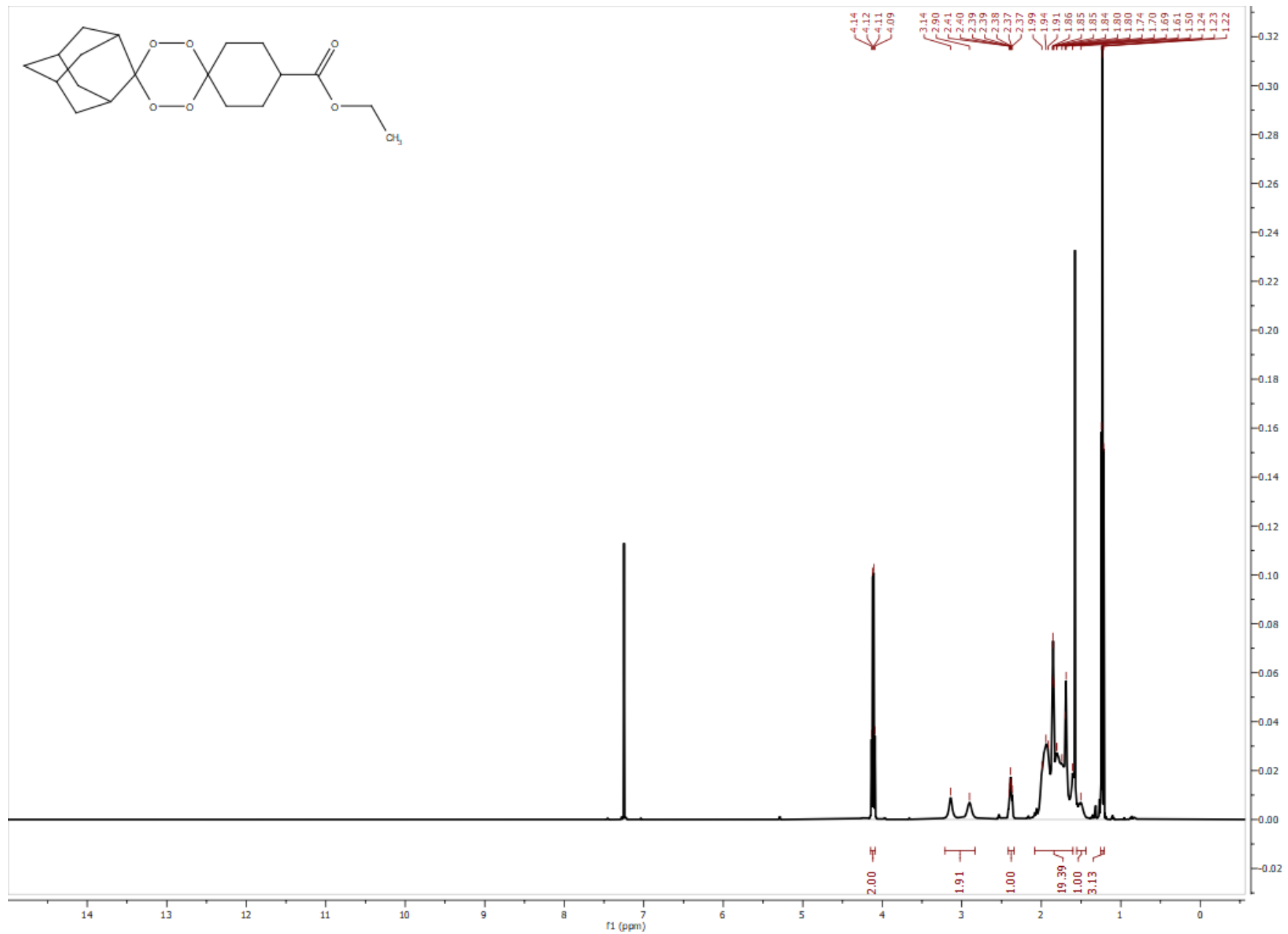


Figure S5. ^1H NMR spectrum (500 MHz) of **2t** in CDCl_3 .

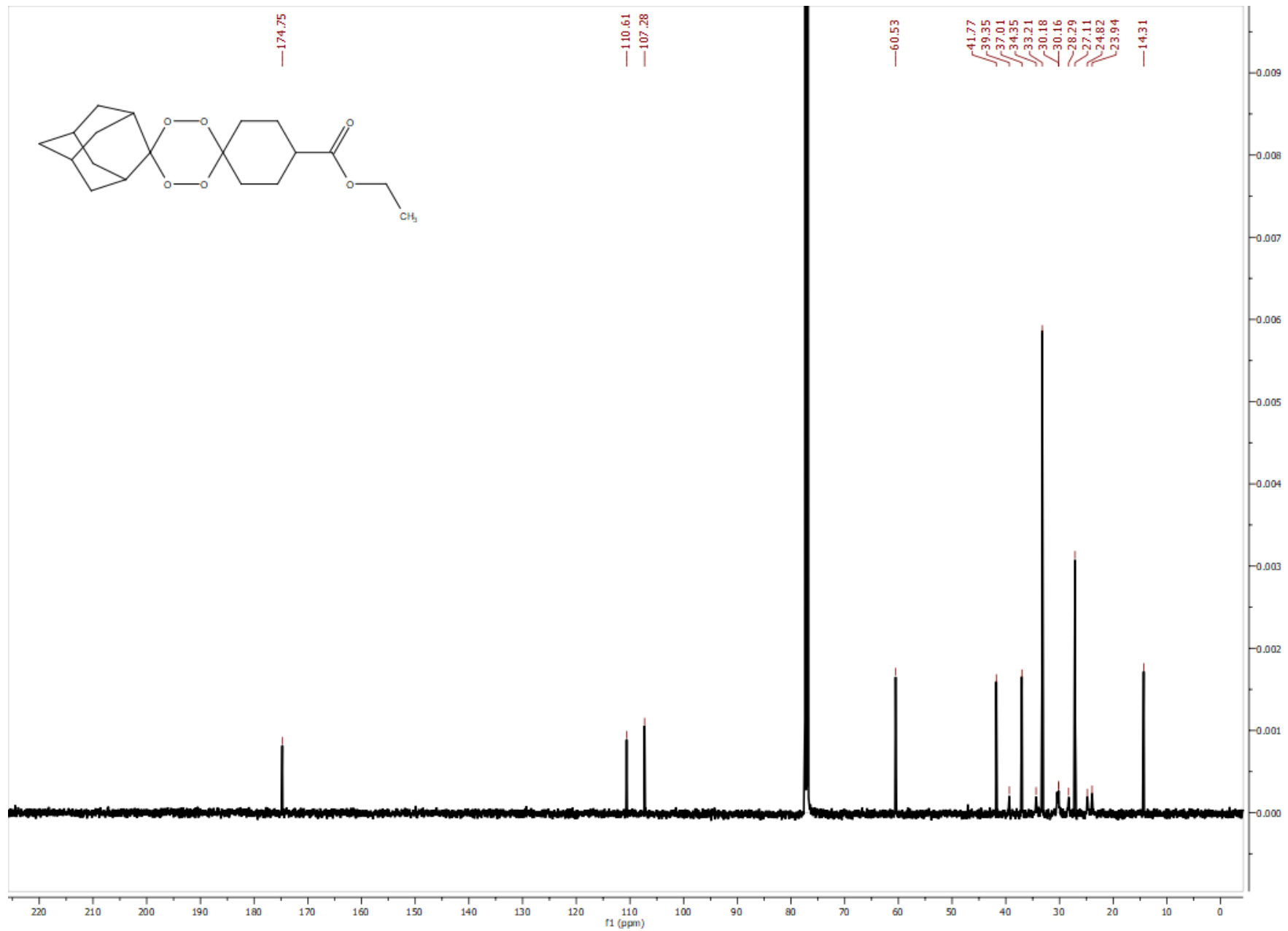


Figure S6. $^{13}\text{C}\{\text{H}\}$ NMR spectrum (126 MHz) of **2t** in CDCl_3 .

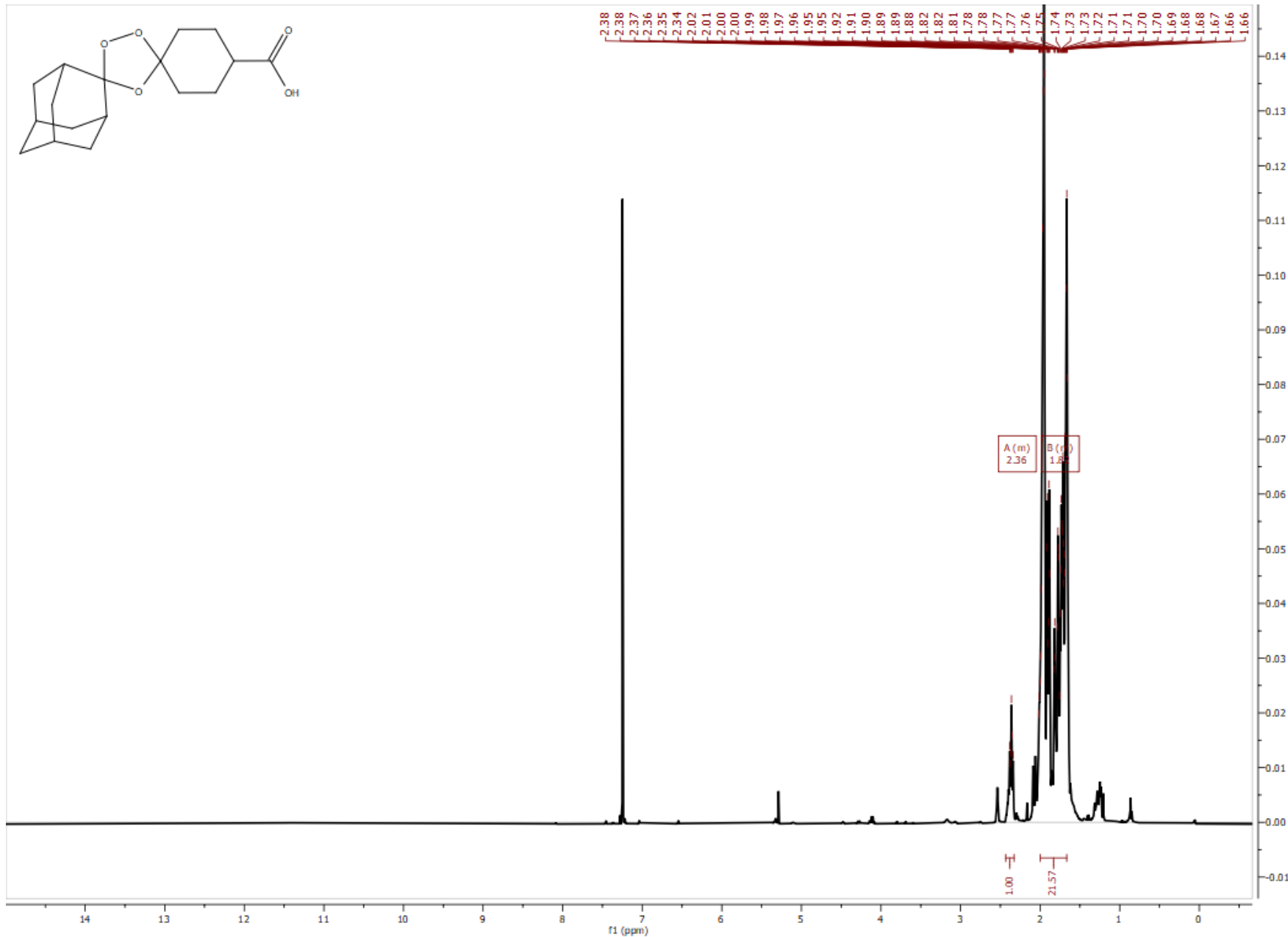


Figure S7. ^1H NMR spectrum (500 MHz) of **3o** in CDCl_3 .

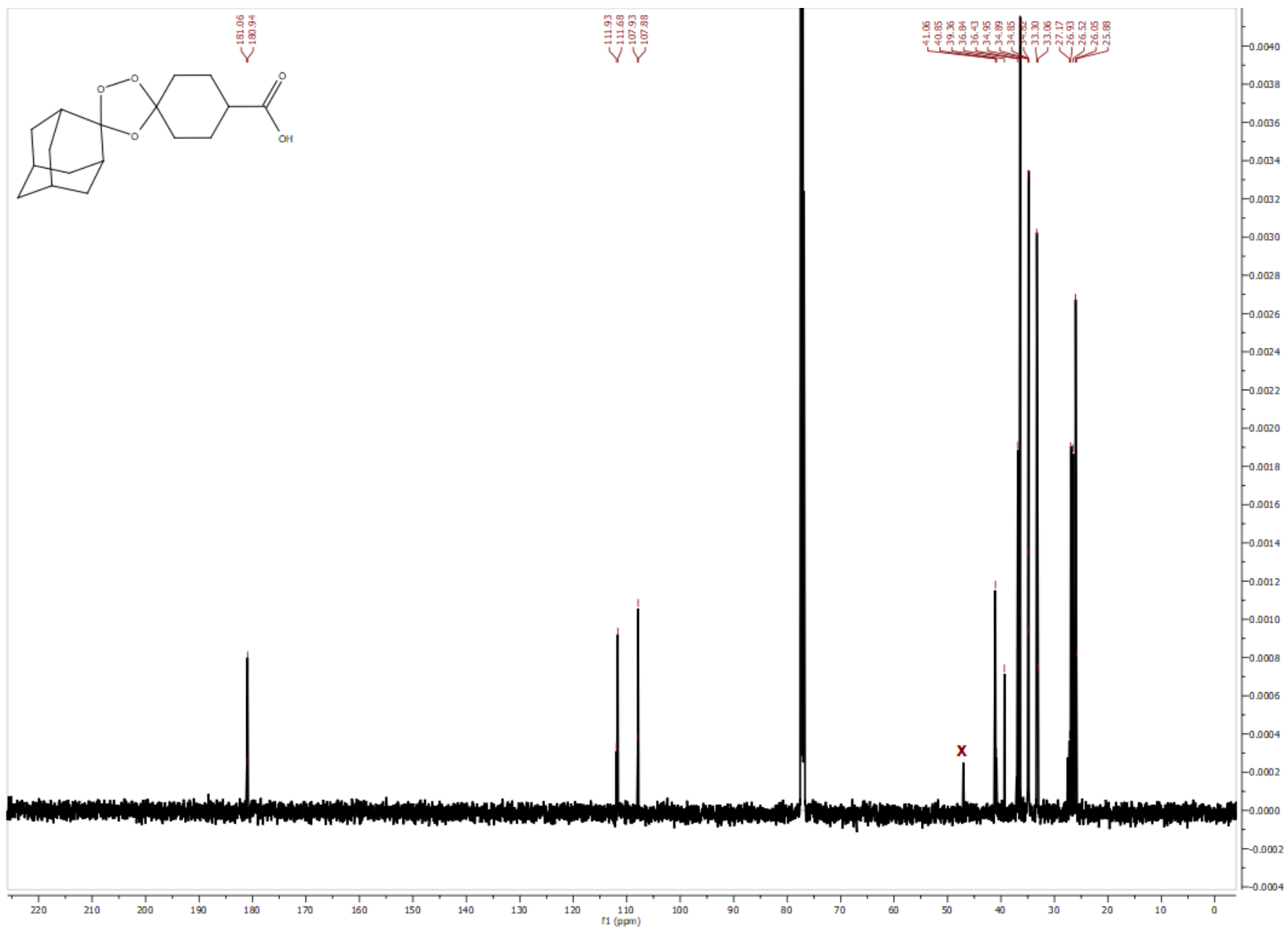


Figure S8. $^{13}\text{C}\{\text{H}\}$ NMR spectrum (126 MHz) of **3o** in CDCl_3 .

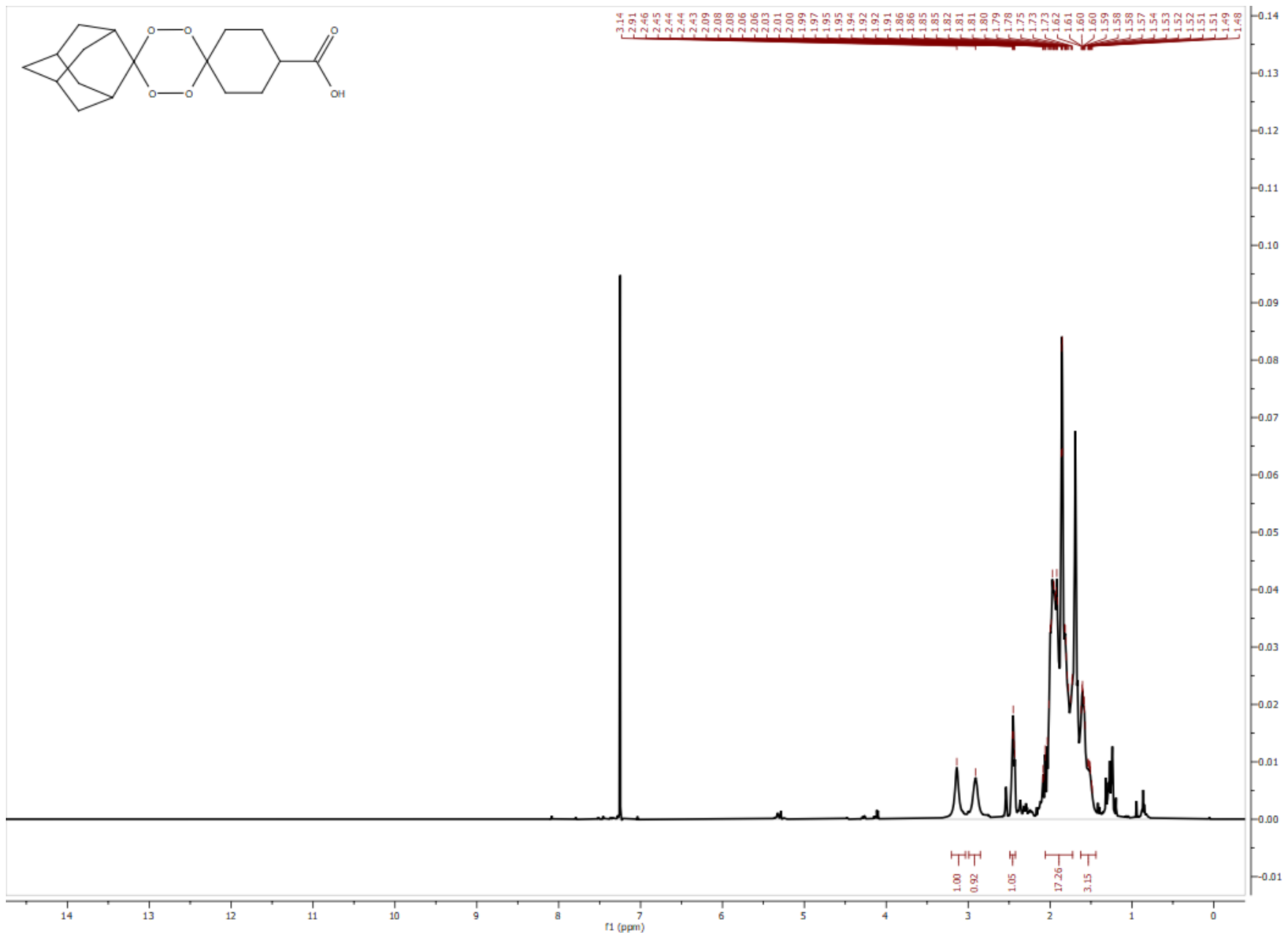


Figure S9. ^1H NMR spectrum (500 MHz) of **3t** in CDCl_3 .

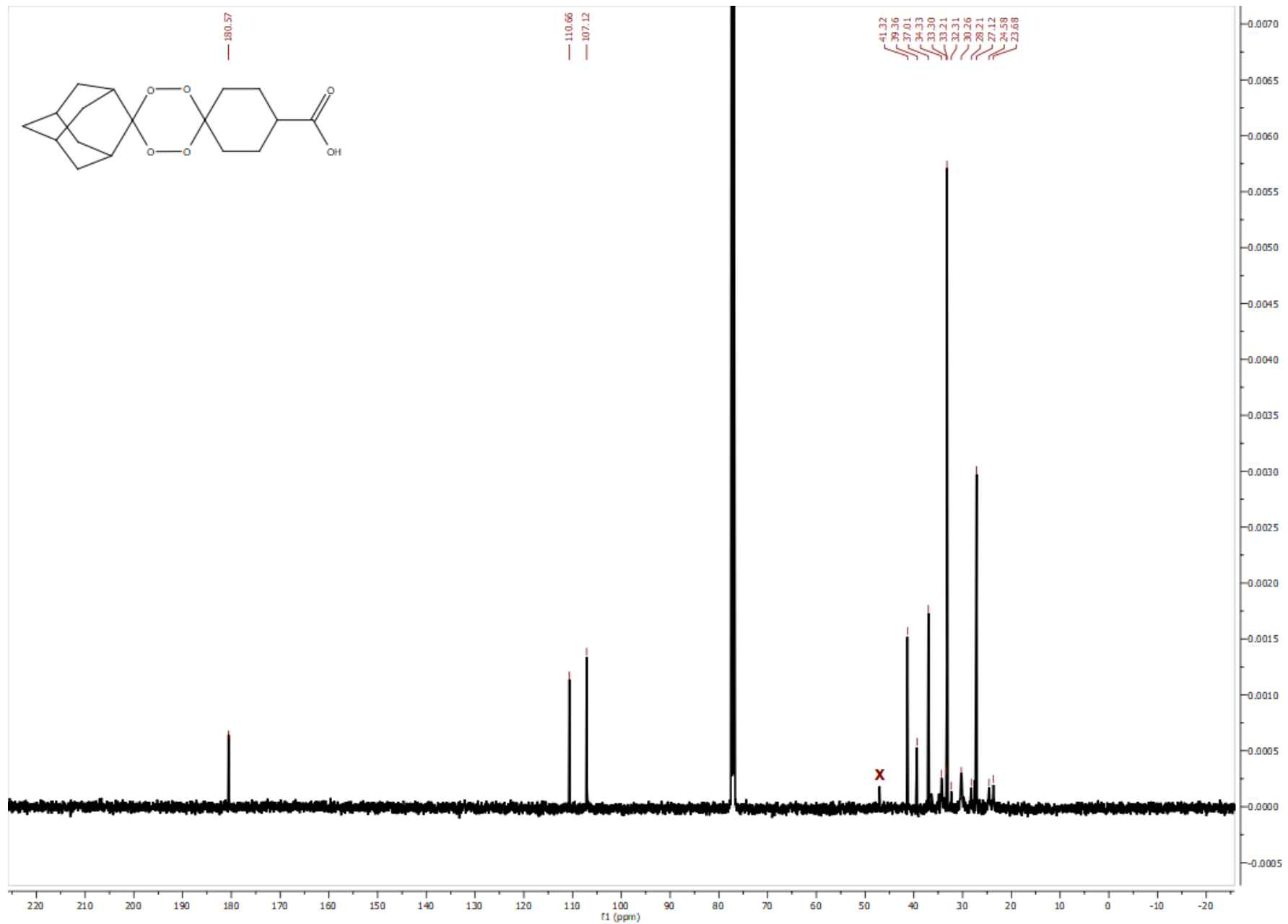
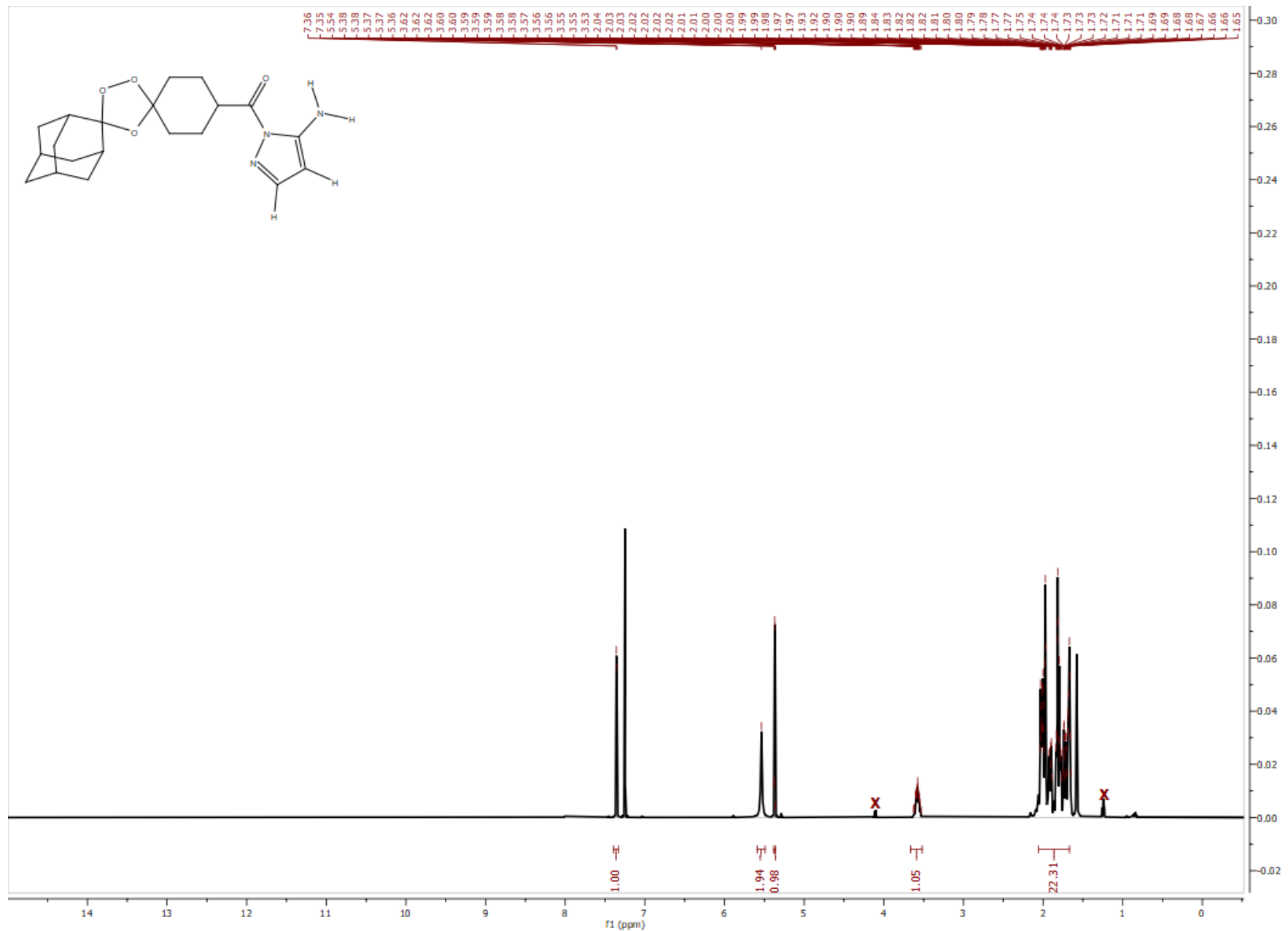


Figure S10. $^{13}\text{C}\{^1\text{H}\}$ NMR spectrum (126 MHz) of **3t** in CDCl_3 .



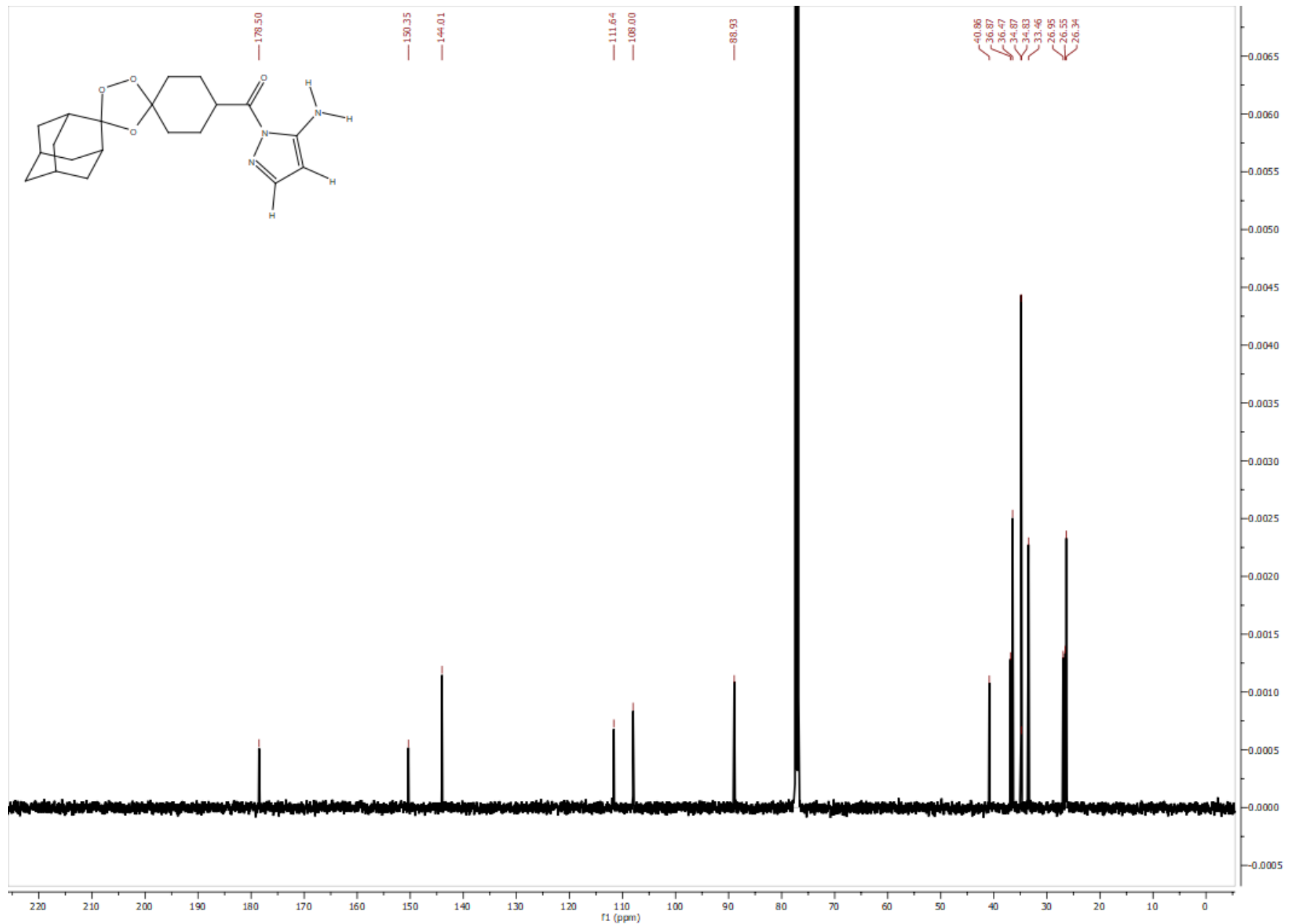


Figure S12. $^{13}\text{C}\{^1\text{H}\}$ NMR spectrum (126 MHz) of **OZ1** in CDCl_3 .

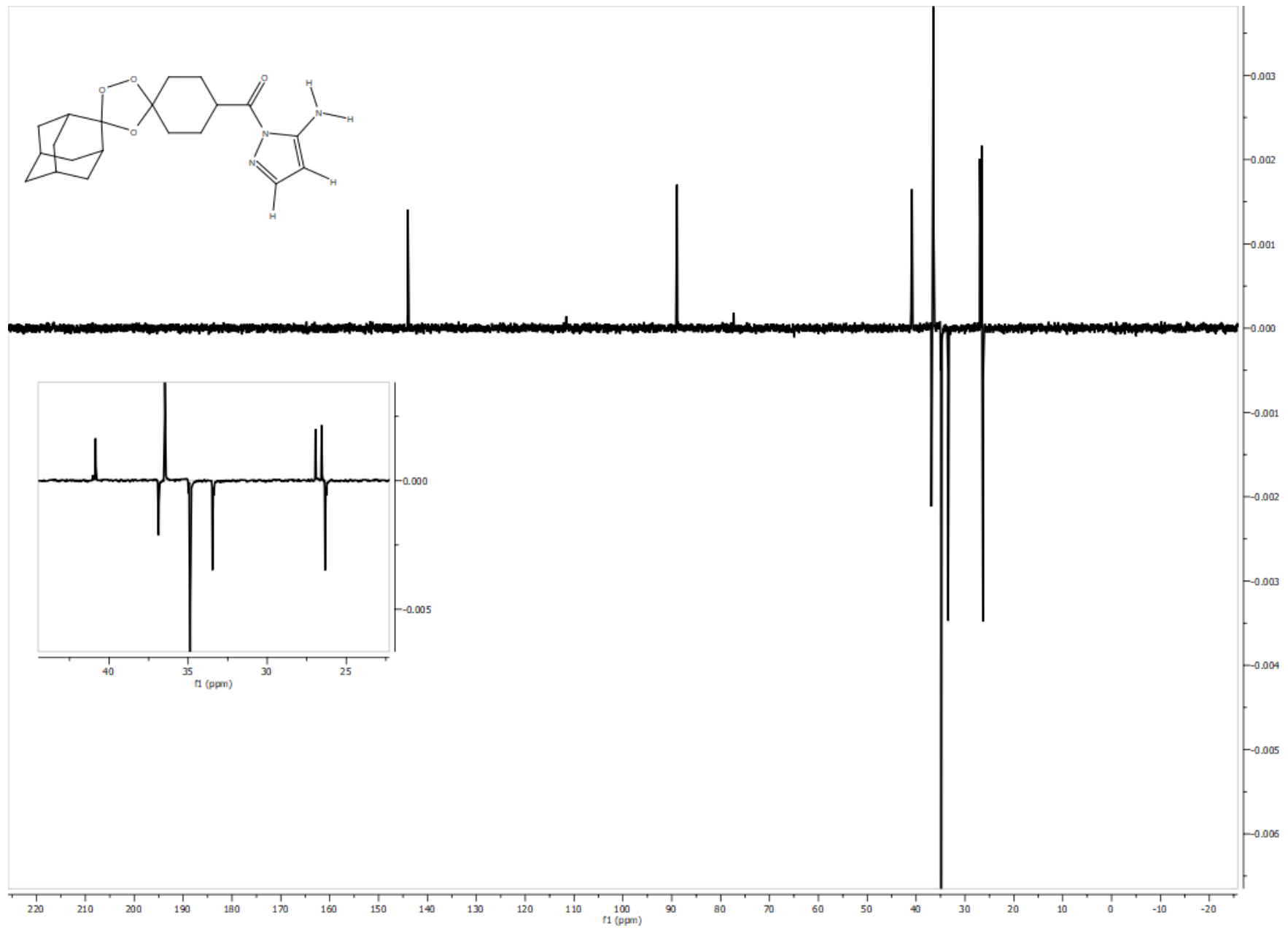


Figure S13. $^{13}\text{C}\{^1\text{H}\}$ DEPT-135 NMR spectrum (126 MHz) of **OZ1** in CDCl₃.

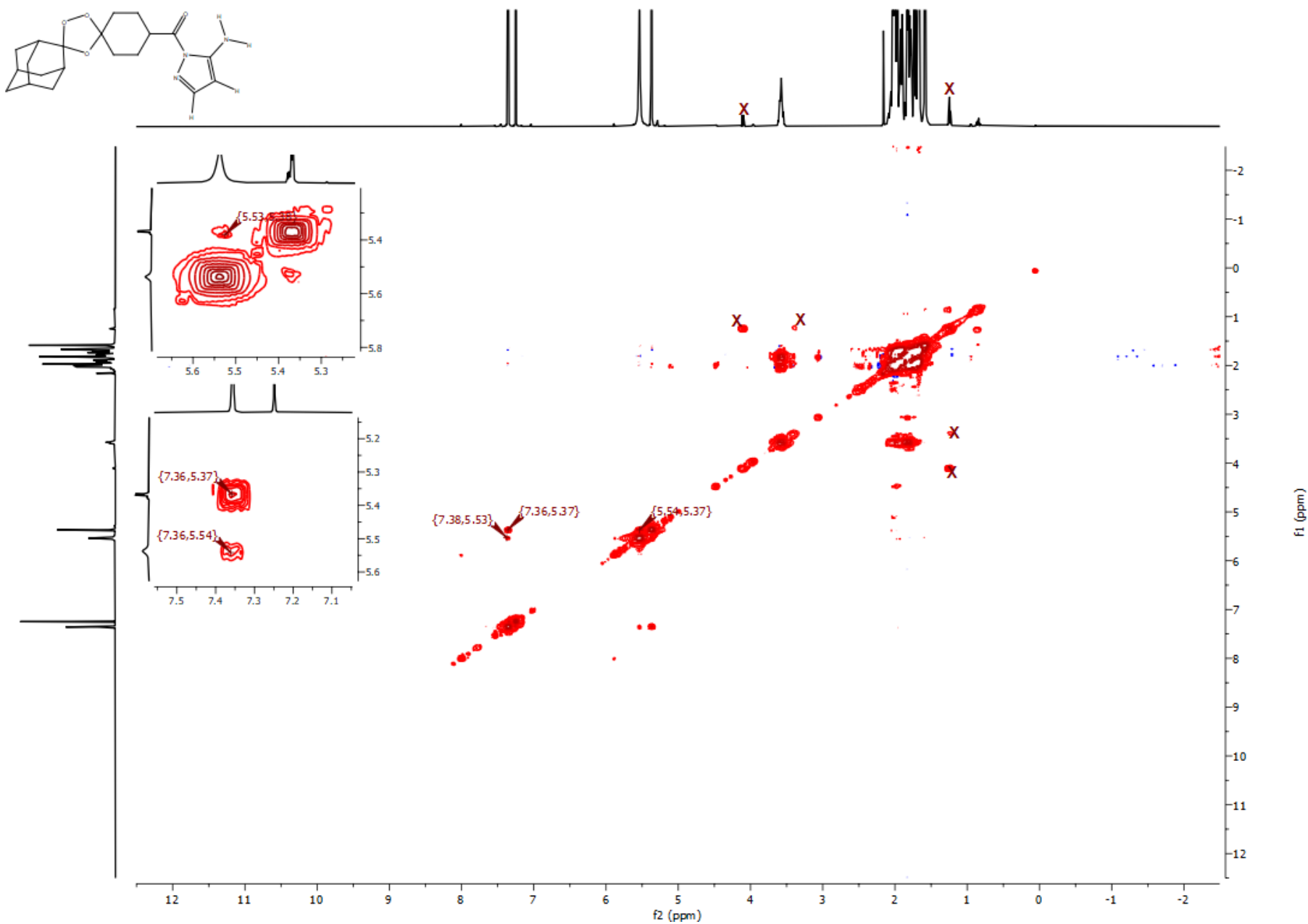


Figure S14. COSY spectrum (500 MHz) of **OZ1** in CDCl₃.

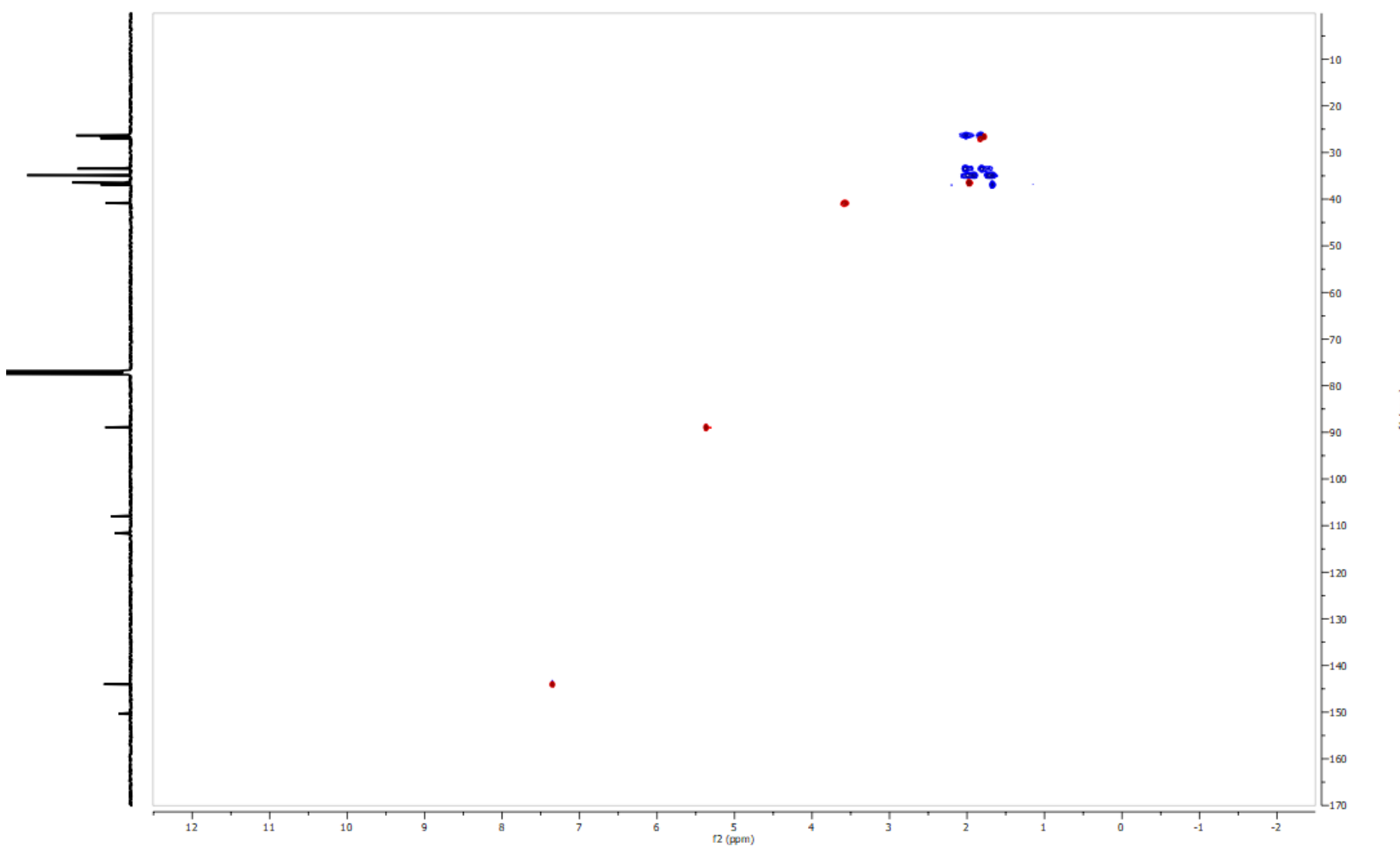
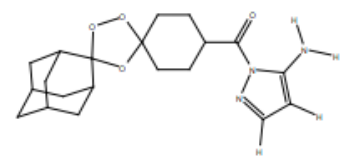


Figure S15. HSQC spectrum (500 MHz) of **OZ1** in CDCl_3 .

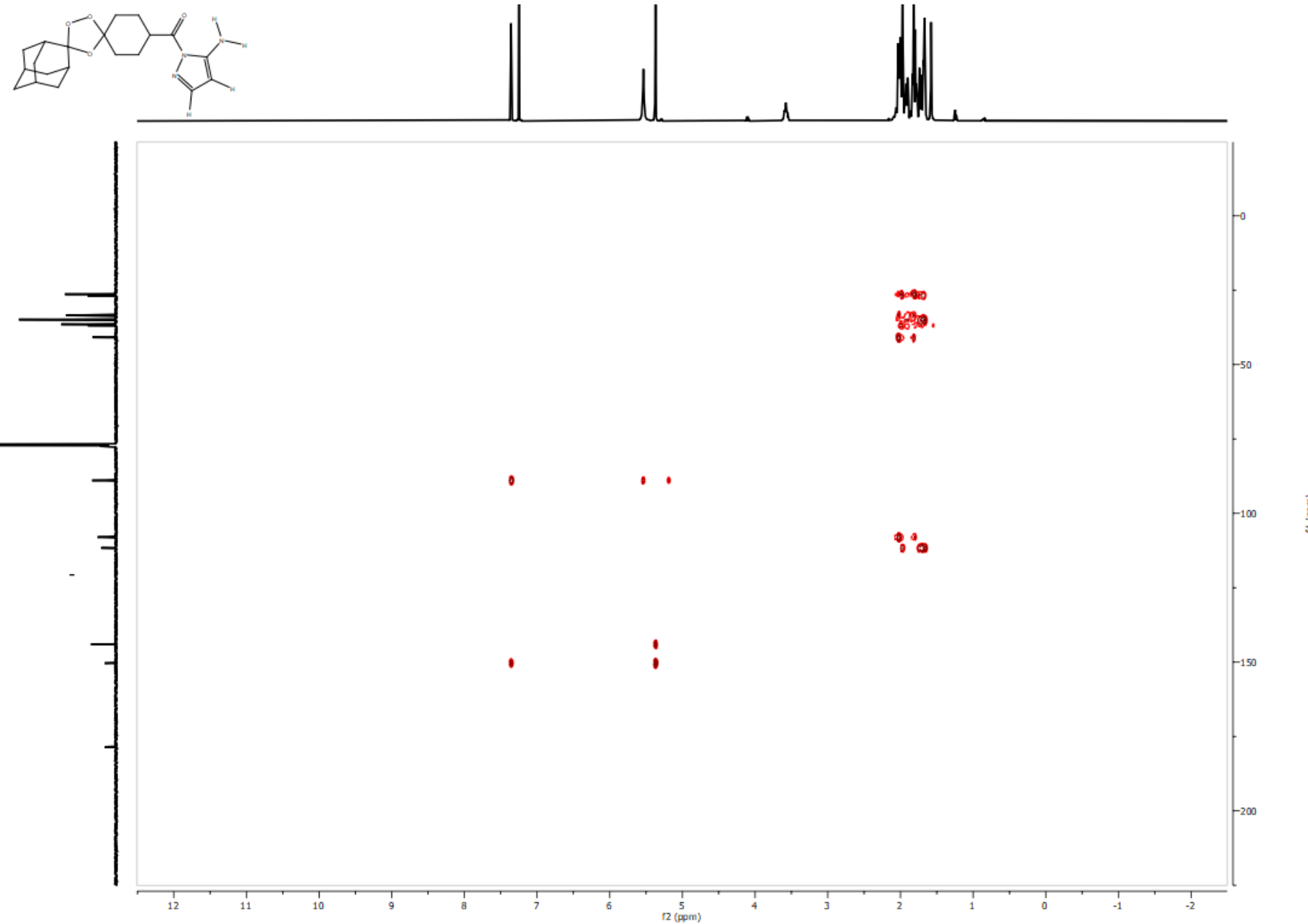


Figure S16. HMBC spectrum (500 MHz) of **OZ1** in CDCl_3 .

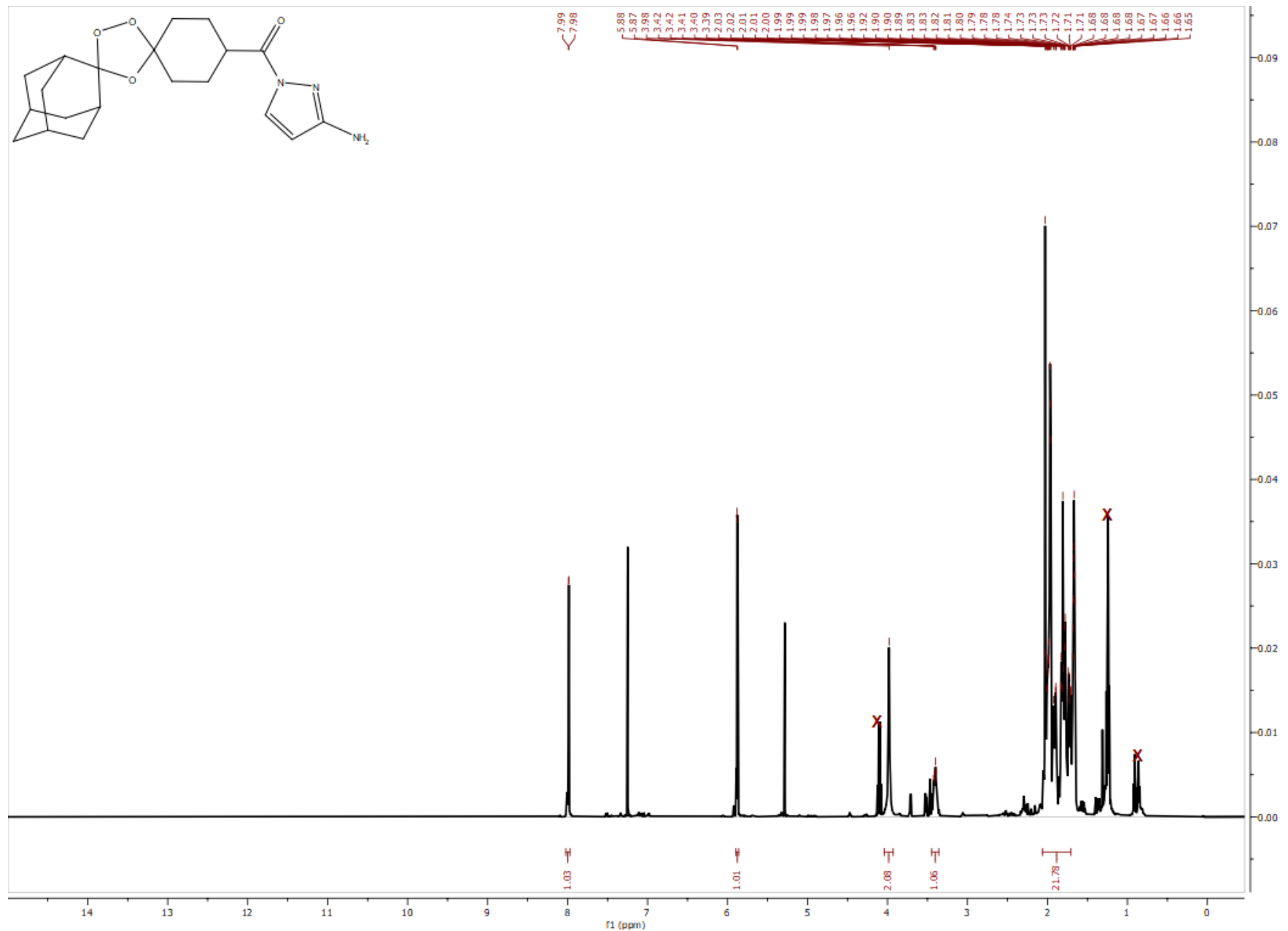


Figure S17. ^1H NMR spectrum (500 MHz) of **OZ2** in CDCl_3 .

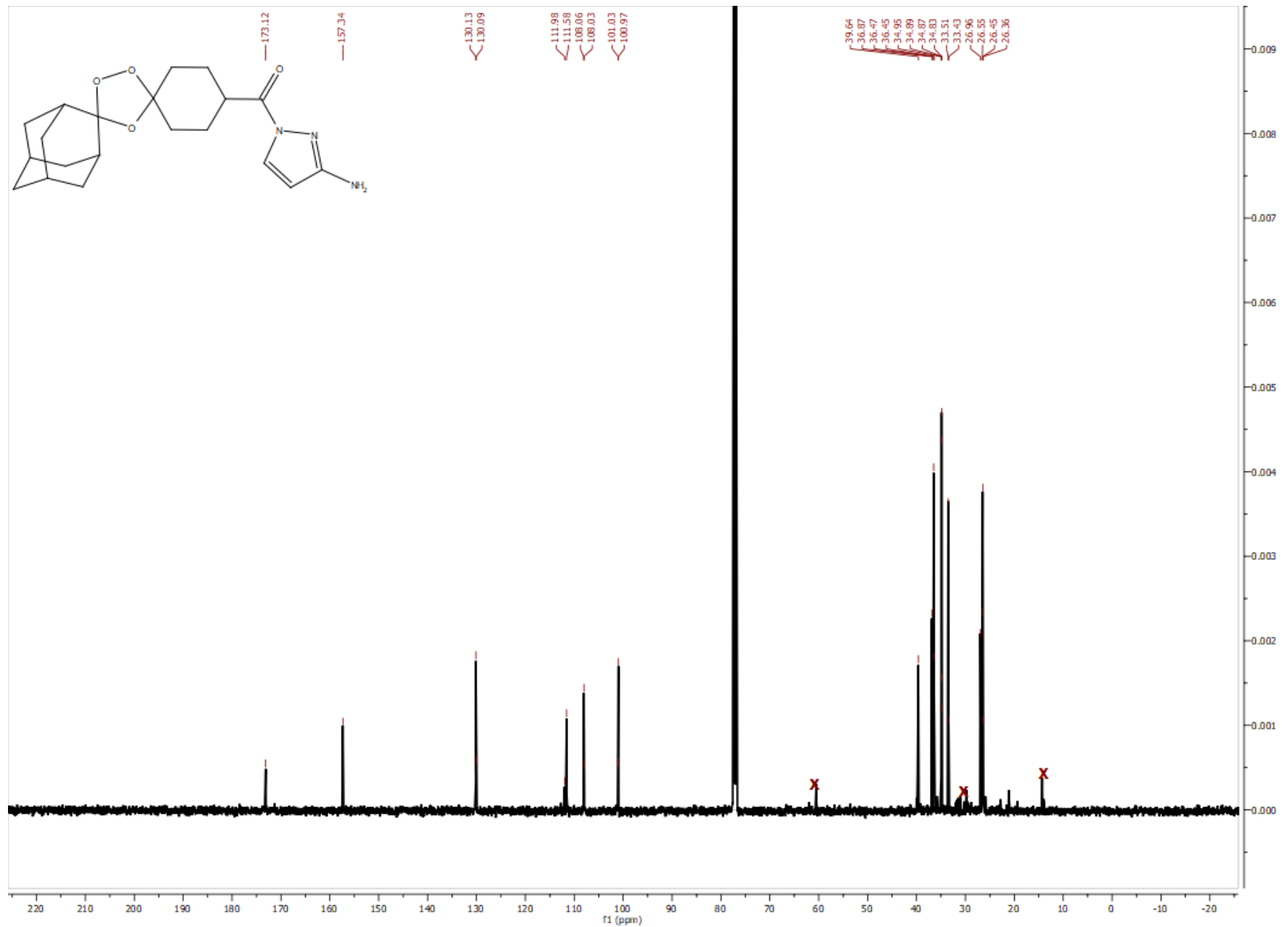


Figure S18. $^{13}\text{C}\{\text{H}\}$ NMR spectrum (126 MHz) of **OZ2** in CDCl_3 .

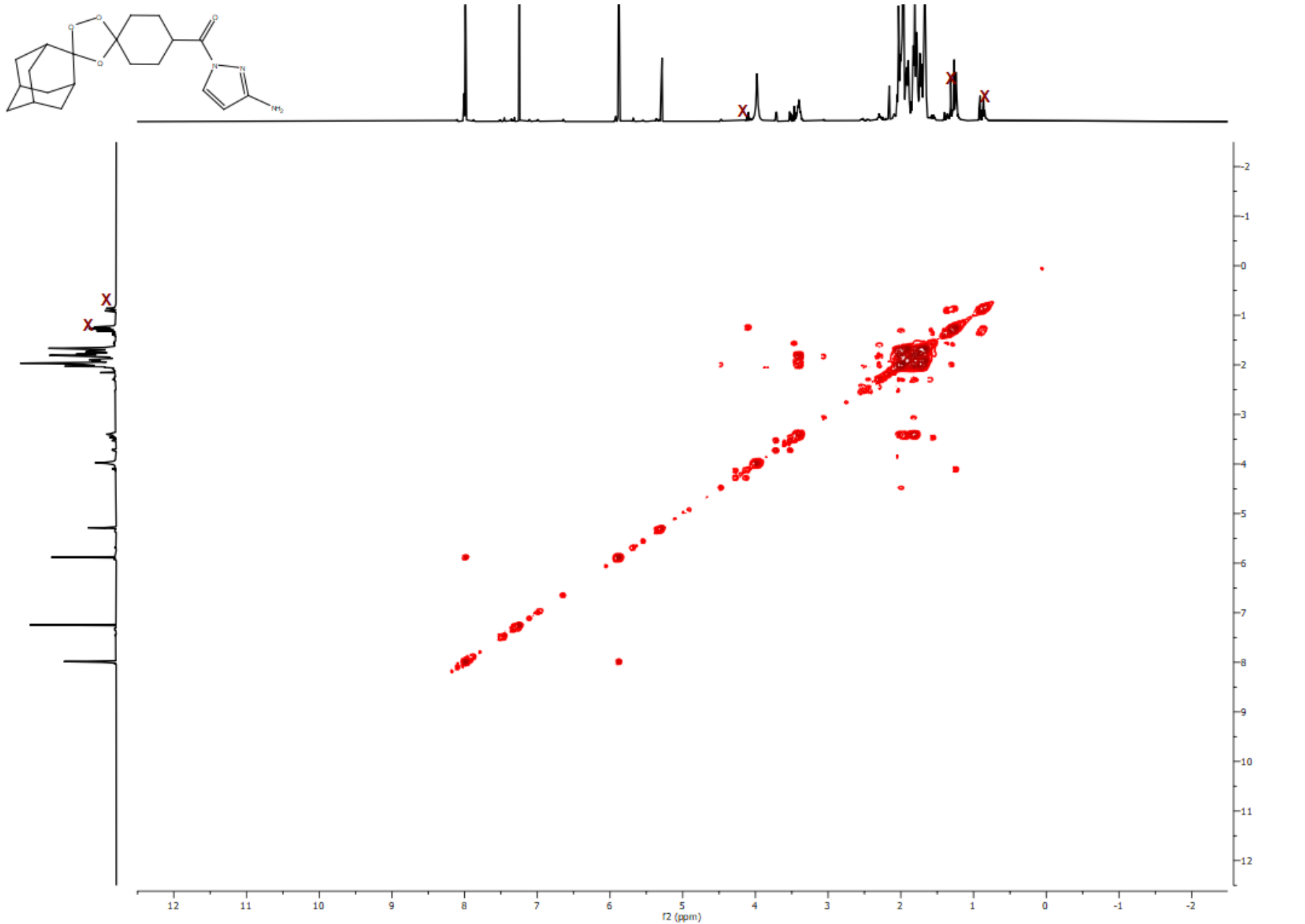


Figure S19. COSY spectrum (500 MHz) of **OZ2** in CDCl_3 .

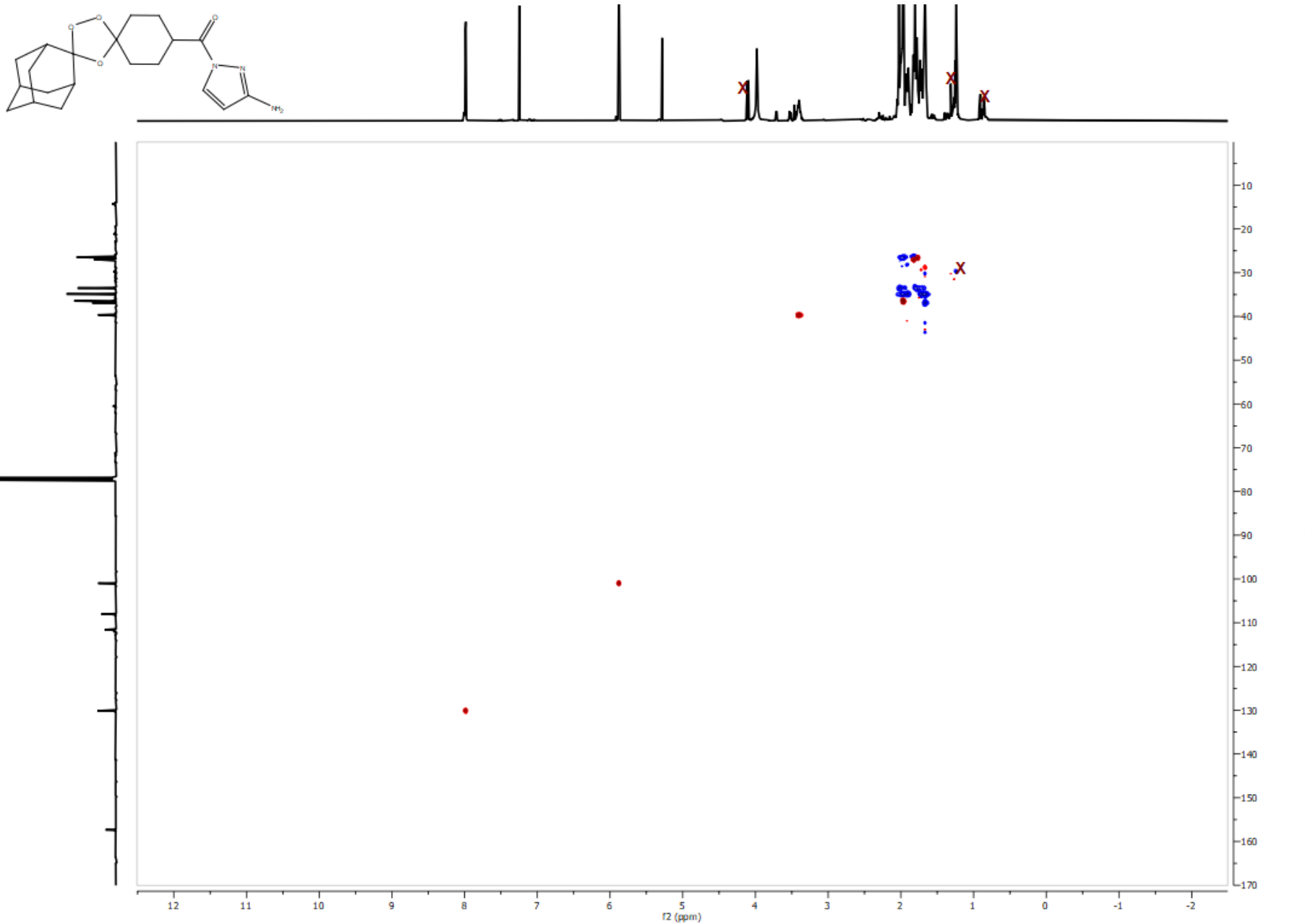


Figure S20. HSQC spectrum (500 MHz) of **OZ2** in CDCl_3 .

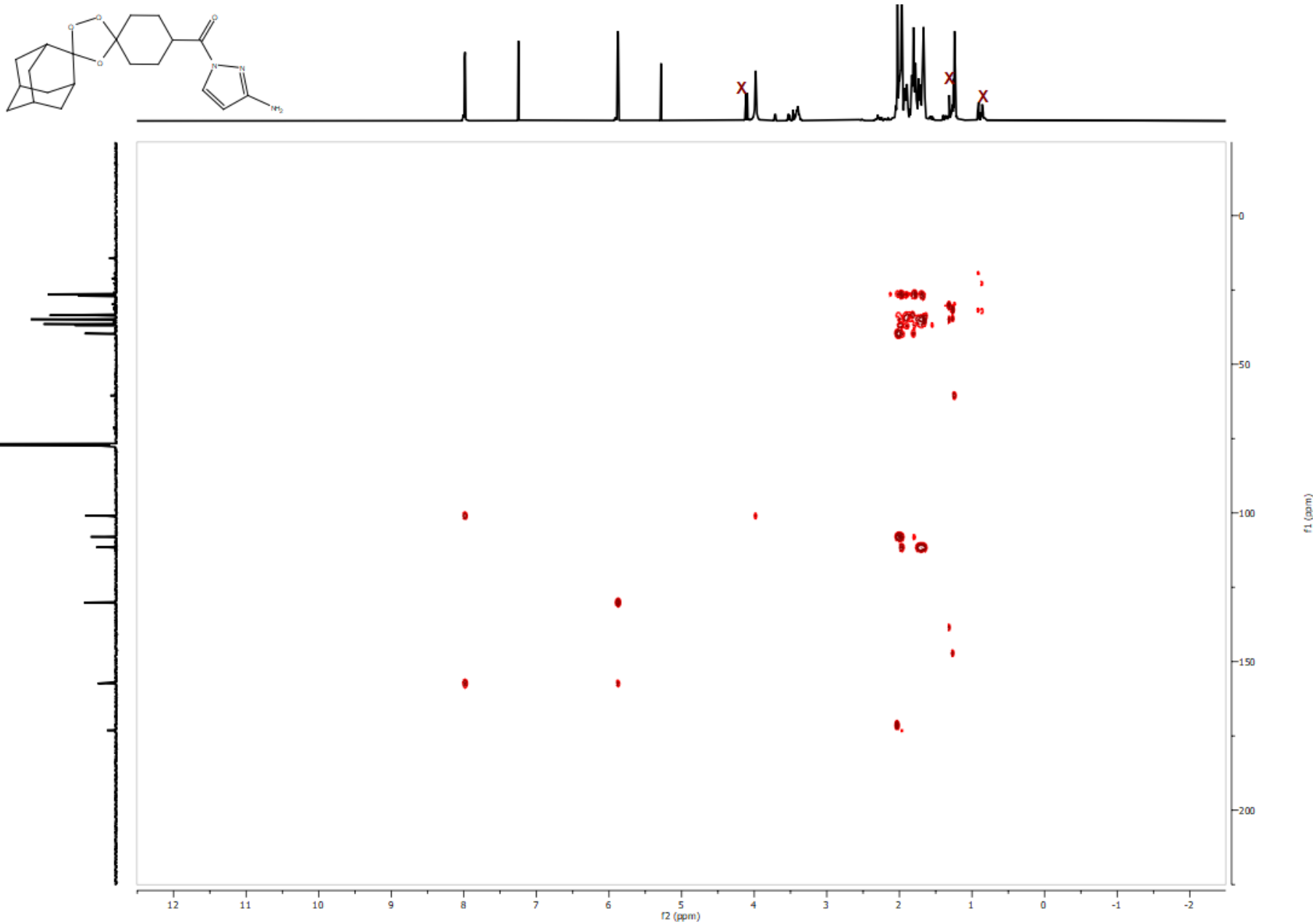


Figure S21. HMBC spectrum (500 MHz) of **OZ2** in CDCl_3 .

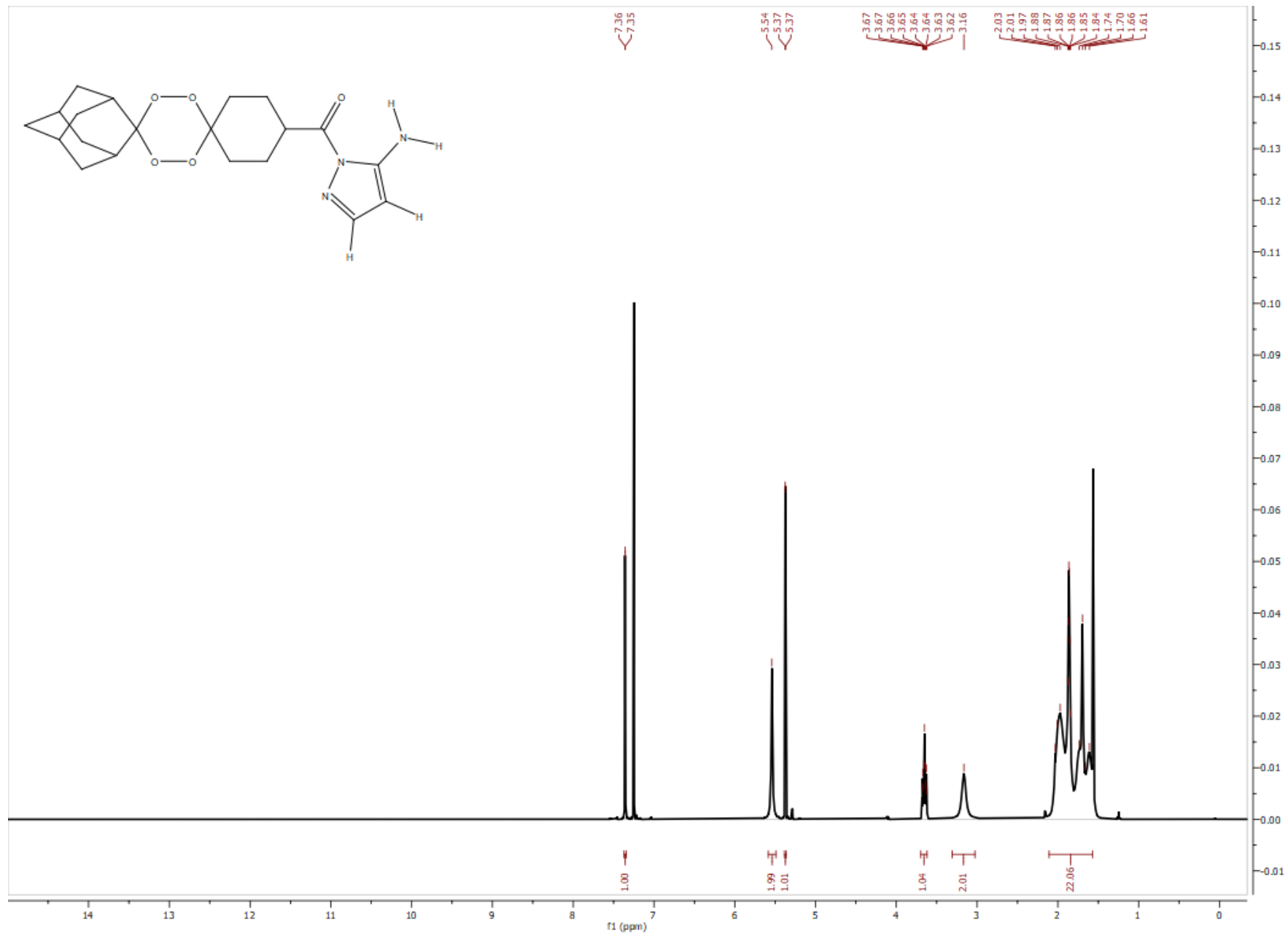


Figure S22. ^1H NMR spectrum (500 MHz) of **T1** in CDCl_3 .

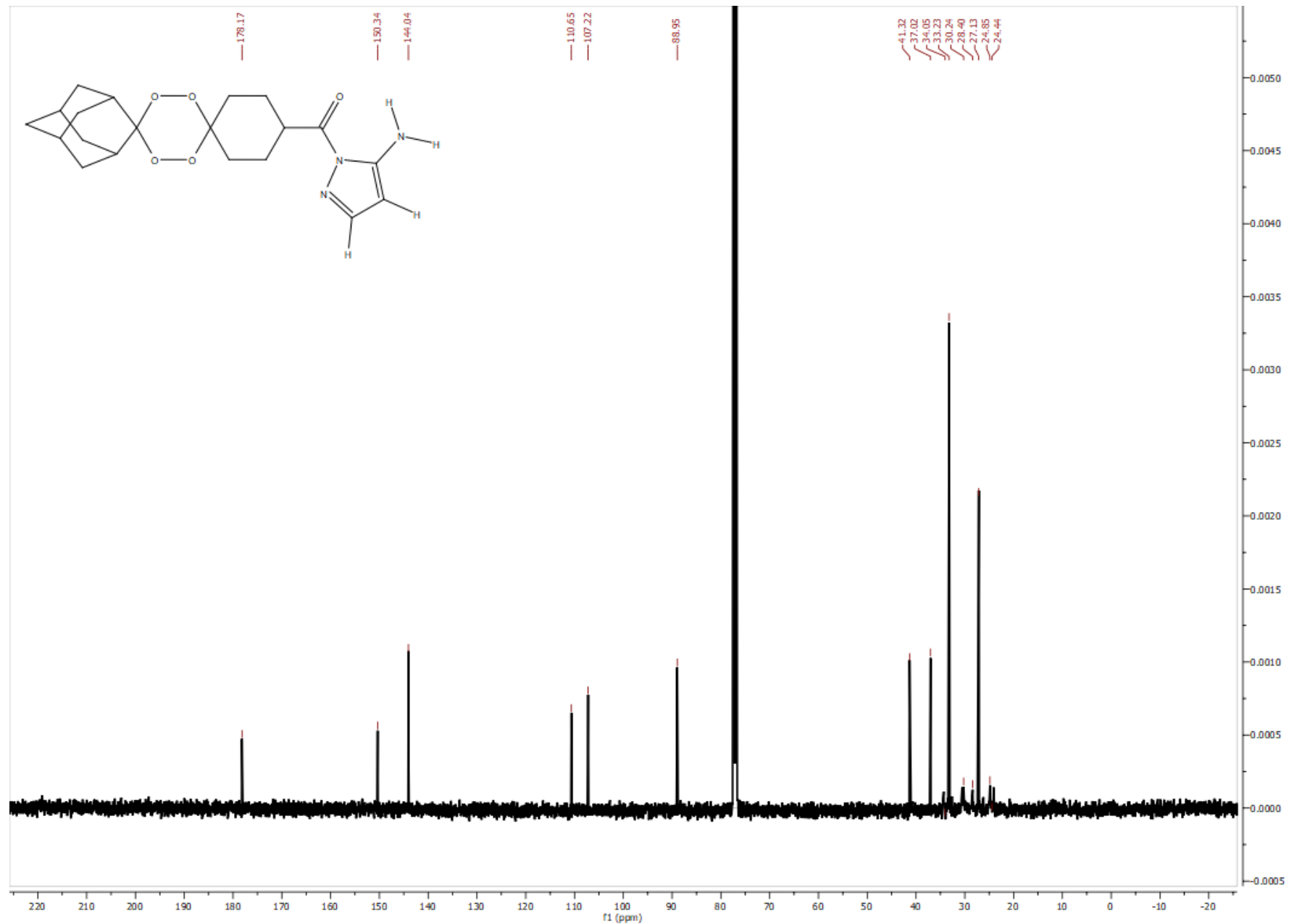


Figure S23. $^{13}\text{C}\{^1\text{H}\}$ NMR spectrum (126 MHz) of **T1** in CDCl_3 .

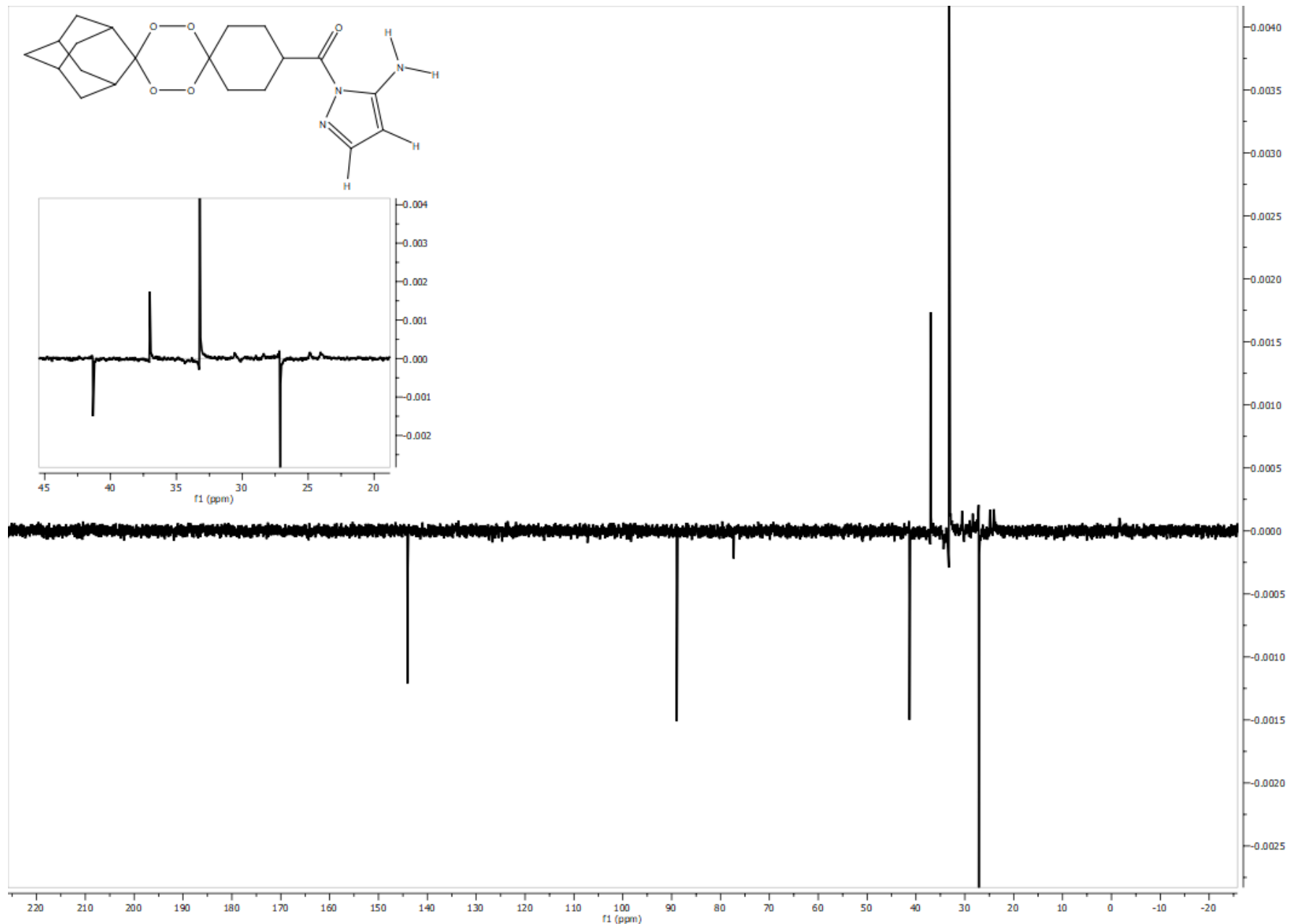


Figure S24. $^{13}\text{C}\{^1\text{H}\}$ DEPT-135 NMR spectrum (126 MHz) of **T1** in CDCl_3 .

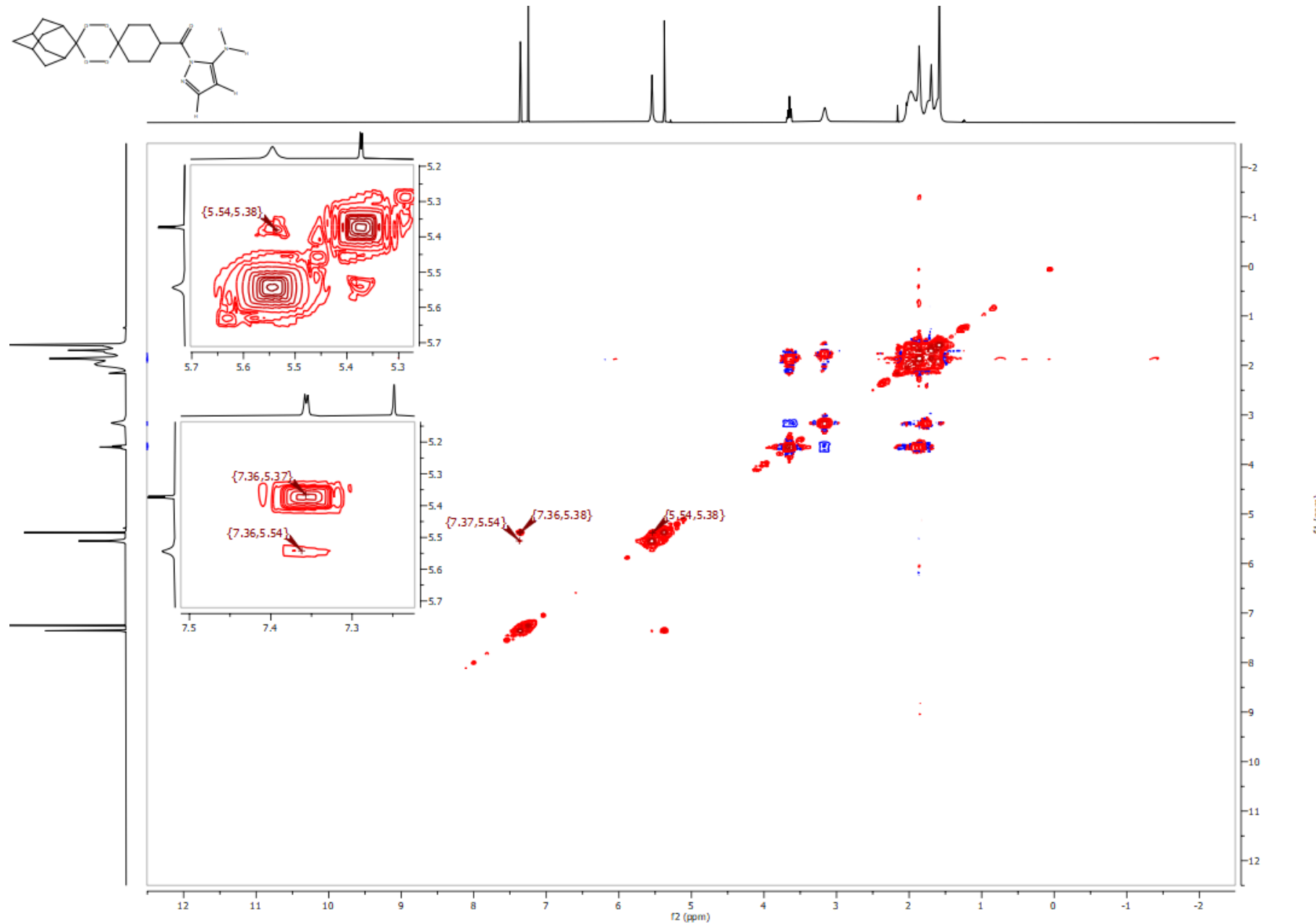


Figure S25. COSY spectrum (500 MHz) of T1 in CDCl_3 .

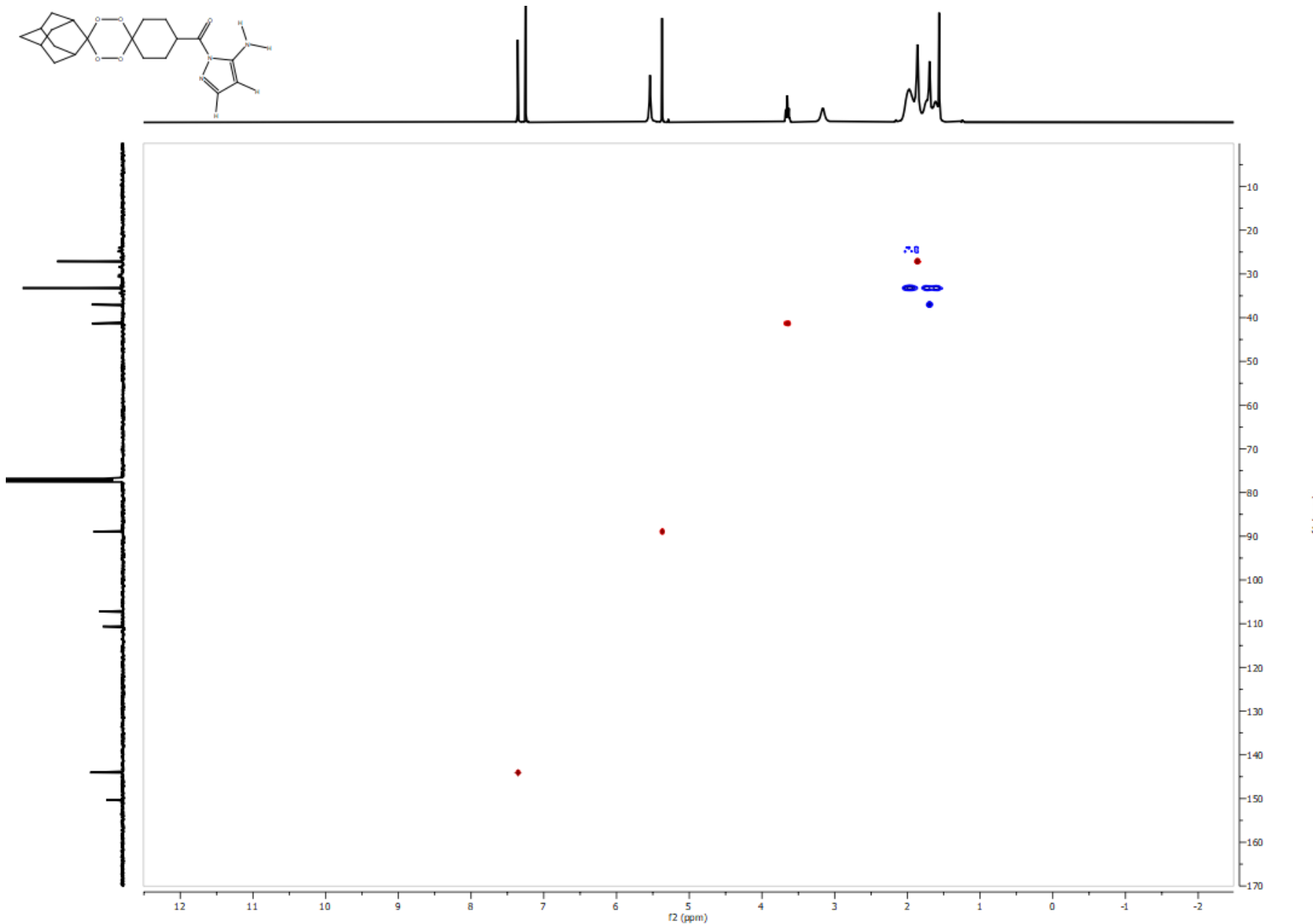


Figure S26. HSQC spectrum (500 MHz) of T1 in CDCl_3 .

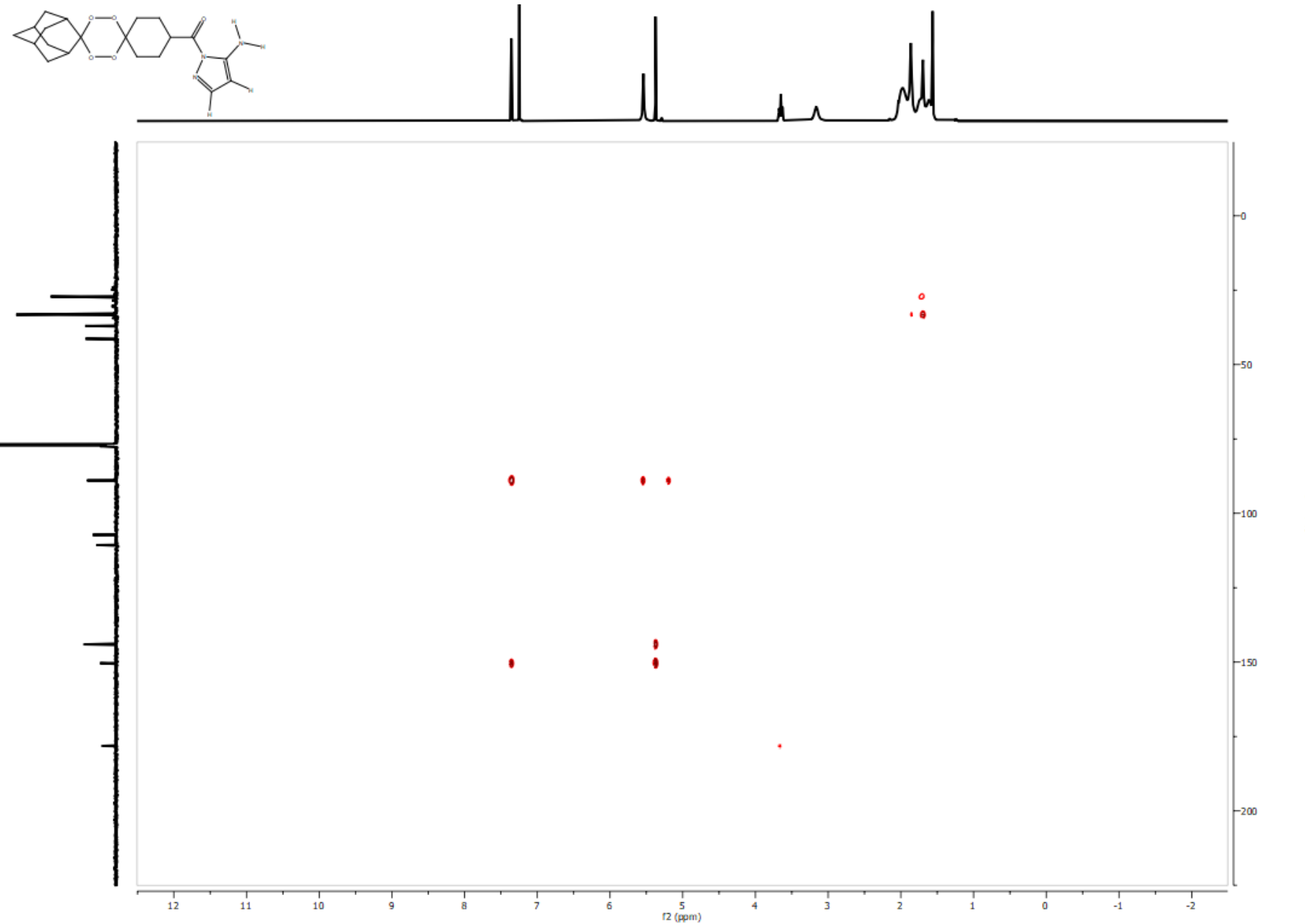


Figure S27. HMBC spectrum (500 MHz) of **T1** in CDCl_3 .

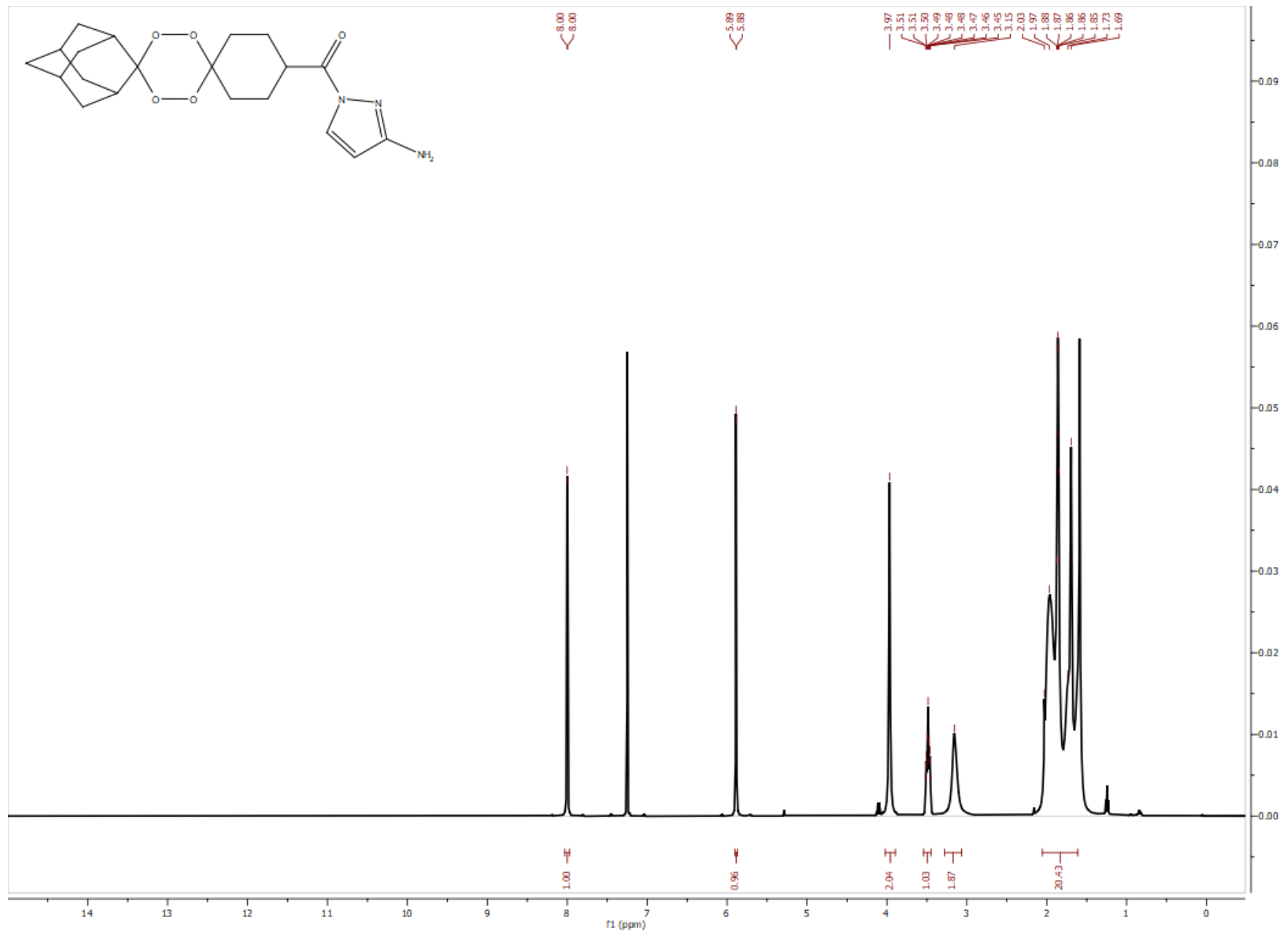


Figure S28. ^1H NMR spectrum (500 MHz) of T2 in CDCl_3 .

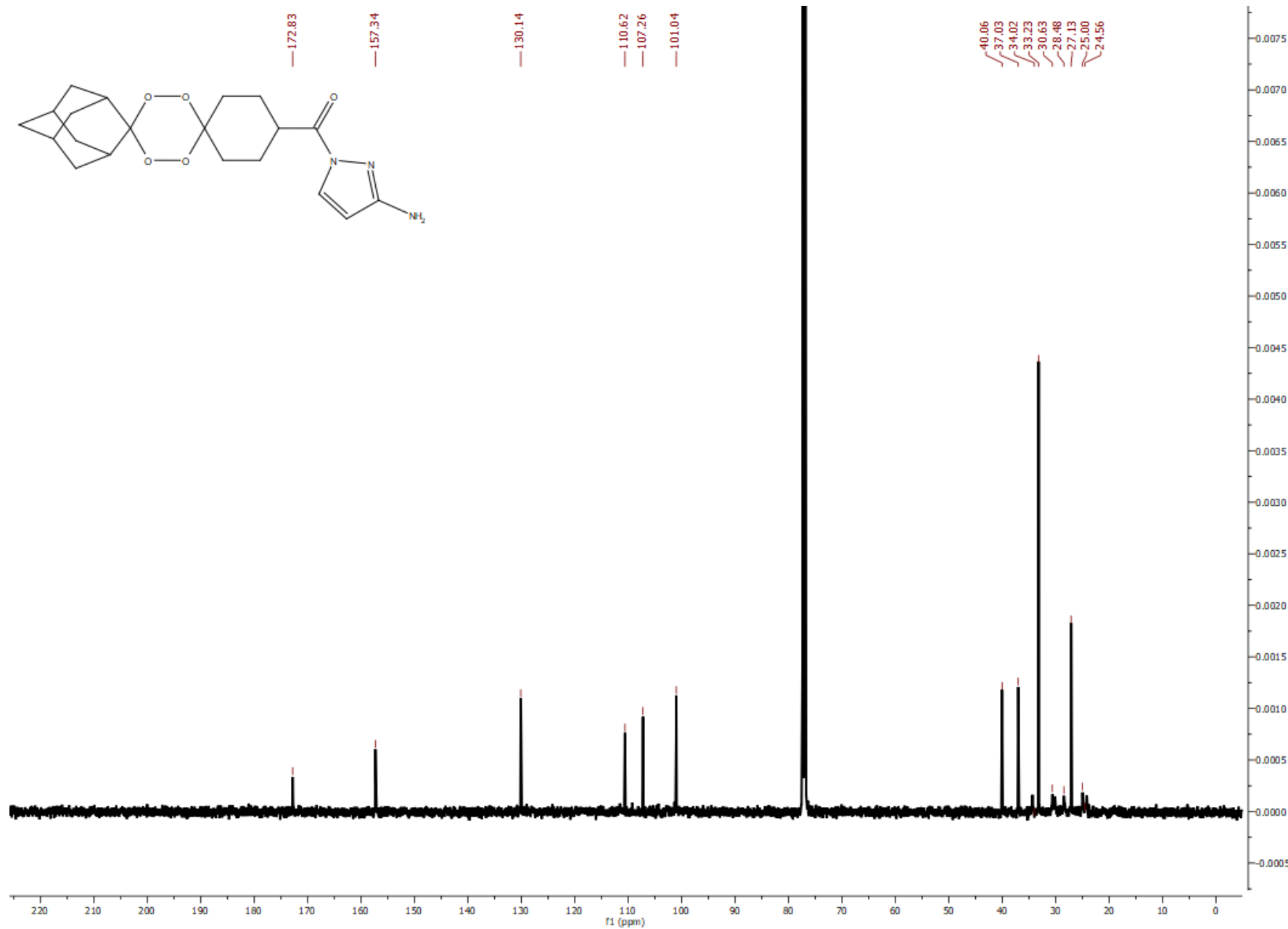


Figure S29. $^{13}\text{C}\{^1\text{H}\}$ NMR spectrum (126 MHz) of **T2** in CDCl_3 .

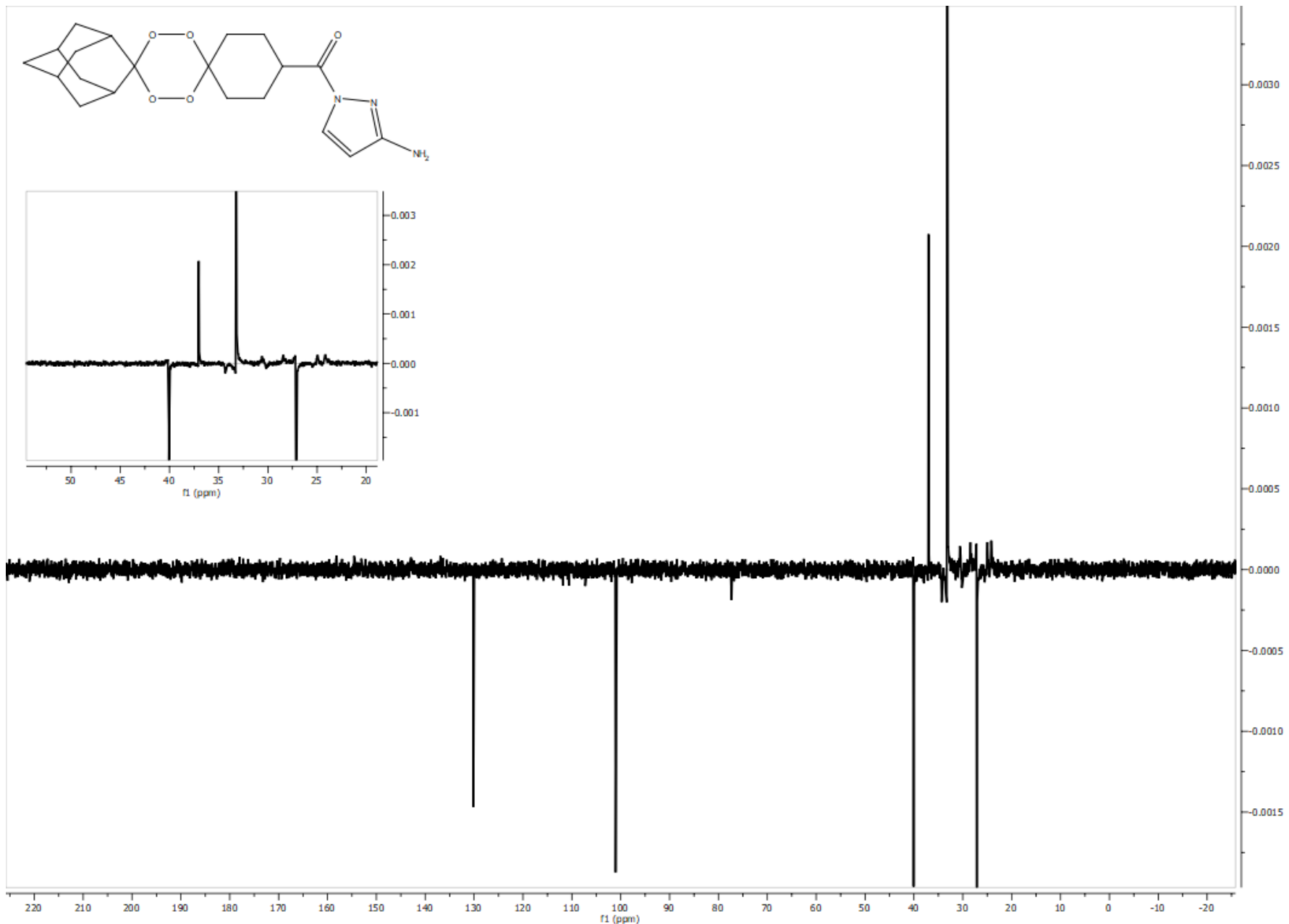


Figure S30. $^{13}\text{C}\{^1\text{H}\}$ DEPT-135 NMR spectrum (126 MHz) of **T2** in CDCl_3 .

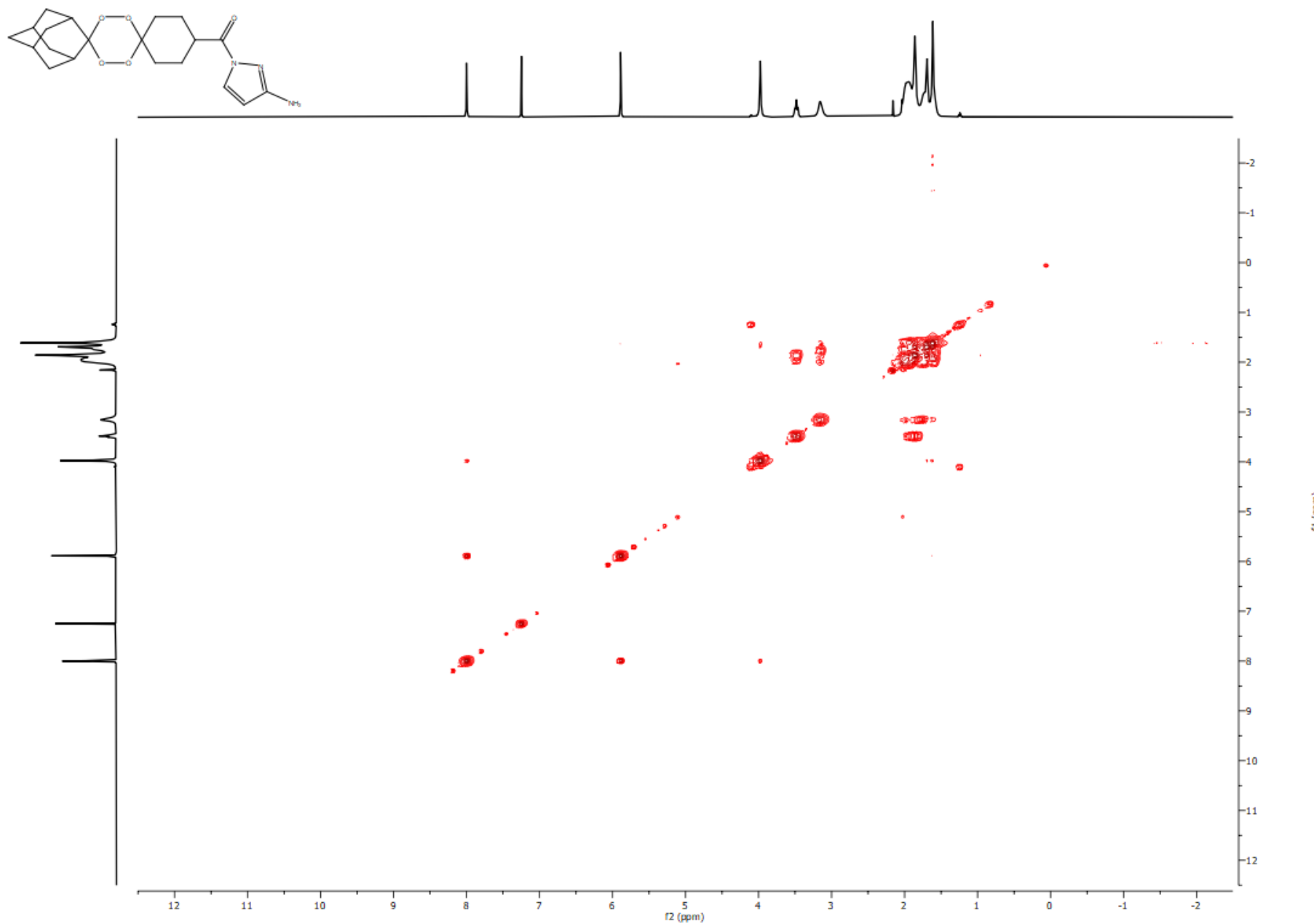


Figure S31. COSY spectrum (500 MHz) of **T2** in CDCl_3 .

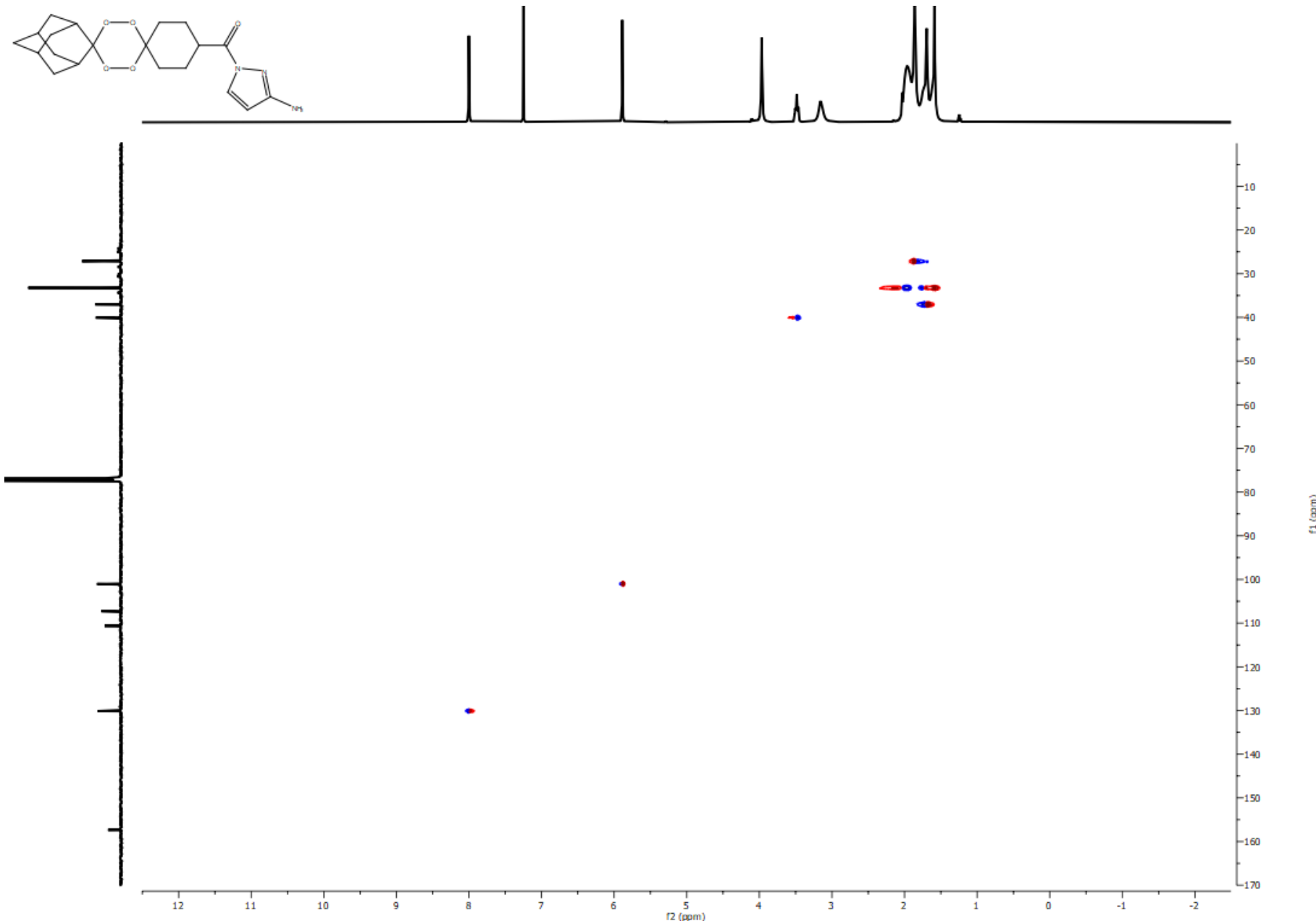


Figure S32. HSQC spectrum (500 MHz) of T2 in CDCl_3 .

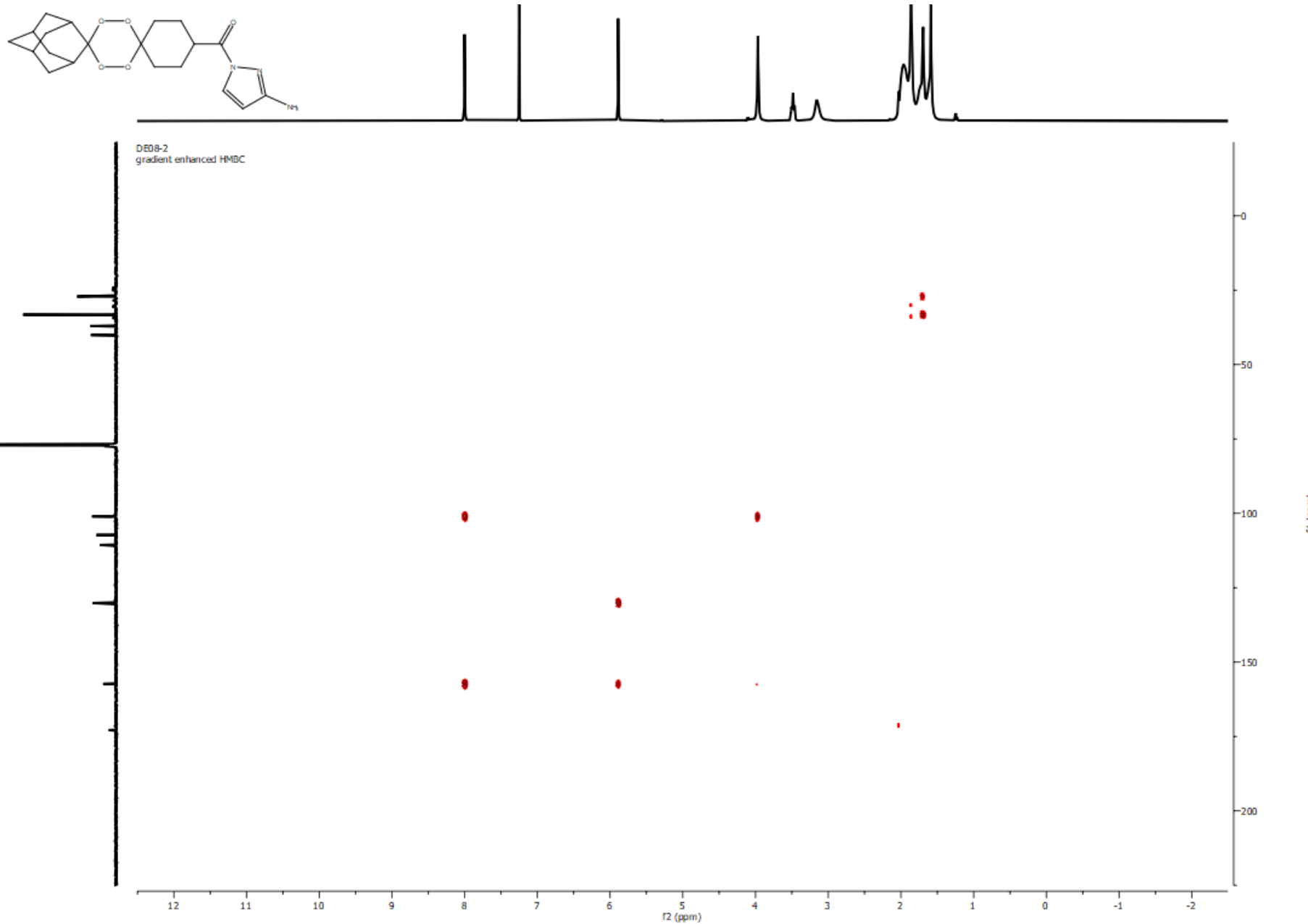


Figure S33. HMBC spectrum (500 MHz) of **T2** in CDCl₃.

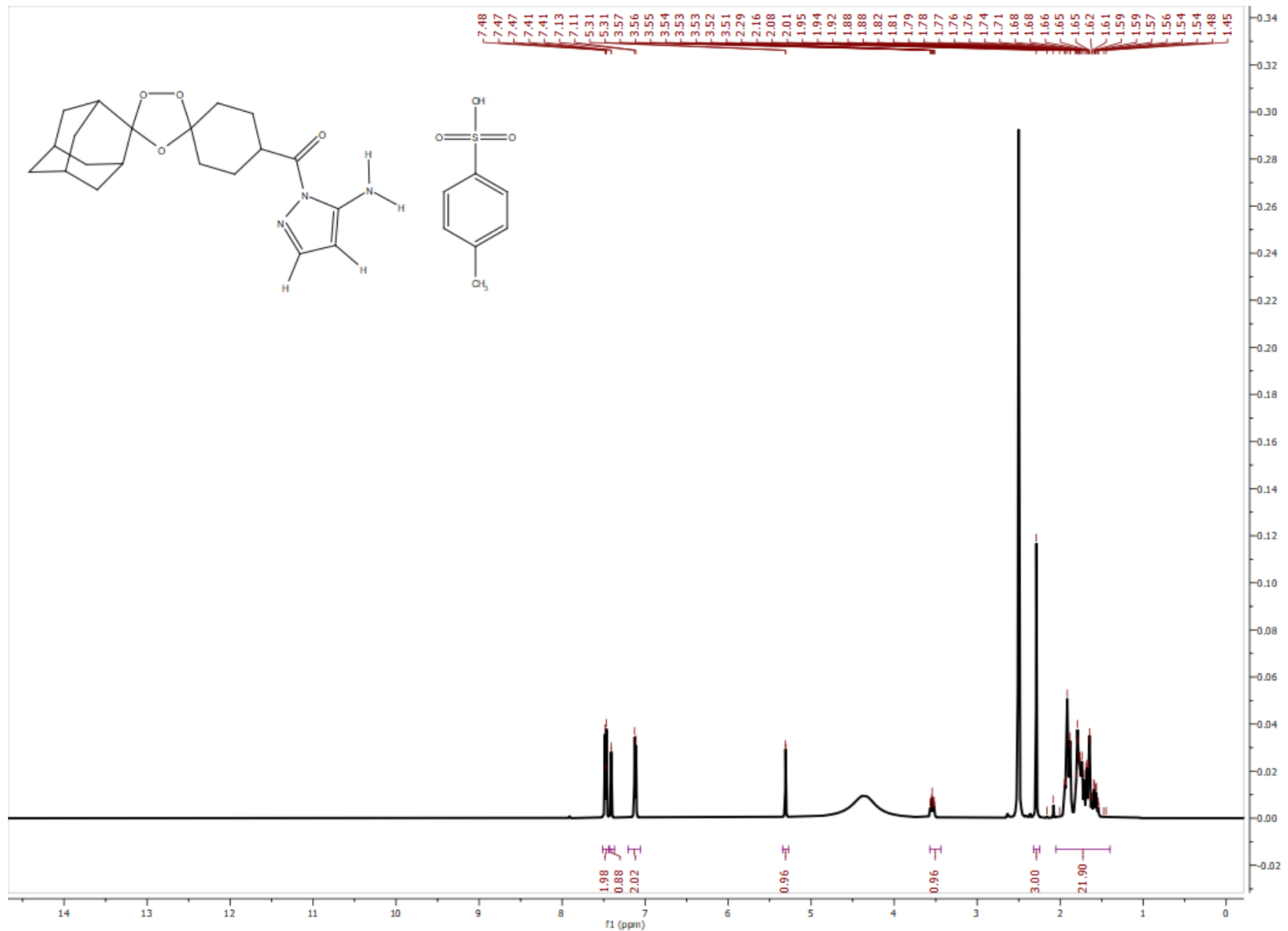


Figure S34. ^1H NMR spectrum (500 MHz) of OZ1•TsOH in $\text{DMSO}-d_6$.

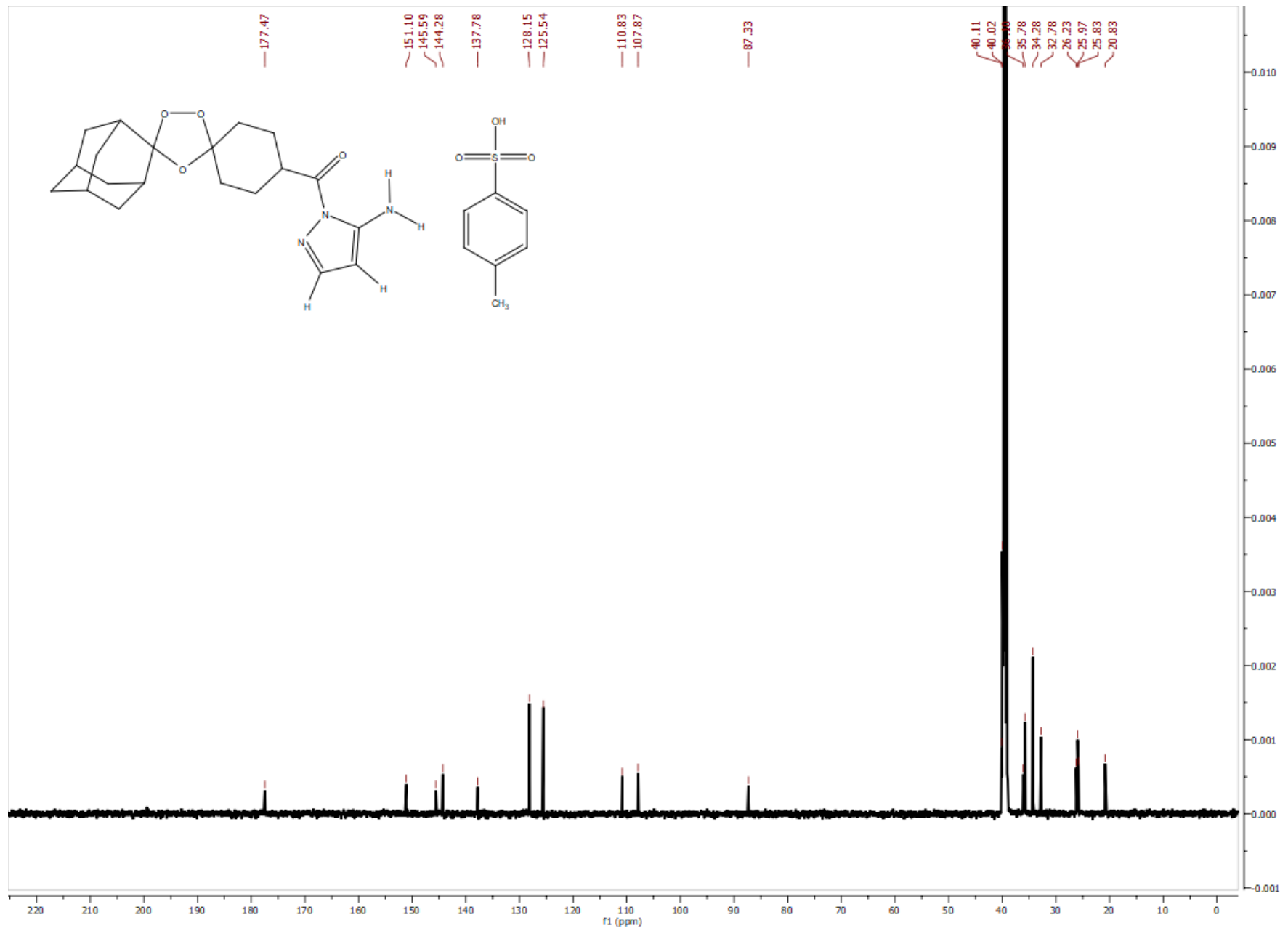


Figure S35. $^{13}\text{C}\{^1\text{H}\}$ NMR spectrum (126 MHz) of **OZ1•TsOH** in $\text{DMSO}-d_6$.

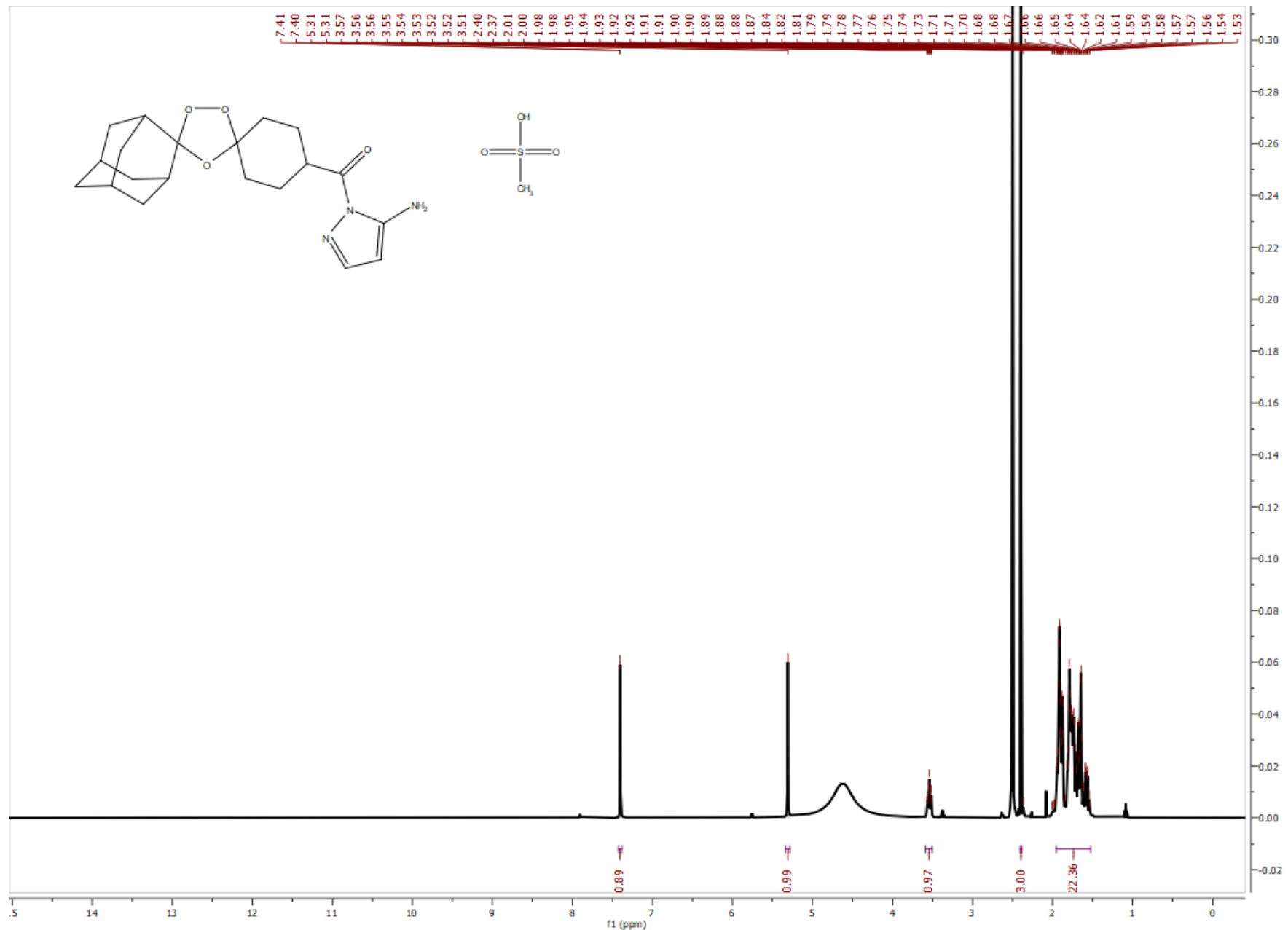


Figure S36. ^1H NMR spectrum (500 MHz) of OZ1•MsOH in $\text{DMSO}-d_6$.

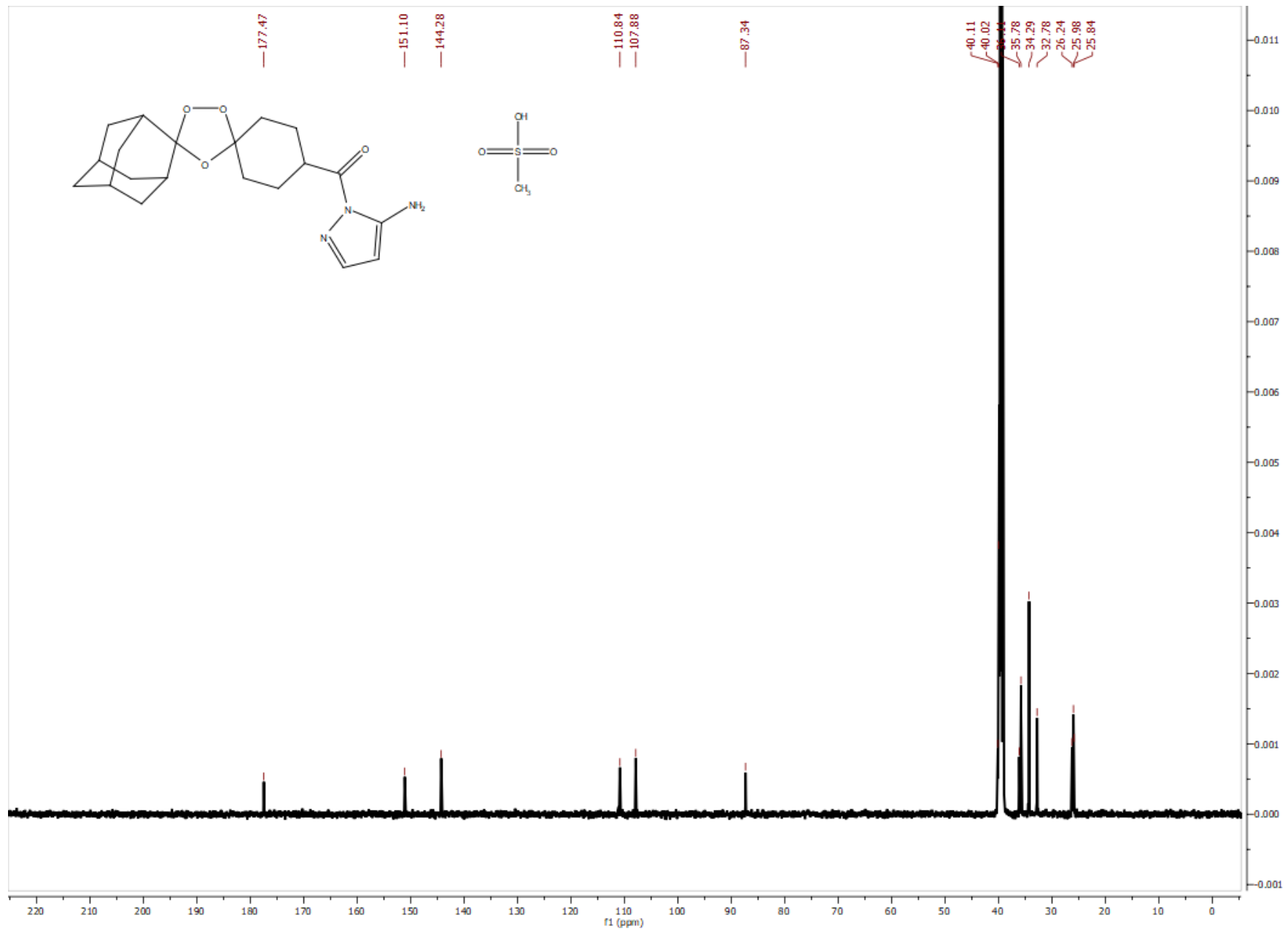


Figure S37. $^{13}\text{C}\{^1\text{H}\}$ NMR spectrum (126 MHz) of **OZ1•MsOH** in $\text{DMSO}-d_6$.

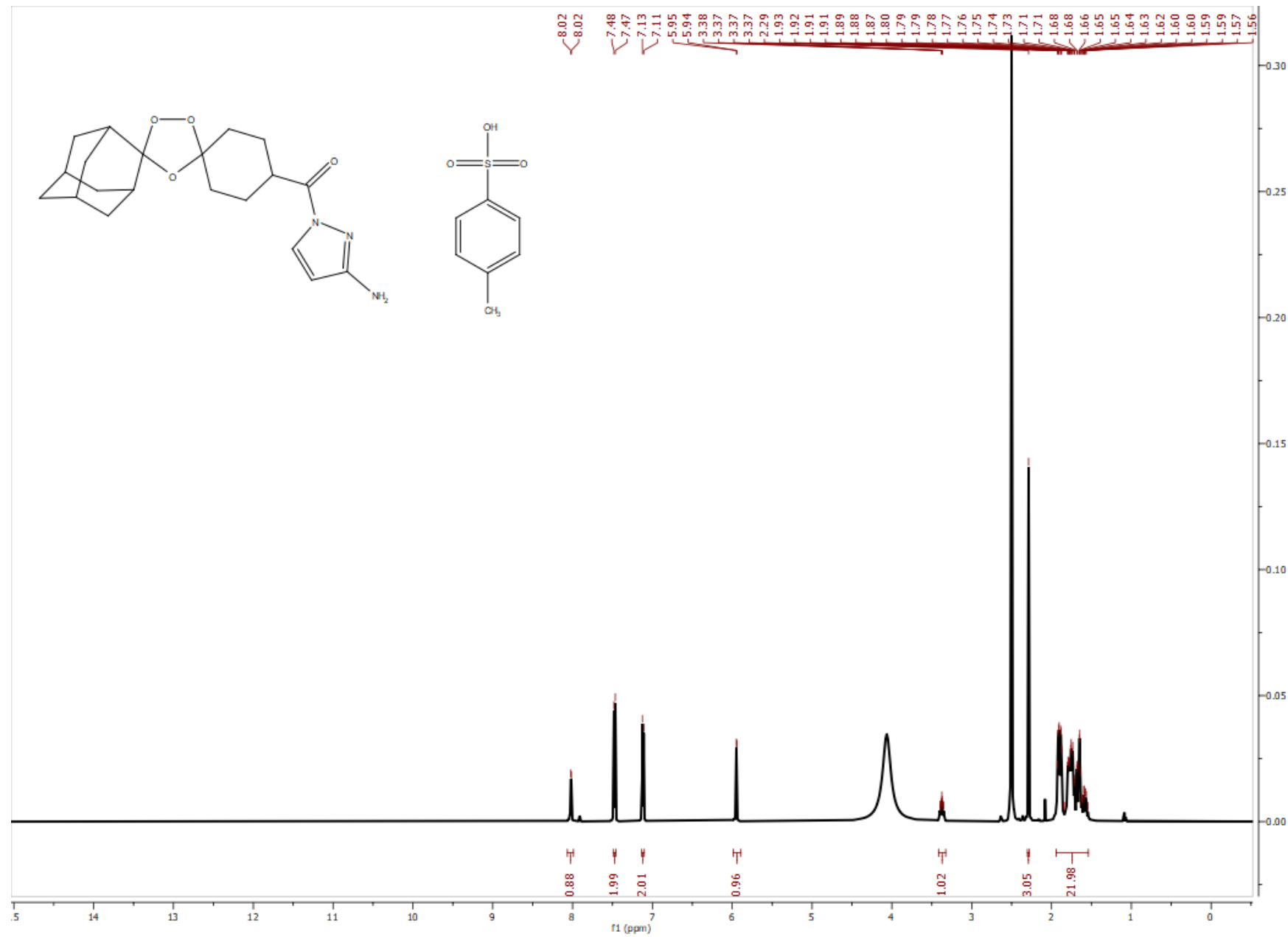


Figure S38. ^1H NMR spectrum (500 MHz) of OZ2•TsOH in $\text{DMSO}-d_6$.

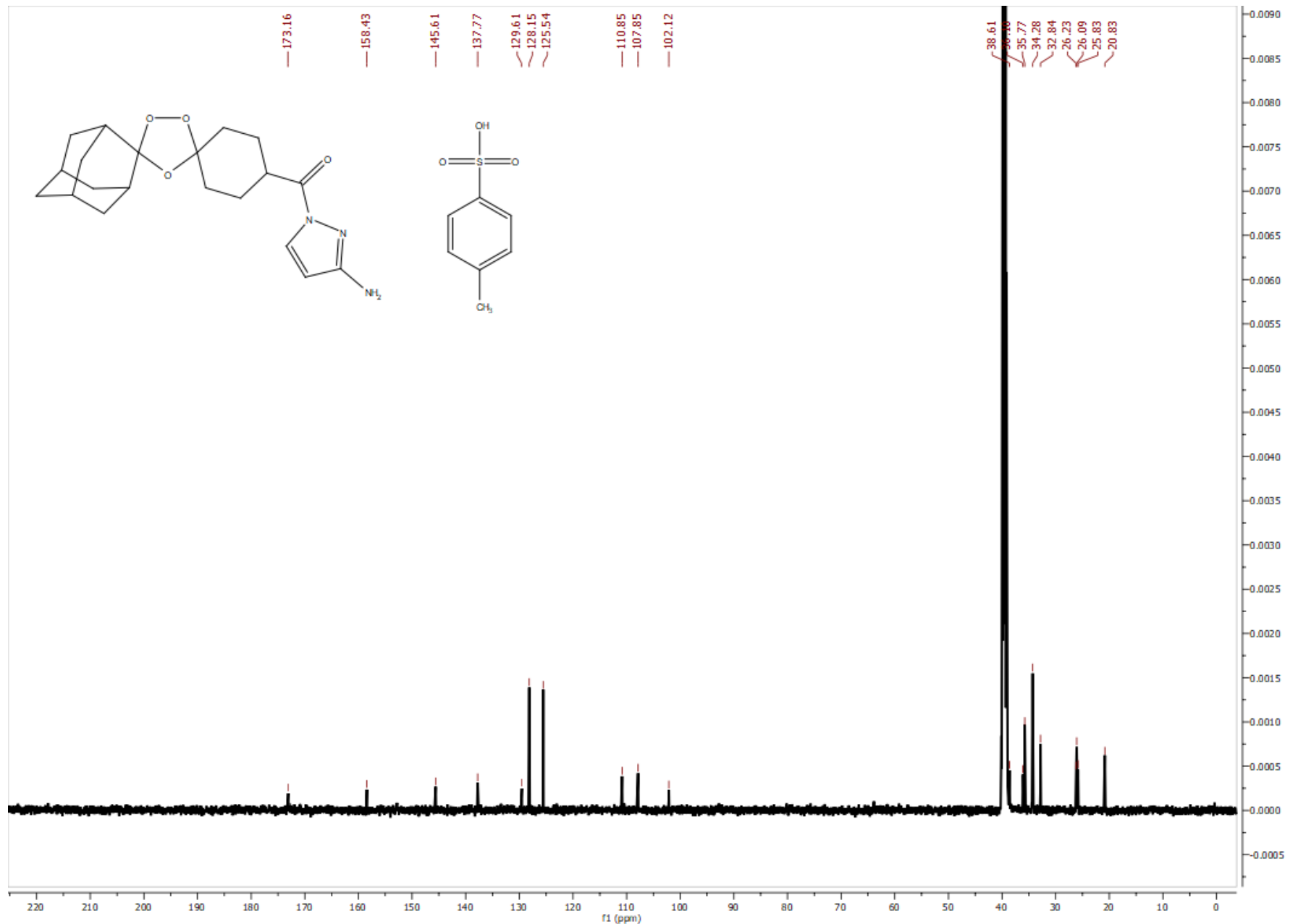


Figure S39. $^{13}\text{C}\{^1\text{H}\}$ NMR spectrum (126 MHz) of **OZ2·TsOH** in $\text{DMSO}-d_6$.

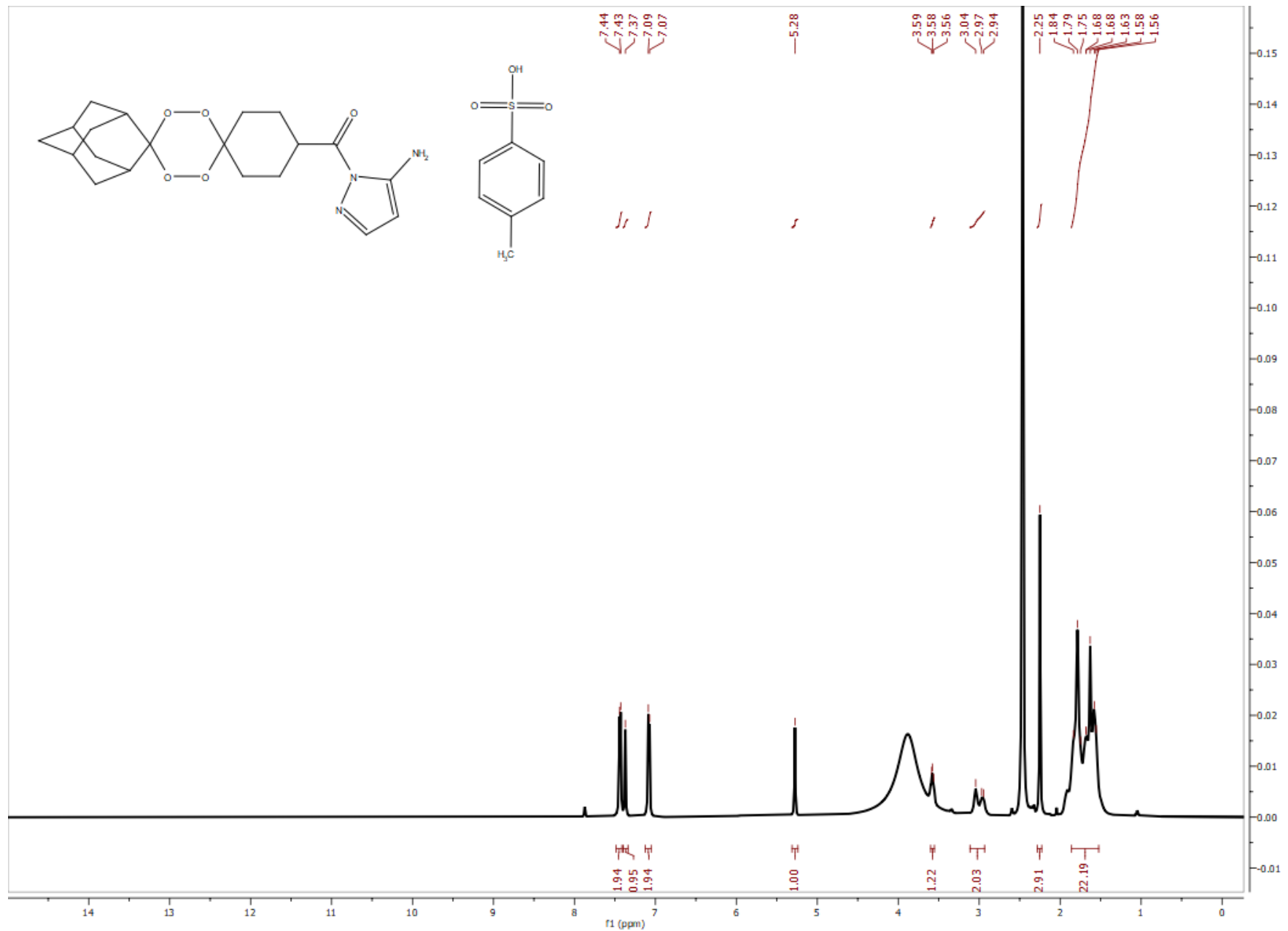


Figure S40. ^1H NMR spectrum (500 MHz) of **T1**•TsOH in DMSO-*d*₆.

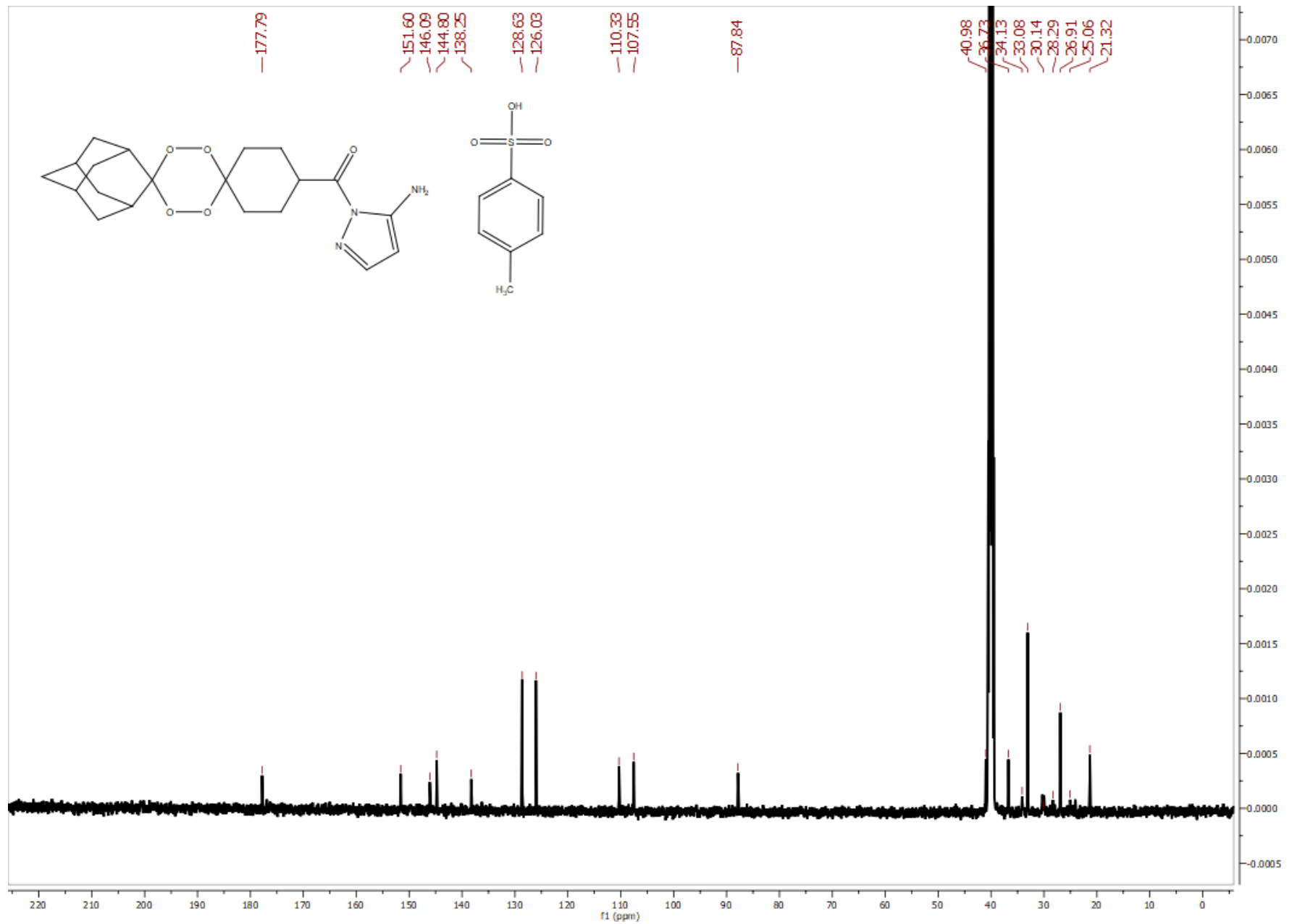


Figure S41. $^{13}\text{C}\{\text{H}\}$ NMR spectrum (126 MHz) of **T1**·TsOH in $\text{DMSO}-d_6$.

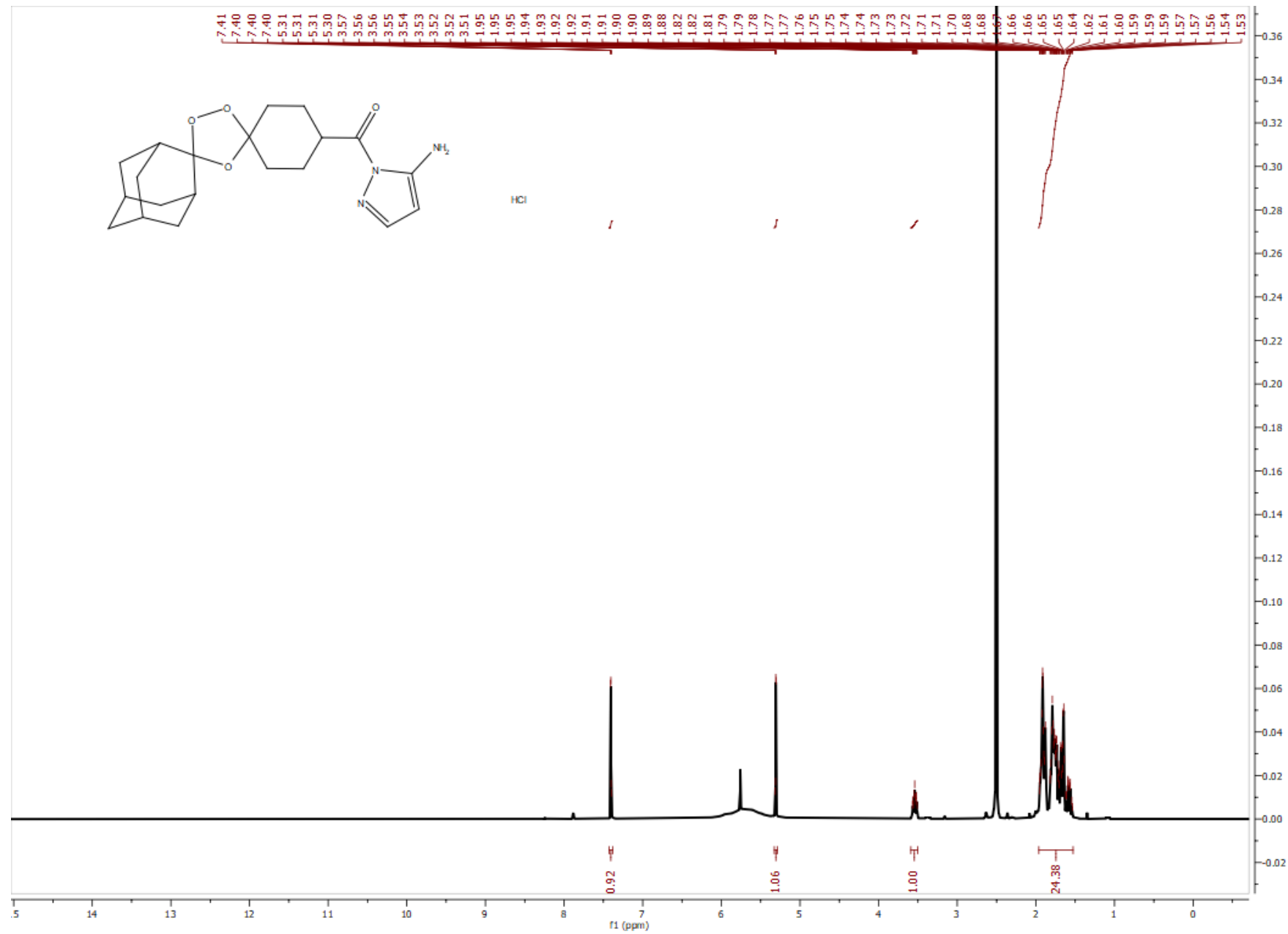


Figure S42. ^1H NMR spectrum (500 MHz) of OZ1•HCl in DMSO-*d*₆.

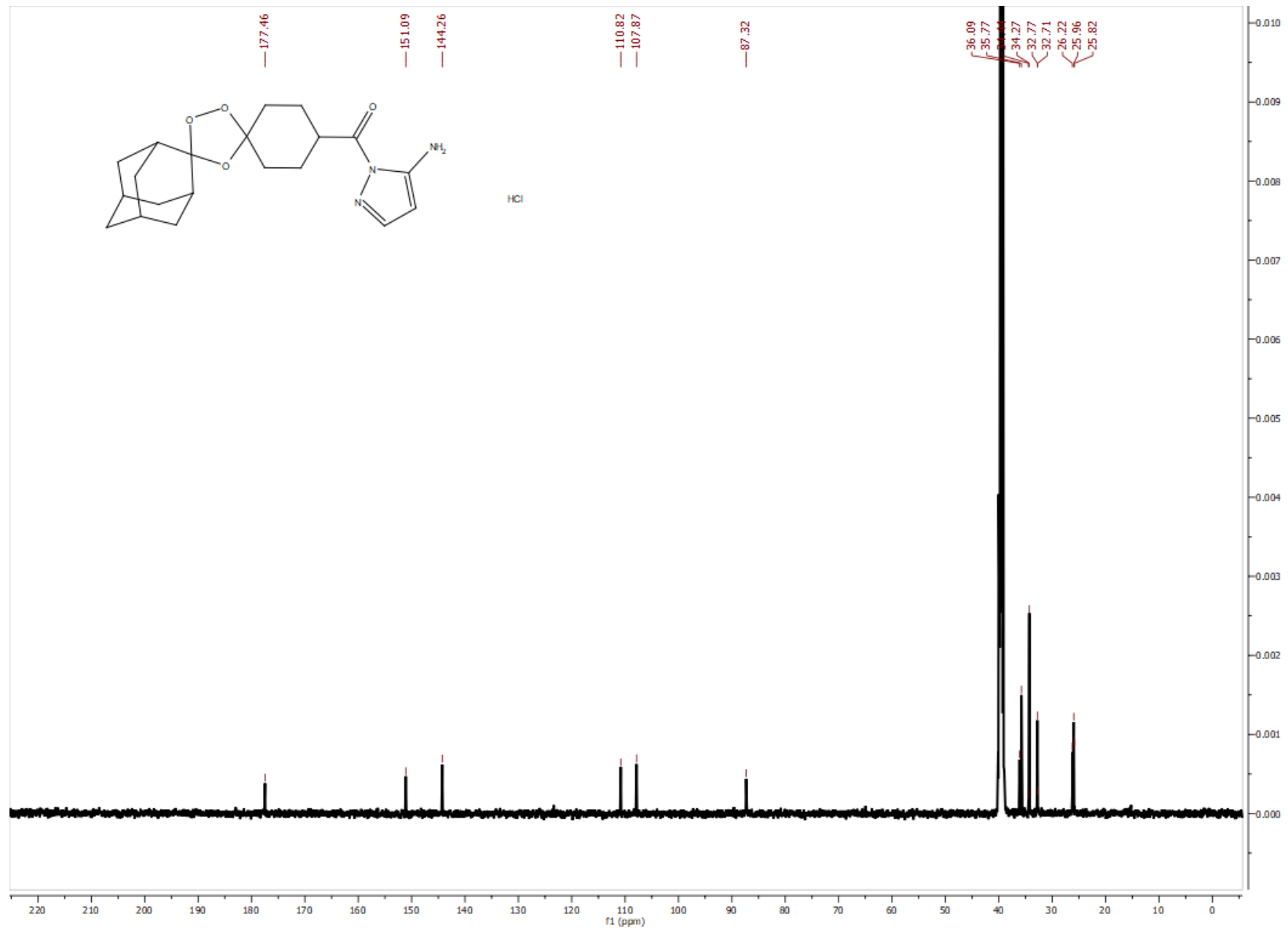


Figure S43. $^{13}\text{C}\{^1\text{H}\}$ NMR spectrum (126 MHz) of **OZ1•HCl** in $\text{DMSO}-d_6$.

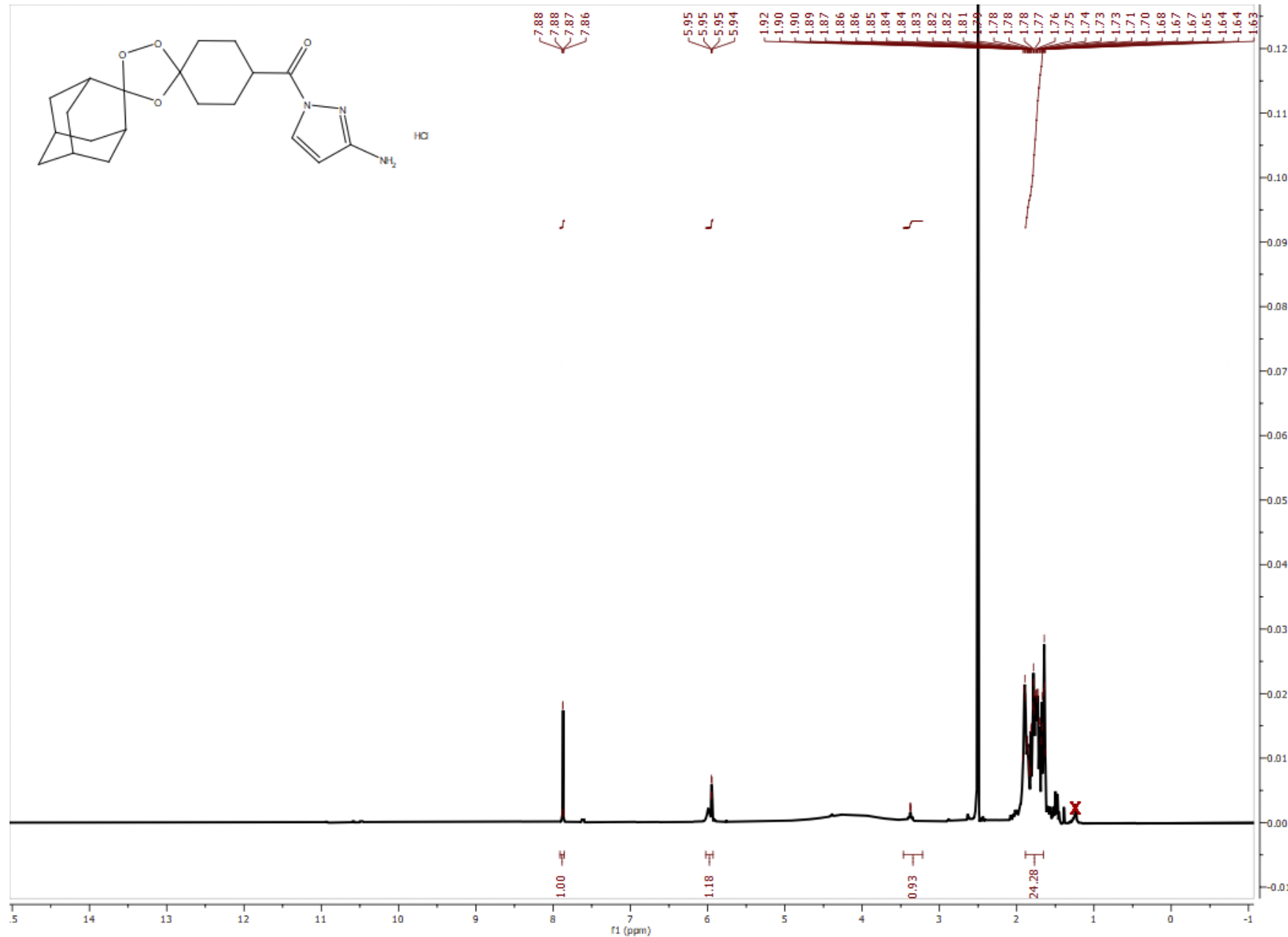


Figure S44. ^1H NMR spectrum (500 MHz) of OZ2•HCl in $\text{DMSO}-d_6$.

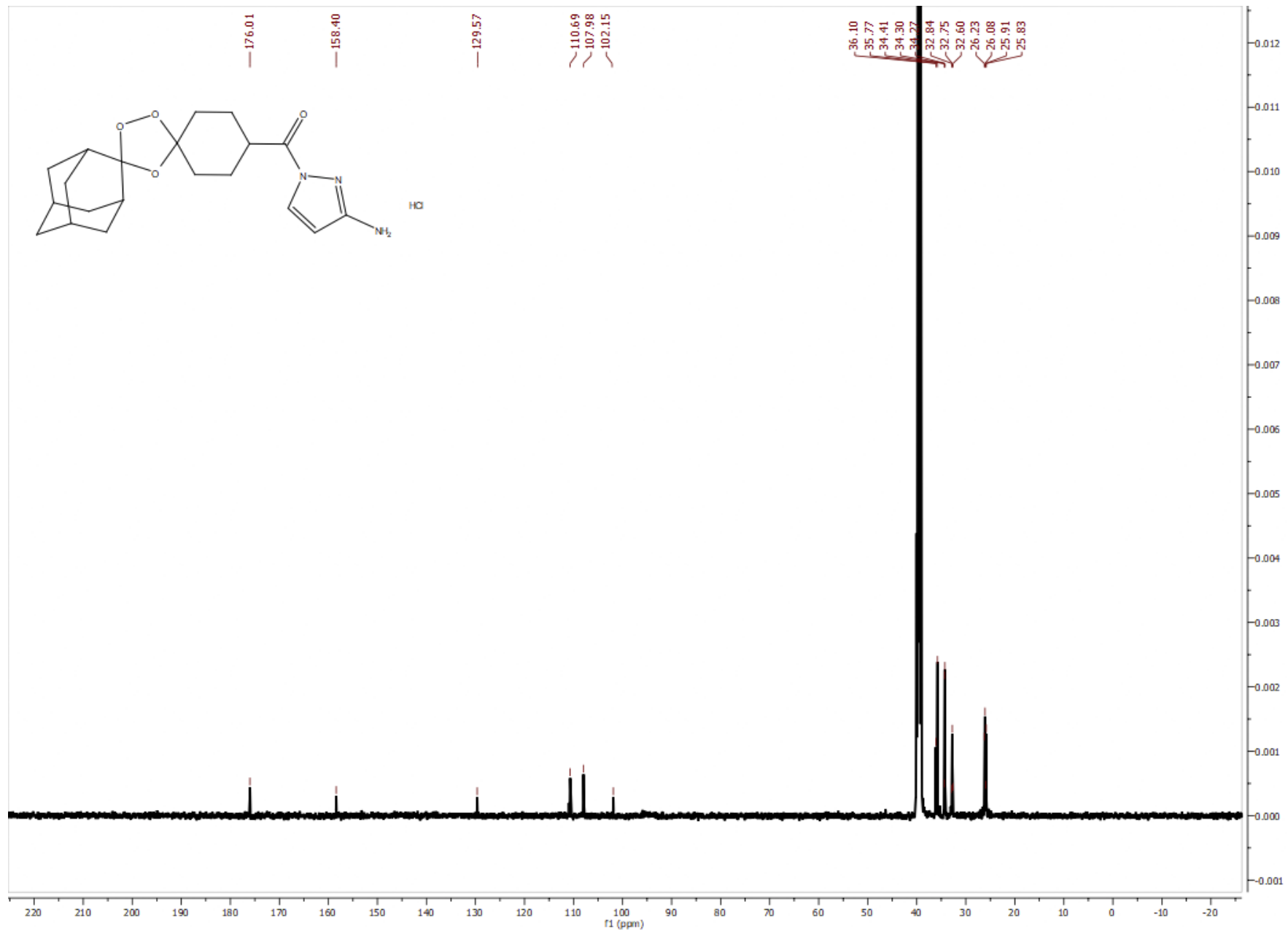
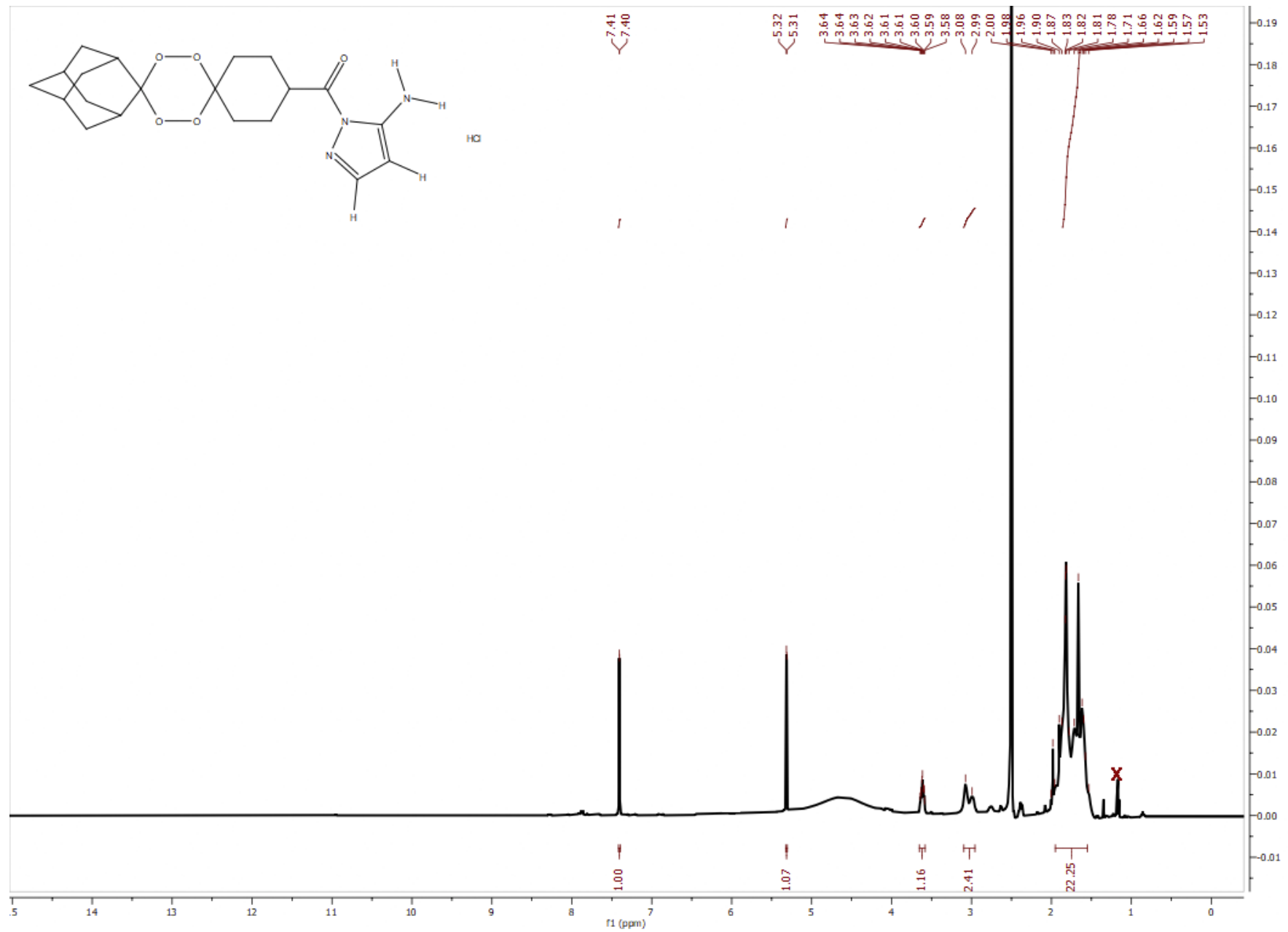


Figure S45. $^{13}\text{C}\{^1\text{H}\}$ NMR spectrum (126 MHz) of **OZ2•HCl** in $\text{DMSO}-d_6$.



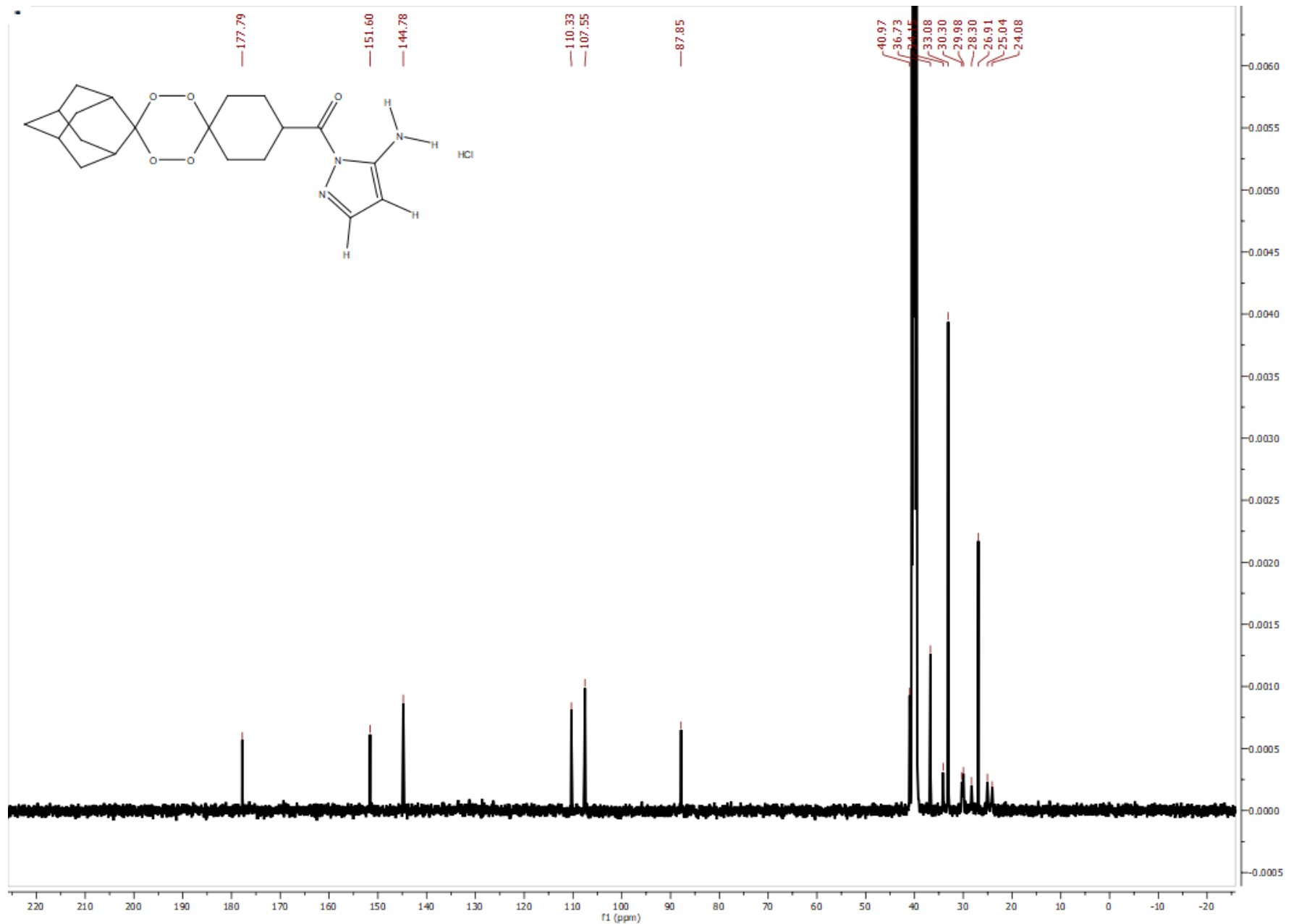


Figure S47. $^{13}\text{C}\{^1\text{H}\}$ NMR spectrum (126 MHz) of **T1•HCl** in $\text{DMSO}-d_6$.

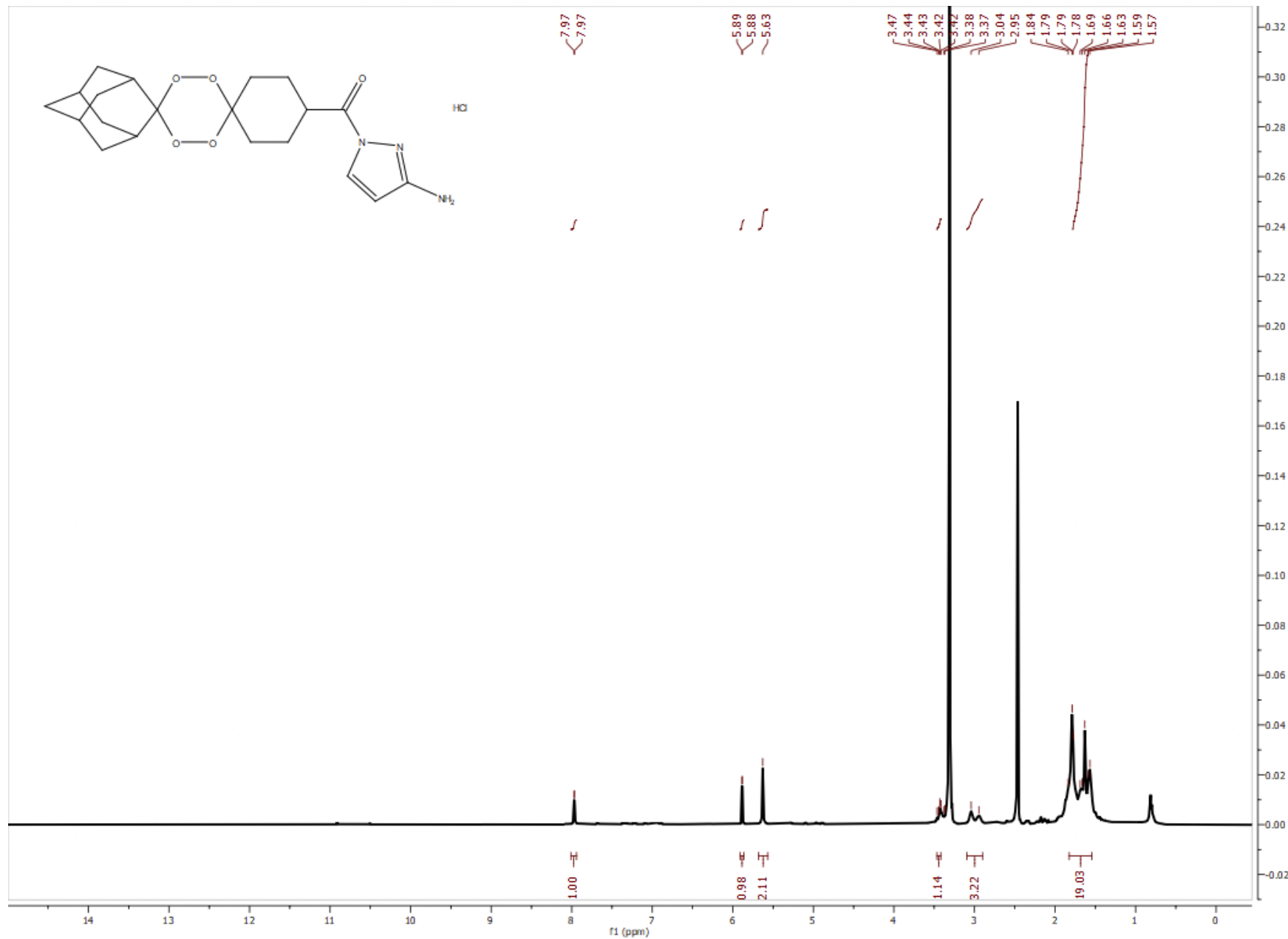


Figure S48. ^1H NMR spectrum (500 MHz) of **T2**•HCl in $\text{DMSO}-d_6$.

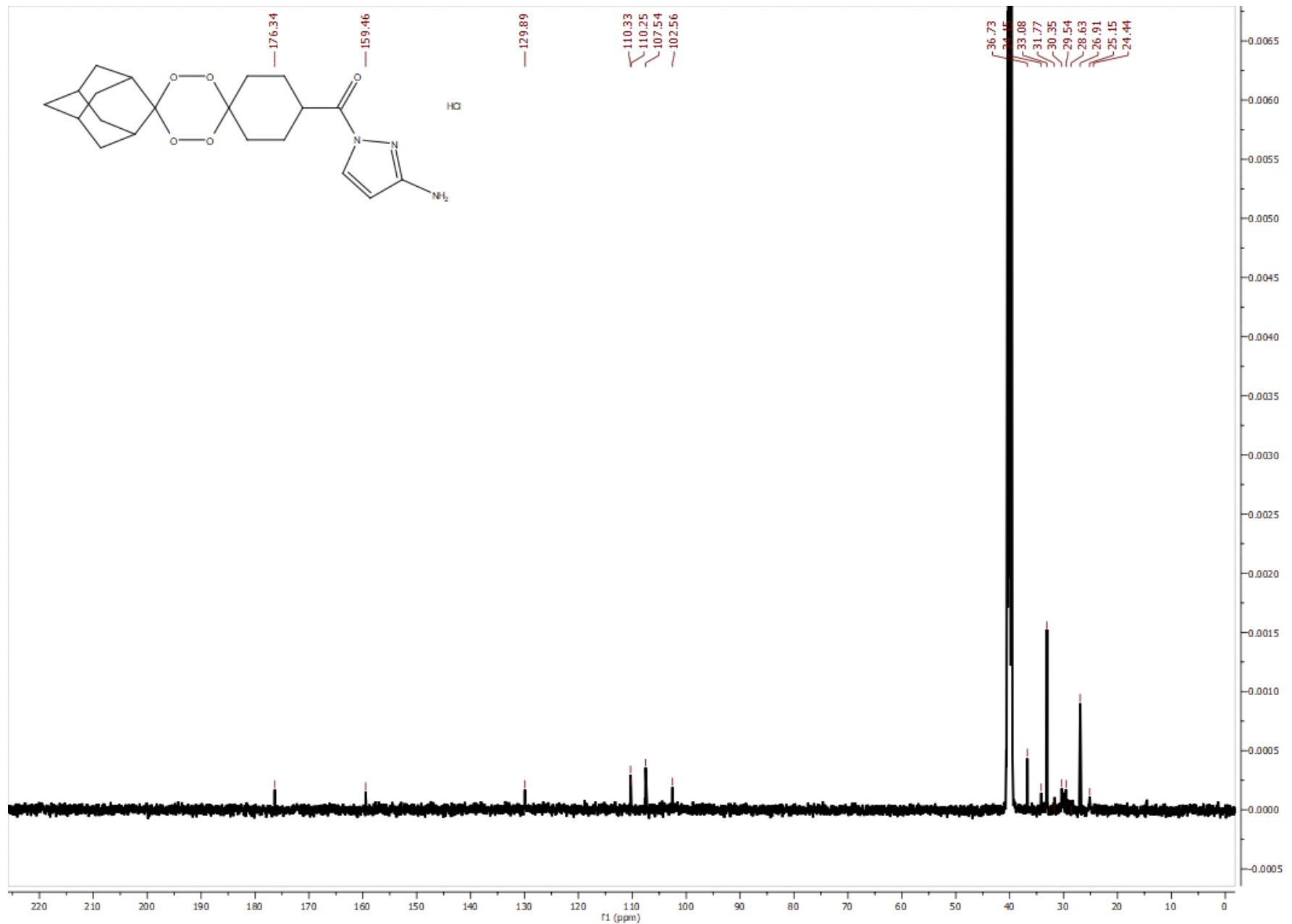
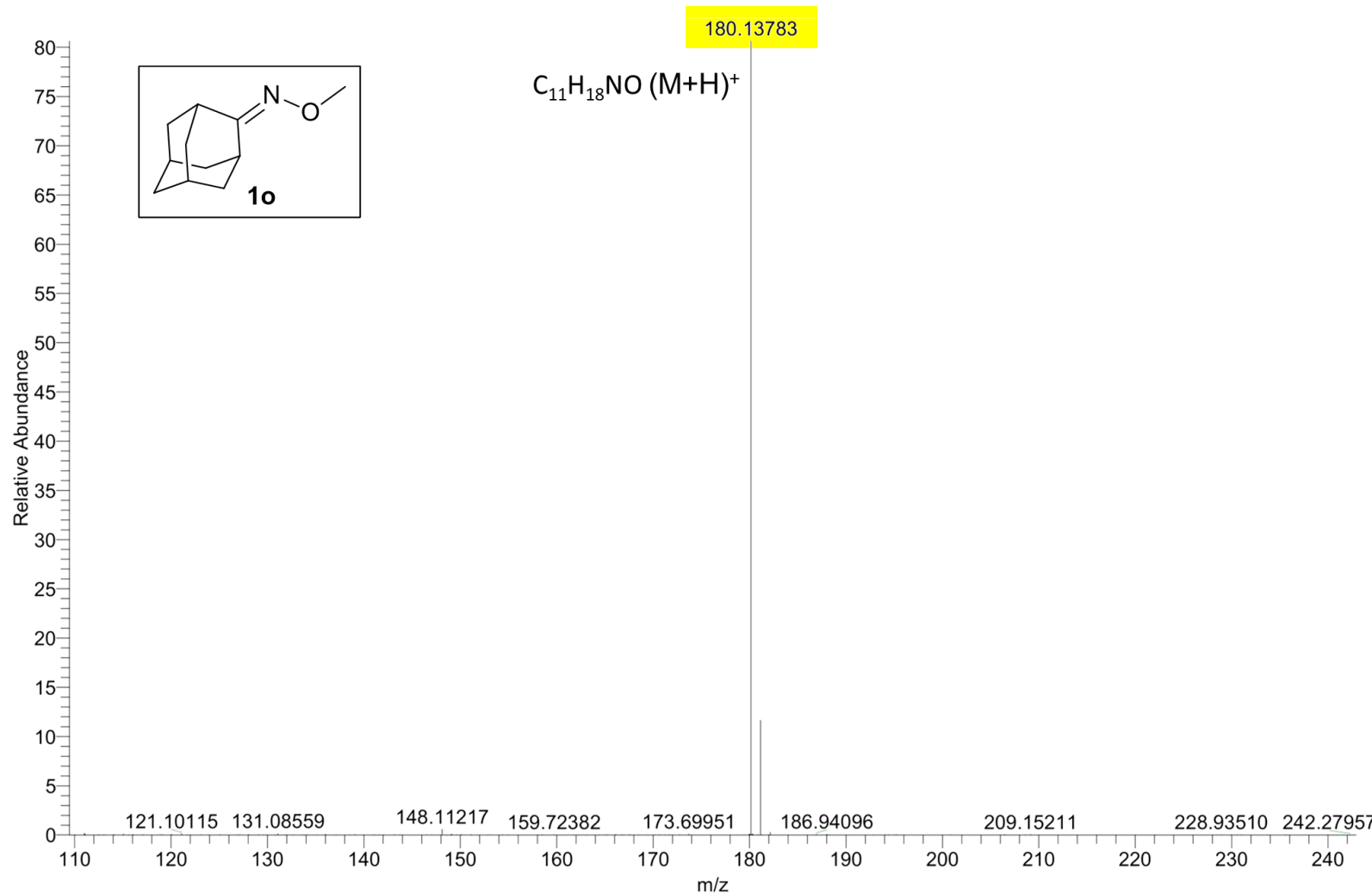


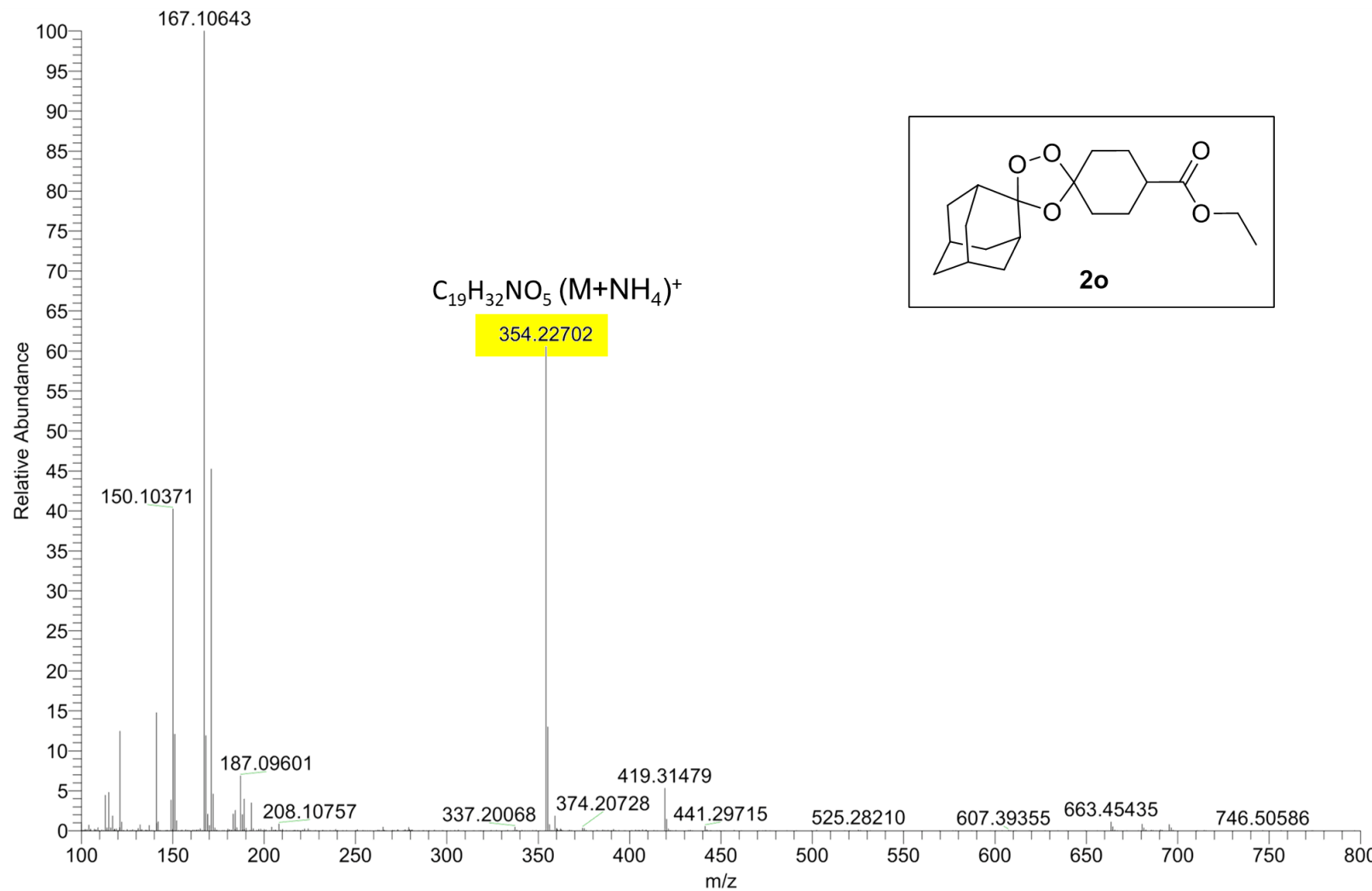
Figure S49. ^1H NMR spectrum (500 MHz) of T2•HCl in $\text{DMSO}-d_6$.

S2. HRMS spectra of the synthesised compounds

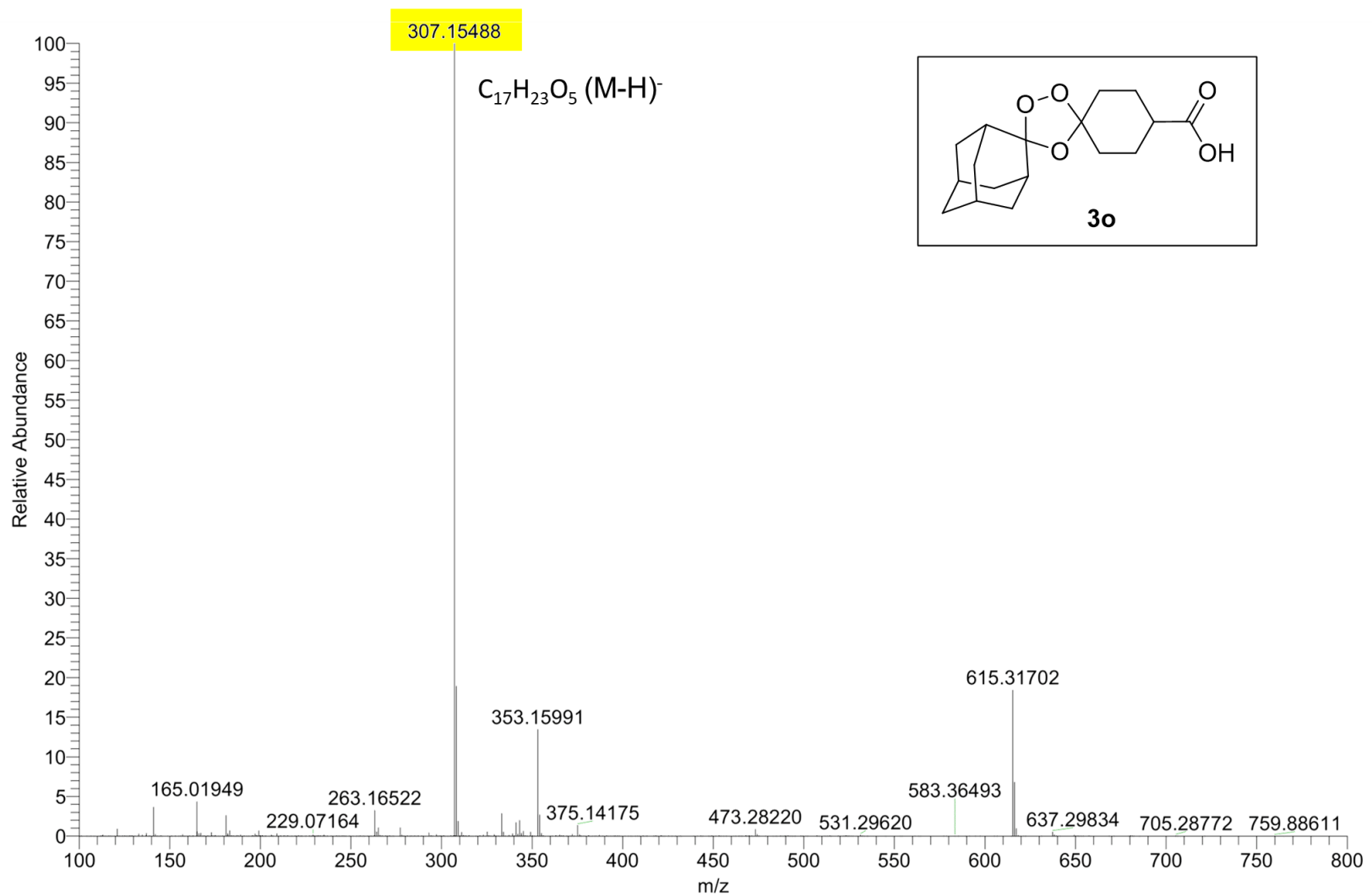
Electrospray ionization mass spectrum in positive-ion mode (HRMS-ESI⁺) of **compound 1o**



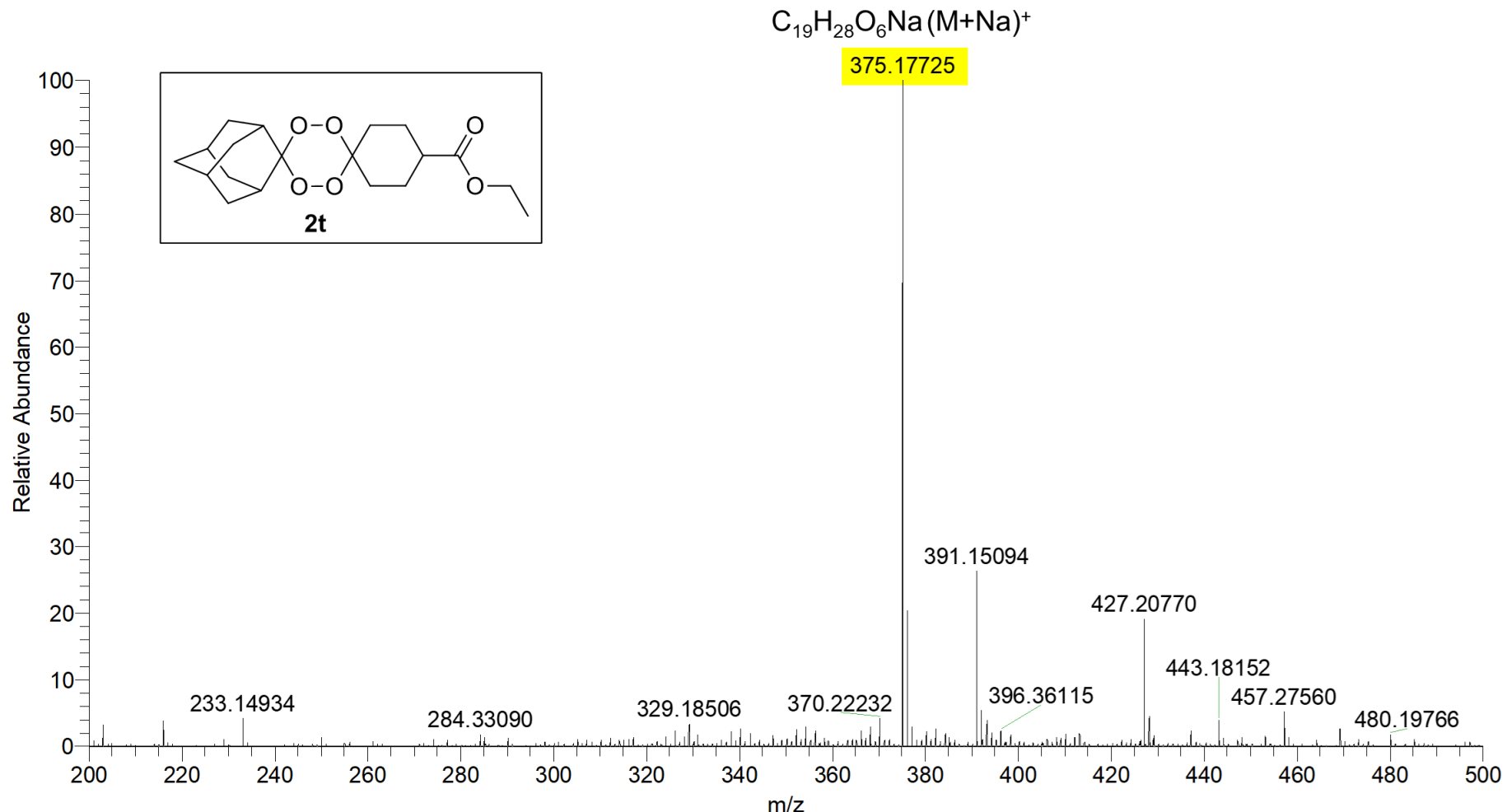
Electrospray ionization mass spectrum in positive-ion mode (HRMS-ESI⁺) of compound **2o**



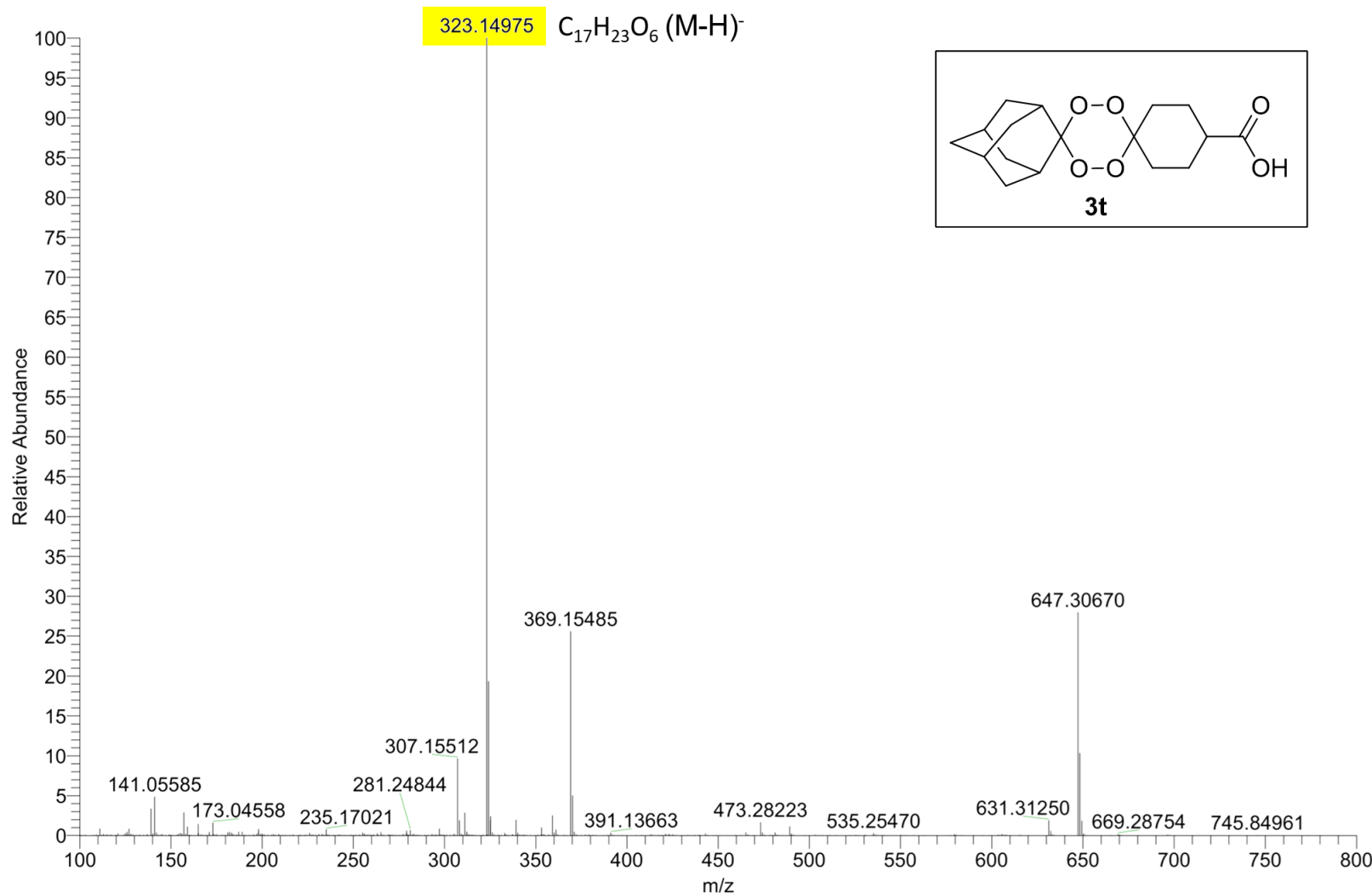
Electrospray ionization mass spectrum in negative-ion mode (HRMS-ESI⁻) of compound **3o**



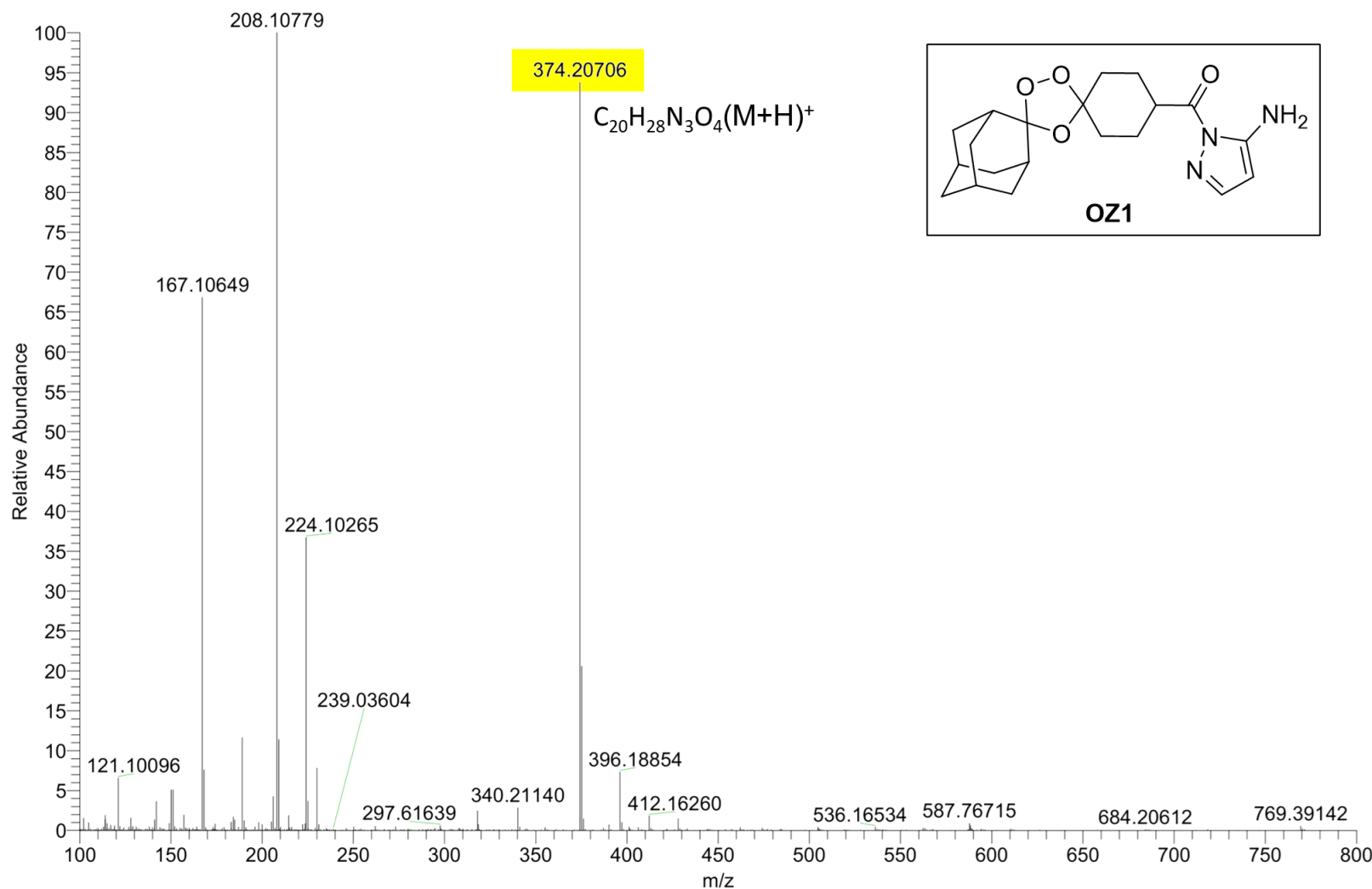
Electrospray ionization mass spectrum in positive-ion mode (HRMS-ESI⁺) of compound **2t**



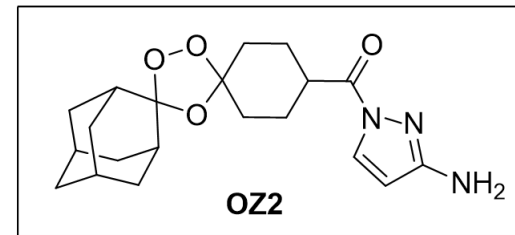
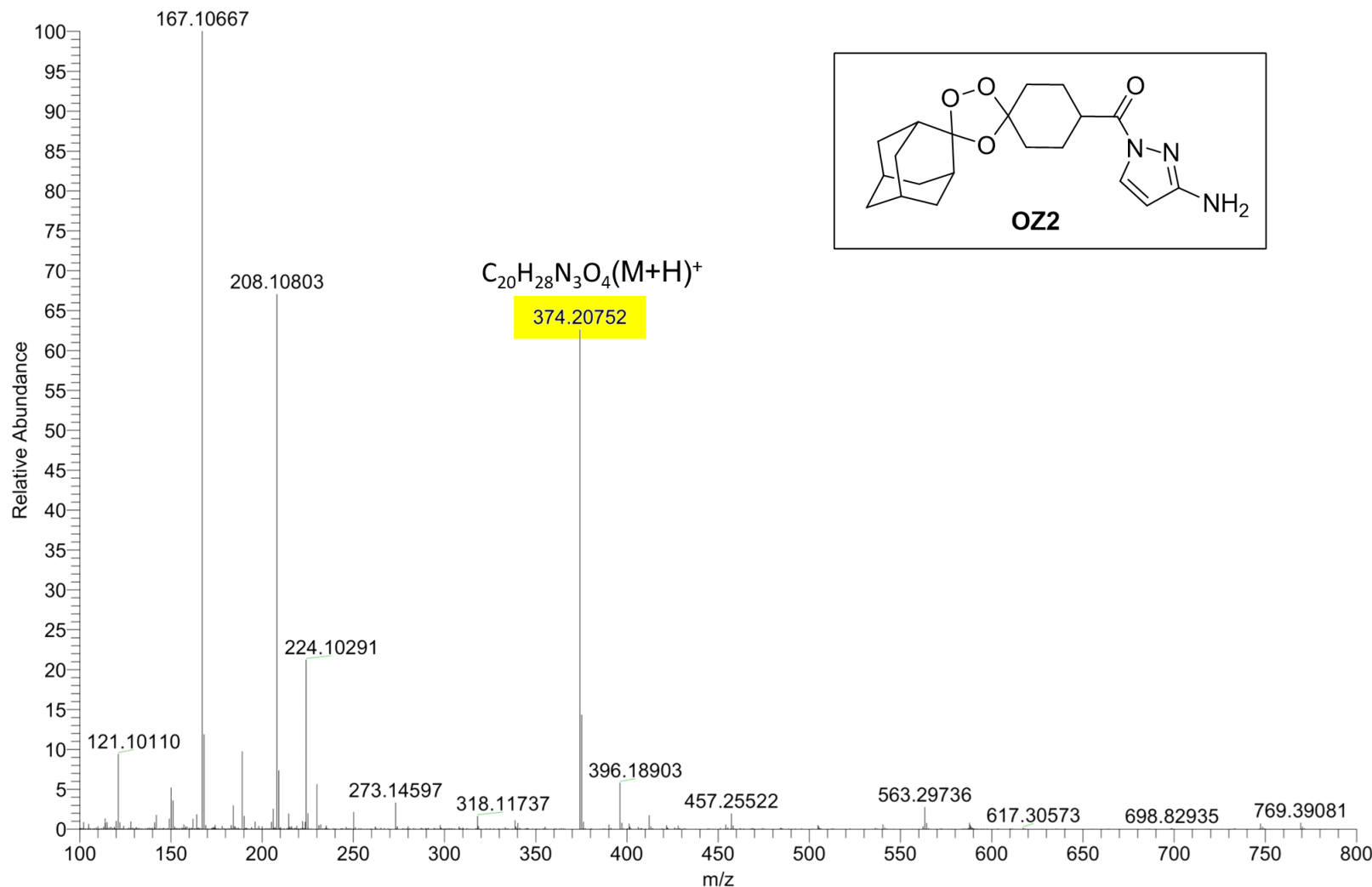
Electrospray ionization mass spectrum in negative-ion mode (HRMS-ESI⁻) of compound 3t



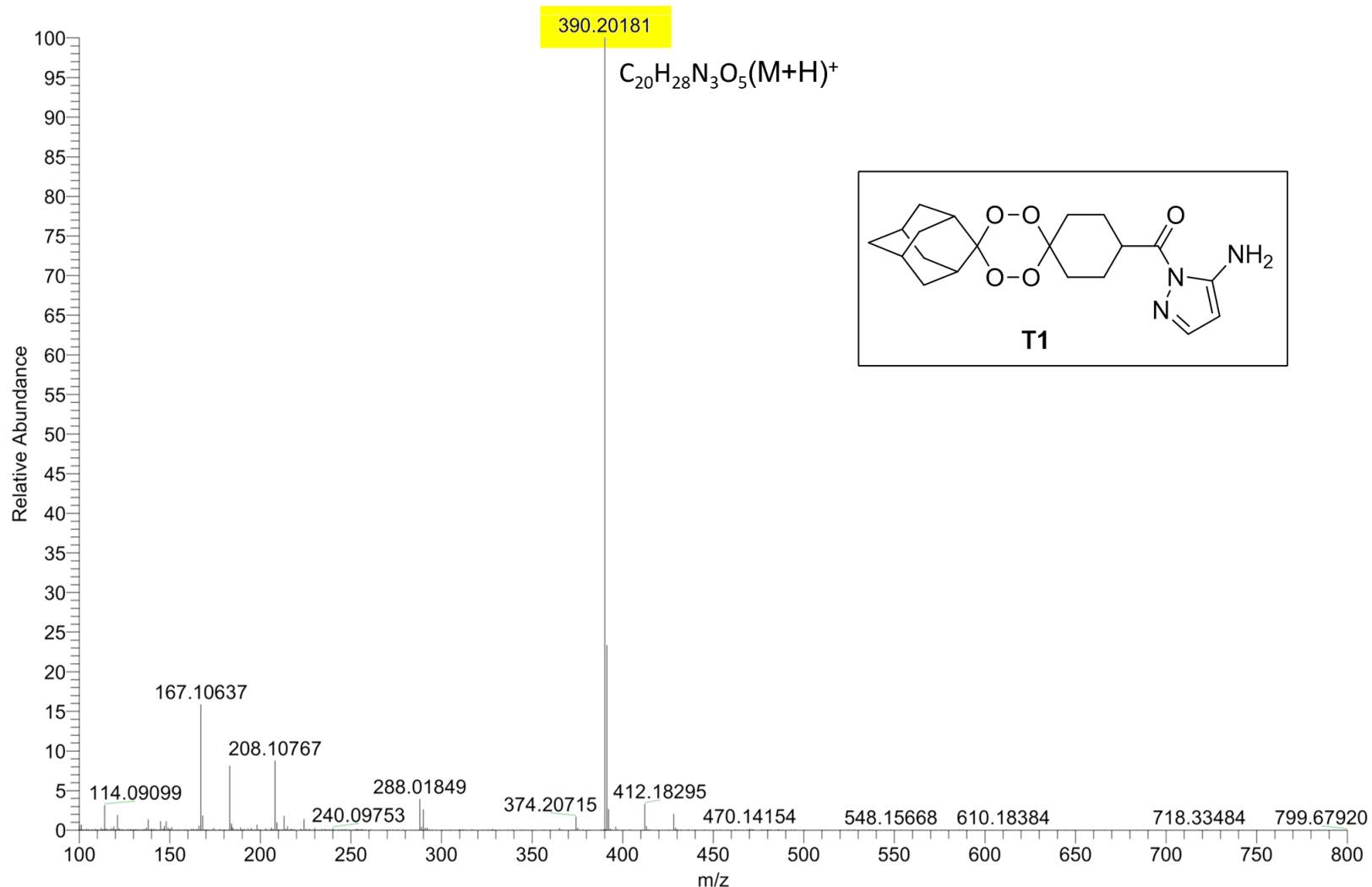
Electrospray ionization mass spectrum in positive-ion mode (HRMS-ESI⁺) of compound OZ1



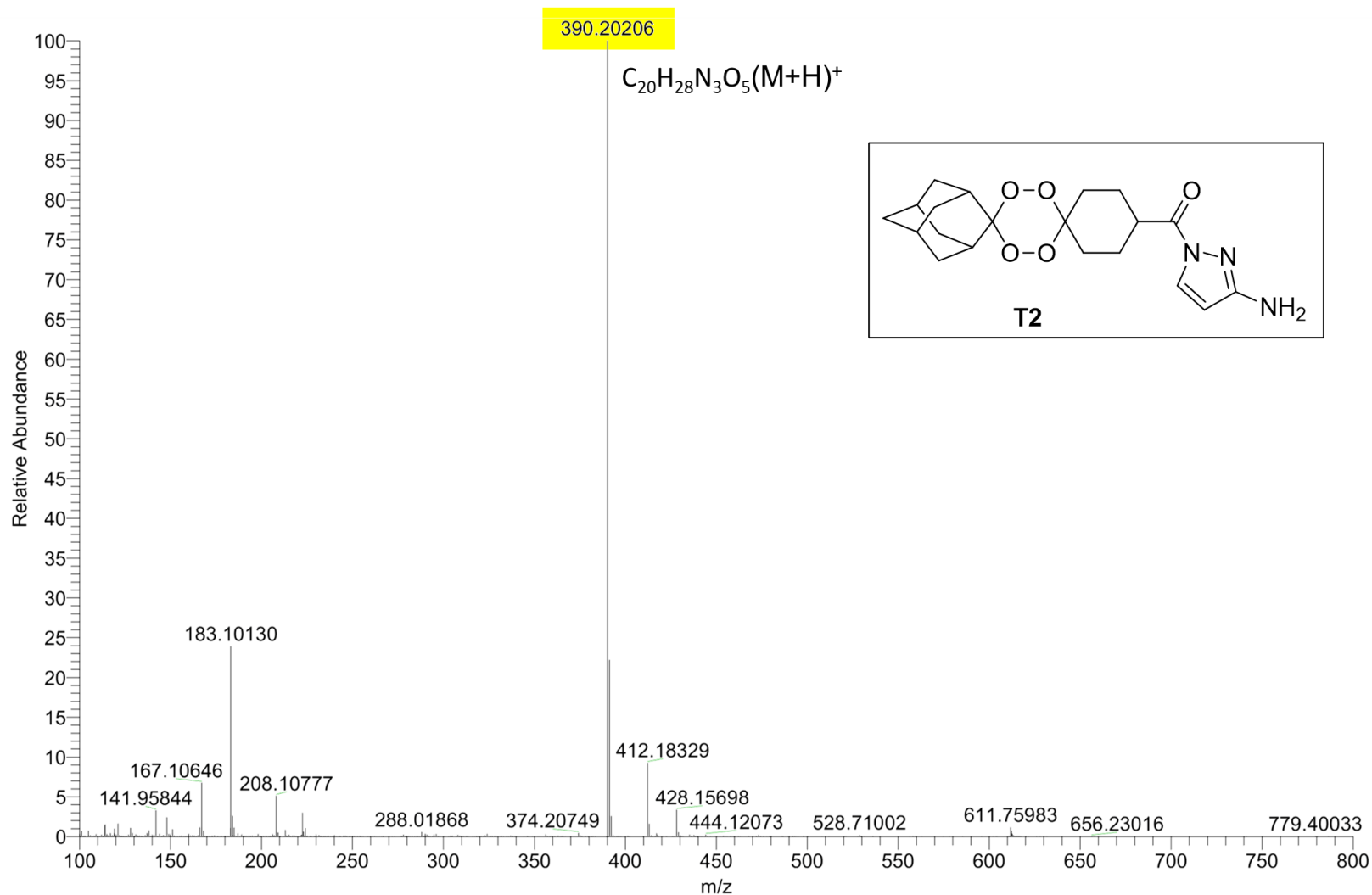
Electrospray ionization mass spectrum in positive-ion mode (HRMS-ESI⁺) of compound OZ2



Electrospray ionization mass spectrum in positive-ion mode (HRMS-ESI⁺) of compound T1



Electrospray ionization mass spectrum in positive-ion mode (HRMS-ESI⁺) of compound T2



S3. X-ray crystallography

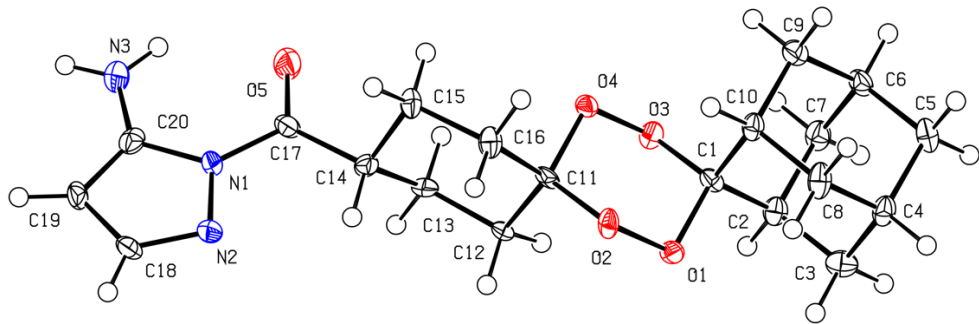


Figure S50. ORTEP drawing of the molecule of (5-amino-*1H*-pyrazol-1-yl) (dispiro[cyclohexane-1,3'-[1,2,4,5]tetraoxane-6',2"-tricyclo[3.3.1.1^{3,7}]decan]-4-yl)-methanone (**T1**). Displacement ellipsoids are drawn at the 50% probability level.

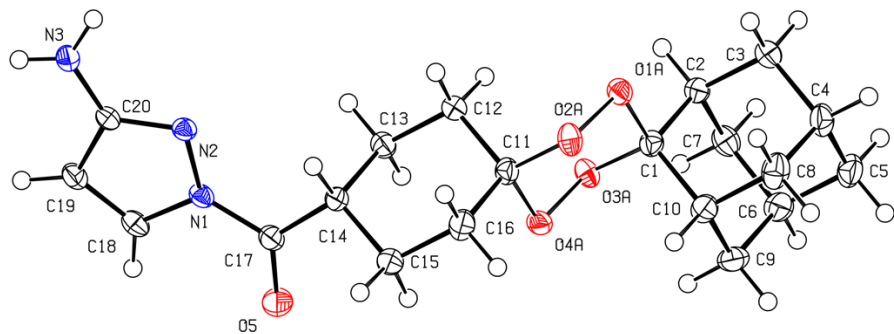


Figure S51. ORTEP drawing of the molecule of (3-amino-*1H*-pyrazol-1-yl) (dispiro[cyclohexane-1,3'-[1,2,4,5]tetraoxane-6',2"-tricyclo[3.3.1.1^{3,7}]decan]-4-yl)-methanone (**T2**). Displacement ellipsoids are drawn at the 50% probability level. The tetraoxane group has minor disorder over two alternate chair conformations; for the sake of clarity, only the major conformation is shown.

CIF files containing supplementary crystallographic data were deposited at the Cambridge Crystallographic Data Centre with references 2151742 (**T1**) and 2151175 (**T2**).